A Midzone-Based Ruler Adjusts Chromosome Compaction to Anaphase Spindle Length

Gabriel Neurohr

TESI DOCTORAL UPF / 2012

Thesis Supervisor

Dr. Manuel Mendoza

Chromosome Segregation and Cytokinesis Laboratory

Cell and Developmental Biology Program

Center for Genomic Regulation (CRG)

Für d’ Andrea

Ich froi mi uf oises grossä Abentür!

Summary

Partitioning of chromatids during mitosis requires that chromosome compaction and spindle length scale appropriately with each other. However, it is not clear whether chromosome condensation and spindle elongation are linked. Here we have used chromosome fusions to examine the impact of increased chromosome length during yeast mitosis. We find that yeast cells could cope with a >50% increase in the length of their longest chromosome arm by decreasing the physical length of the mitotic chromosome arm through 1) reducing the number of copies of the repetitive *rDNA* array and 2) by increasing the level of mitotic condensation. Consistently, cells carrying the fused chromosomes became more sensitive to loss of condensin- and its regulator polo kinase/Cdc5. Length-dependent stimulation of condensation took place during anaphase and depended on aurora/Ipl1 activity, its localization to the spindle midzone, and phosphorylation of histone H3 on Ser10, a known Ipl1 substrate. The anaphase spindle therefore may function as a ruler to adapt the condensation of chromosomes to spindle length. Consistent with this, chromosome condensation levels correlate with the length of anaphase spindles.

Resum

La correcta segregació de les cromàtides germanes durant mitosi requereix que la compactació dels cromosomes i la llargada del fus mitòtic s'escalin un amb l'altre. Tot i això, no està clar si la condensació de cromosomes i l'elongació del fus mitotic són processos directament relacionats. En aquesta publicació hem descrit que les cèl·lules de llevat poden suportar un increment de més del 50% de la llargada del braç cromosòmic més llarg. Aquestes cèl·lules sobreviuen gràcies a la disminució de la llargada física del braç del cromosoma mitjançant 1) la reducció de la llargada de la regió del DNA ribosòmic i 2) l'increment de la condensació del DNA. De manera concordant, les cèl·lules amb cromosomes fusionats esdevenen més sensibles a la pèrdua de la condensina i l'activitat quinasa de polo/Cdc5.

L'estimulació de la condensació depèn de la longitud del cromosoma. En l'estudi hem descrit que aquesta condensació té lloc durant anafase i depèn de l'activitat de la quinasa Ipl1, localitzada al fus, concretament a la *zona de solapament dels microtúbuls,* i de la fosforilació a la Serina 10 de l'histona H3. A més, Ipl1 ajuda a resoldre les cromàtides germanes durant anafase. Per tant, durant anafase, el fus mitòtic pot funcionar com un regle que adapta la condensació dels cromosomes a la seva llargada. Conseqüentment, els nivells de condensació es correlacionen amb la mida del fus mitòtic durant anafase.

Preface

In this work we present evidence that the level of anaphase chromosome condensation and the length of the mitotic spindle are coordinated with each other. Especially the size of the mitotic spindle can vary substantially between different cell types of a species and it was not clear so far how these differently scaled chromosome segregation machineries are able separate the same set of chromosomes. Our findings help to explain this question.

Not only the length of the mitotic spindle is however variable, but also chromosomes can change their size. Changes in chromosome arm length as a consequence of chromosomal translocations are frequently observed in cancer cells. The results presented here suggest a way how such alterations in chromosome size may be tolerated and are therefore medically relevant.

A note on author contributions

The “long chromosome project” was initiated in the laboratory of Yves Barral at ETH Zürich under the supervision of Manuel Mendoza, then a postdoctoral fellow. The initial aim was to test whether long chromosomes would lead to incompletely segregated chromatin during anaphase and study its impact on cytokinesis.

A first strategy to fuse yeast chromosomes, based on Cre-mediated recombination, was developed by undergraduate student Dominik Theler in 2006/2007. Another undergraduate student, Basil Greber, then started investigating the effects of chromosome fusion on the progression of cytokinesis. Surprisingly however the oversized chromosomes did not interfere with cytokinesis, suggesting that the long chromosomes were segregated efficiently (Spring 2007).

In summer 2007 I joined the project and two developments accelerated the progress: 1) We learned to visualize the segregation of yeast chromosomes using time lapse microscopy. 2) Dominik Theler had the idea for a less efficient but much faster approach to fuse chromosomes, which luckily turned out to work in my hands. Together this allowed us for the first time to directly look at fused chromosomes, which led to the initial discoveries of this work, namely chromosome hyper-condensation, shown in Figures 10, 12 and 14A-C.

After my undergraduate studies were finished I joined the laboratory of Manuel Mendoza in fall 2008 as a PhD student at the CRG in Barcelona, where I continued to work on the project. At the same time another undergraduate student, Andreas Nägeli, continued part of the project in the laboratory of Yves Barral. A very fruitful phase of collaboration between the two labs was finally crowned by the publication of the long chromosome paper in April 2011 [1], a copy of which can be found in the appendix. A substantial fraction of both text and figures in the results section presented here are directly taken from that publication.

Because Andreas Nägeli has made significant findings that are essential for our current understanding, his results are presented as part of this thesis. Specifically the data shown in Figures 16, 19, 22, 23A-C and 24B were generated by him.

Another collaborator that I want to mention here is Javier Diez from the laboratory of Toni Gabaldon at the CRG in Barcelona. He assembled and analyzed the results of the whole genome sequencing which we have performed and which are shown in Figure 11.

After this short historical perspective I wish the reader the same pleasure reading this work as I had writing it.

Table of Contents

I. Introduction

In order to fully partition chromosome arms during mitosis, chromosome arms must condense enough to be segregated by the anaphase spindle. However, both the size of chromosome arms and the length of the mitotic spindle can vary between different cells of a species. In this study we addressed the question whether chromosome condensation and the size of the mitotic spindle are somehow coordinated with each other. In the introduction I would thus like to consider what is known about how chromosomes fold and segregate during mitosis. This requires a quick review of the eukaryotic cell cycle and the structure of chromosomes.

1. Overview of the eukaryotic cell cycle and mitosis

1.1. The core cell cycle machinery is conserved from yeasts to vertebrates

The series of events required to fully duplicate and divide a cell into two daughter cells is termed cell cycle. In eukaryotic cells we distinguish between meiotic and mitotic cell cycles. The more common and probably older mitotic cycle generates two genetically identical daughter cells, while the DNA content in a meiotic cycle is reduced to half of the original content. Here I will focus on the mitotic cell cycle, which can be divided in four phases termed G1 (growth or gap phase 1), S (synthesis phase), G2 and M (Mitosis) (**Fig. 1**). During G1 phase, high rates of protein synthesis increase cell size and mass. This is followed by duplication of the DNA content and the centrioles during S phase. The duration of the second growth phase G2 is very variable and in some species, like *S. cerevisiae*, almost completely absent. Finally cells

segregate the DNA and organelles and divide into two independent daughters in M phase [2].

Early efforts to uncover the molecular nature of the cell cycle were genetic screens in the yeast species *S. cerevisiae* and *S. pombe* [3-5]**.** These studies identified mutants that arrested at different stages of the cell division cycle and were thus termed “cdc” mutants. This observation led to the idea that a cell cycle is a series of events in which a new step is always initiated once a previous step is completed, this is also known as the domino model of the cell cycle [6].

A different view came from experiments on oocytes from the frog *X. laevis*. Injection of cytoplasm collected from mature oocytes, which are arrested in metaphase II of meiosis, induced immature oocytes to start meiosis [7]. Thus a maturation-promoting factor (MPF) was present in the cytoplasm of metaphase II arrested eggs. MPF activity periodically increased and decreased as cells passed through mitotic divisions and hence MPF is also referred to as mitosis-promoting factor [6]. In contrast to the observations made in yeast however, perturbation of mitosis, for example by interfering with mitotic spindle formation, did not arrest the MPF oscillator [8, 9]. This led to the idea of an intrinsic clock that drives the cell cycle independently of the progression of individual cell cycle steps [6].

The two apparent different modes of regulation of the cell cycle in yeast and frog eggs could be reconciled by two main subsequent findings: First, that the core machinery responsible for the cell cycle is conserved in yeast, frog oocytes and mammals; second, that this machinery is regulated by feedback mechanisms in somatic cells but not in embryonic systems. These “checkpoints” ensure that initiation of late events is dependent on conclusion of early events [10].

In budding yeast *CDC28* was identified to be an important gene required for cell cycle entry in G1 [5]. Surprisingly *CDC28* could fully replace a mutated version of *cdc2* in fission yeast [11]. This was remarkable because *cdc2* mutants arrested mainly in G2 [3]. The G1/S transition in budding yeast thus

depended on the same machinery as the G2/M transition in fission yeast. Functional replacement of *S. pombe cdc2* was even possible with the human gene *CDC2* gene [12]. The three functionally redundant genes *cdc2 (Sp), CDC28 (Sc)* and *CDC2 (Hs)* encode a protein kinase. Interestingly isolated MPF also contained a kinase of approximately the same size. The kinases in MPF and Cdc2 turned out to be very similar, as MPF can be inhibited by a molecule which can also block *S. pombe* Cdc2 activity [13]. Thus the basic cell cycle machinery is conserved amongst species from yeasts to vertebrates and consists of a master regulator kinase.

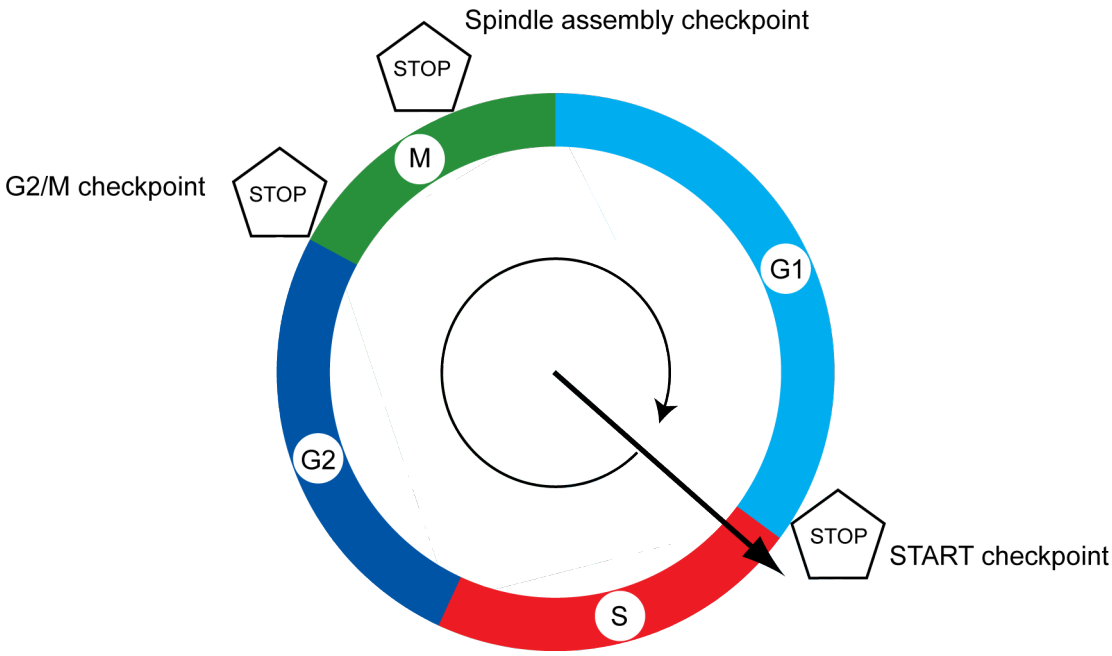

Figure 1: Regulation of the cell cycle.
The eukaryotic cell cycle is driven by a Cyclin/Cdk oscillator represented here as the hand of a clock. The oscillator triggers the essential processes such as DNA replication, mitosis and cytokinesis at the right time of the cell cycle. Checkpoints integrate intra- and extracellular information and are able to block cell cycle progression if exctracellular conditions are not favorable or if previous cell cycle events have not been completed. Figure adapted from [14].

The Cdc2/Cdc28 kinase forms a complex with co-activator proteins termed cyclins, because they appear and disappear periodically with the cell cycle

[15]. Accordingly the Cdc2/Cdc28 kinase was called cyclin dependent kinase (Cdk). During the different phases of the cell cycle, specific cyclins are synthesized and degraded in a regulated manner. The different cyclins determine the activity and in part the specificity of the kinase towards its substrates [16]. In yeasts the same Cdk kinase, but bound to different cyclins, promotes DNA replication in S-phase and chromosome segregation in M-phase. In animal cells multiple Cdks interact with an even higher number of cyclin proteins [17]. The core cell cycle machinery thus consists of a central Cyclin/Cdk oscillator that drives the cell cycle in both yeasts and vertebrates (**Fig. 1**).

1.2. Transition between different cell cycle stages is tightly regulated

It is of crucial importance that the different steps required for cell duplication happen in the right temporal order. To ensure this, cell cycle checkpoints monitor accurate completion of the processes of a cell cycle phase. If a process is not finished or an error is detected, these checkpoints can prevent progression of the cell cycle (**Fig. 1**).

The G1/S transition: The transition from G1 to S-phase is called restriction point, or START in yeast, as it represents a commitment of the cell to divide. At the START point dividing cells need to overcome transcriptional repression of the G1/S-cyclins and inactivate Cdk inhibitors (CKI) through degradation [18]**.** This allows cells to enter S-phase and duplicate their genome.

Before entering the cell cycle cells make sure they are ready to divide. This decision is regulated by a combination of internal and external signals. In budding yeast the most important external signals are the availability of nutrients and the presence of mating pheromone, which prevents entry into the cell cycle. In multicellular organisms growth factors stimulate or inhibit cell proliferation. Loss of the coordination between cell division and environmental cues is detrimental especially in multicellular organisms as it might lead to

uncontrolled cell proliferation, an important step in cancer. Internal signals that regulate cell cycle entry are cell size, growth rate and different forms of stress [18]. DNA damage for example can block passage through START in budding yeast [19].

The G2/M transition: In cell cycle models with an extended G2 phase like *S. pombe* and mammalian cell lines, Cdk activity increases rapidly as cells enter mitosis. This switch-like activation of Cdk is regulated through an inhibitory phosphorylation on Cdk. One important inhibitory kinase is Wee1, which is present in all eukaryotes. Cdk becomes active after dephosphorylation by the Cdc25 phosphatase. Both Wee1 and Cdc25 are phosphorylated by Cdk. This inhibits Wee1 but activates Cdc25, creating two feedback loops that make the entry into M-phase an irreversible switch-like step [20].
In *S. pombe* and vertebrates, DNA damage occurring in S- or G2 phase prevents entry into mitosis through inactivating Cdc25. This hinders cells from attempting to segregate damaged chromosomes. In *S. cerevisiae* damaged DNA prevents the onset of anaphase, but the molecular basis for this is not entirely clear [21].

The M/G1 transition: At the transition from M- to G1-phase, also called exit from mitosis, cells need to switch form a state with high Cdk activity to a state with low Cdk activity. This transition is regulated on several levels. Reduction of Cdk activity is achieved mainly through degradation of mitotic cyclins and through stabilization of Cdk inhibitors. In addition mitotic exit depends on phosphatases that dephosphorylate Cdk substrates.
Exit from mitosis is controlled by the spindle assembly checkpoint (SAC), which detects chromosomes that are not attached to the mitotic spindle. The SAC prevents activation of the anaphase promoting complex (APC), which is needed to initiate chromosome separation, degradation of cyclins and activation of mitotic exit phosphatases [22].

1.3. Mitosis

Entry into mitosis is marked by a steep increase in the activity of the mitosis specific Cdk/CyclinB complex. This initiates a series of events that ultimately lead to the segregation of the cellular material and the cleavage of the cell into two daughters. Typically mitosis is subdivided into prophase, prometaphase, metaphase, anaphase, telophase and cytokinesis. This classification is mostly based on cytological analysis of an open mitosis as it is observed in vertebrate cells (**Fig. 2**) [23].

1.3.1 Overview of an open mitosis

Prophase: The first microscopically visible signs of mitosis are changes in chromosome structure termed chromosome condensation. During this process, the replicated DNA molecule, consisting of two connected sister chromatids, is organized into mitotic chromosomes.

Prometaphase: In higher eukaryotes like plants and animals, the nuclear envelope disassembles in prometaphase. Coinciding with the breakdown of the nuclear envelope cells start to organize their microtubules into a complex bipolar structure, called the mitotic spindle. These spindle microtubules now gain access to the chromosomes and attach to a protein complex present on each sister chromatid, the kinetochore.

Metaphase: Molecular motors and microtubule dynamics move chromosomes along microtubules to the equator of the mitotic spindle. In order to equally partition the chromosomes, the kinetochores on the two sister chromatids of a chromosome need to attach to opposite poles of the mitotic spindle. Cells delay anaphase onset through activation of the spindle assembly checkpoint (SAC) until all chromosomes are correctly attached.

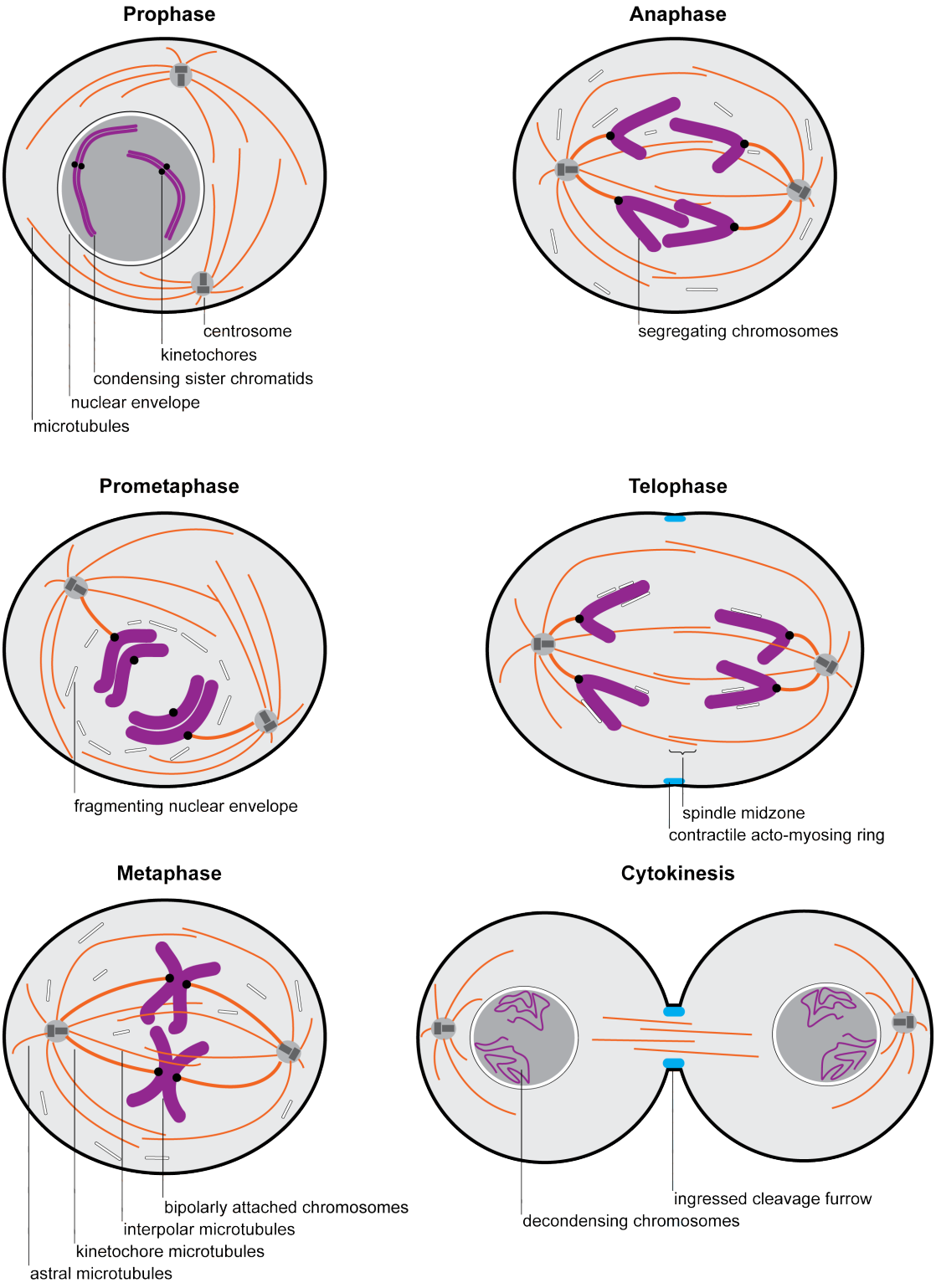

Figure 2: Overview of an on open mitosis in vertebrate cells.
The cartoon shows important mitotic structures at different stages of mitosis. The important steps taking place in each phase are described in the text. The figure is based on [23].

Anaphase: Once all chromosomes are bipolarly attached, cells initiate anaphase through activation of the anaphase promoting complex APC, which initiates a series of reactions leading to simultaneous inactivation of Cdk and of sister chromatid cohesion. Microtubules then pull the duplicated chromosomes towards opposite poles of the cell.

Telophase: In telophase the chromosomes start to decondense and the nuclear envelope is re-assembled around the chromatin. A contractile ring consisting of actin and myosin assembles below the plasma membrane between the segregating chromosomes.

Cytokinesis and Abscission: The contractile ring now pulls the plasma membrane inside, generating a cleavage furrow and dividing the cytoplasm. This process is called cytokinesis. The acto-myosin ring then needs to be disassembled before cells can be completely cleaved from each other by a membrane fission event termed abscission.

1.3.2. Mitosis in budding yeast

In order to segregate its chromosomes budding yeast has to perform the same tasks as described above. There are however some important alterations to the mitosis observed in vertebrates.

One main difference is that budding yeast performs a closed mitosis: the nuclear envelope is not disassembled. The mitotic spindle therefore has to form inside of the nucleus and the spindle poles are embedded in the nuclear envelope (**Fig. 3**). A small spindle is assembled soon after spindle pole duplication in S-phase. In contrast to vertebrate cells, microtubules have access to chromosomes throughout the cell cycle and bipolar attachment of chromosomes to the mitotic spindle is already achieved in S-phase, before spindles have fully matured [24].

During anaphase the mitotic spindle elongates, giving the nuclear envelope an elongated shape. Towards the end of anaphase a thin channel connects the two future daughter nuclei giving the nucleus the appearance of a

dumbbell (**Fig. 3**). Due to this geometry, the segregating chromosomes are subjected to spatial restrictions that are absent in open mitosis.

In contrast to vertebrate cells the plane of cytokinetic division in budding yeast is already defined in G1. This is important because yeast cells have a rigid cell wall and the right geometry for division needs to be established through polarized growth of the bud. Bud growth is constant from entry into S-phase until mitotic exit. The size of the bud is a very useful morphological trait to identify the cell cycle stage. Cytokinesis itself also relies on a contractile acto-myosin ring, but in addition a new cell wall, the septum, is deposited between mother and daughter cell [25].

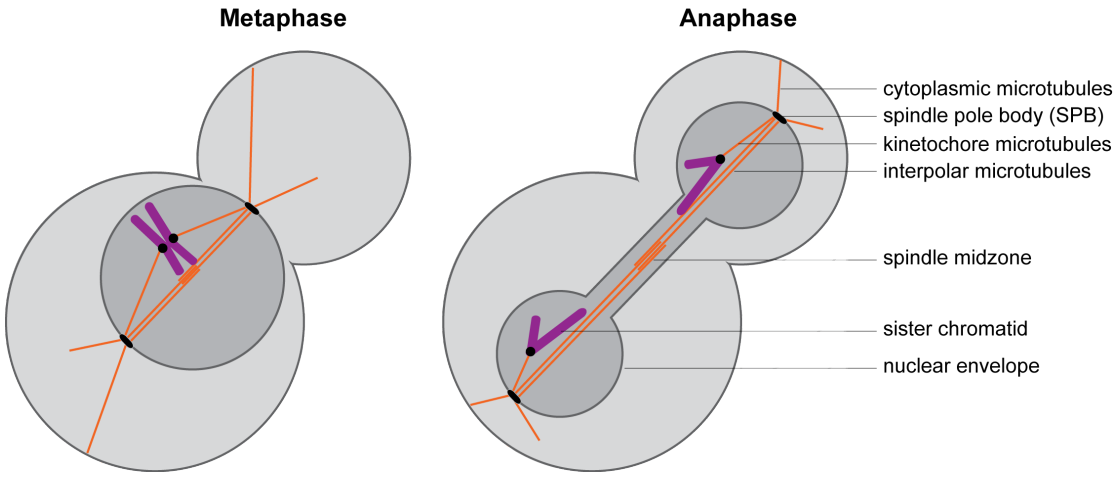

Figure 3: The budding yeast mitotic spindle.
A metaphase (left) and an elongated anaphase (right) spindle are shown. Each spindle pole nucleates about 18 nuclear microtubules. Each of the 32 kinetochores is contacted by a single microtubule. In addition one or two interpolar microtubules emanate from each pole. The region of overlapping interpolar microtubules defines the spindle midzone. A few cytoplasmic microtubules connect the SPBs to the cell cortex and help to position the spindle in meta- and anaphase [26, 27].

1.4. The mitotic spindle

The main component of the mitotic spindle are microtubules (MTs). These are giant polymeric assemblies of tubulin proteins, that form hollow tubes of 25nm diameter. The basic building unit is a heterodimer of α- and β-tubulin, which polymerize in a polarized fashion to form MT filaments with a plus and a

minus end. The polymerization is started at the minus end of the filament, where α-tubulin binds to a complex of the tubulin variant γ-tubulin and associated proteins. Further heterodimers are then added on top of theses MT seeds making the MT grow in plus end direction [28].
The tubulin subunits are GTP binding proteins. Shortly after incorporation of an α-, β-tubulin dimer, the GTP in the β-subunit gets hydrolized to GDP. Most of the tubulin dimers along a MT are thus in the GDP bound form. On growing MT fibers there is however always a small cap of tubulin bound to GTP. GTP hydrolysis induces a small conformational change in the tubulin subunit that destabilizes the polymer. If the GTP hydrolysis proceeds faster than addition of new GTP-bound tubulin dimers, the protective GTP cap is lost and the tip of the growing MT is destabilized. This induces the disassembly of the MT. When a new GTP cap is formed through addition of GTP-tubulin dimers the disassembly is stopped and the MT starts to grow again. Thus MTs switch stochastically between phases of growth and disassembly. This behavior is called dynamic instability [28].

During mitosis MTs reorganize to form a specialized bipolar structure, the mitotic spindle, which is capable of physically separating the sister chromatids (**Fig. 2, 3**). The minus ends of the MTs are anchored in two opposed microtubule organizing centers (MTOCs), called centrosomes in animal cells or spindle pole bodies (SPBs) in yeast. As yeast performs a closed mitosis, the SPBs are embedded in the nuclear envelope and nucleate both cytoplasmatic and nuclear microtubules [27].
The spindle is made up of three types of MTs. Astral MTs connect the MTOC with the cortex of the cell and help to position the mitotic spindle. Interpolar MTs emanate from the two poles and form a set of overlapping antiparallel MTs, which interact with each other and link the two halves of the spindles. In yeast about four interpolar MTs extend from each spindle pole body while more than 100 interpolar microtubules are present in a mammalian metaphase spindle. Kinetochore microtubules bind to the kinetochores and

thus connect the chromosomes to the mitotic spindle. In mammalian cells around 30 microtubules contact each kinetochore. Yeast kinetochores bind to a single microtubule [27].

The microtubules of the mitotic spindle are organized into a network by a number of additional proteins that regulate the MT stability, crosslink and move MTs relative to each other. Mass spectrometric analysis of purified human spindles identified around 800 spindle associated proteins [29].

At anaphase onset the dynamics in the spindle change and two processes contribute to the segregation of the sister chromatids. First shortening of the kinetochore fibers, without detaching from the kinetochores, moves the chromatids closer to the poles. This is called anaphase A.

In addition microtubule motors slide antiparallel MTs against each other. This moves the spindle poles apart in anaphase B, increasing the length of the mitotic spindle. Anaphase B is supported by a set of proteins that get recruited to the region of overlapping interpolar microtubules during anaphase in a process is termed spindle midzone maturation.

The relative contribution of anaphase A and anaphase B to chromosome separation varies between organisms. In *S. cerevisiae*, the 2µm metaphase spindle elongates to about 8µm in anaphase, thus chromosome segregation is mostly driven by anaphase B [22].

1.5. Mitotic Kinases

Cdks are the master regulators of mitotic progression. In addition a number of other protein kinases control important steps during mitosis. The most prominent ones are Aurora kinases and polo like kinase.

Aurora B/Ipl1 kinase: In mammalian cells there are three members of the Aurora kinase family, Aurora A, Aurora B and Aurora C. The single family member found in *S. cerevisiae* most closely resembles Aurora B and is called

Ipl1. Aurora B/Ipl1 is part of the chromosomal passenger complex (CPC), which also contains Survivin/Bir1, INCENP/Sli15 and Borealin/Nbl1 [30, 31].
Aurora B/Ipl1 activation requires the interaction with INCENP. Activity is further stimulated through phosphorylation of INCENP/Sli15 by Aurora B/Ipl1 and an auto-phosphorylation of the T-loop (activation loop) in the Aurora B/Ipl1 kinase domain [30].
In mammalian cells the CPC locates on chromosome arms during prophase and accumulates at the centromeres during prometaphase [30]. In budding yeast Ipl1 localizes to centromeres from G1 to metaphase [32]. In all eukaryotes, the CPC translocates to the mitotic spindle after anaphase onset [30].
Aurora B has conserved roles from yeast to humans in establishing bipolar chromosome attachment to the mitotic spindle, chromosome condensation, spindle maturation and cytokinesis. The specific role of Aurora B in some of these processes will be discussed in more detail later (Sections 2.2.; 2.4. and 3.1.).

Polo-like kinase: In all eukaryotic species there is one active polo like kinase during mitosis, in mammalian cells Plk1 in *S. cerevisiae* Cdc5 [33]. Plk1/Cdc5 accumulate at the beginning of mitosis [34, 35] and are degraded by the anaphase promoting complex at the end of mitosis [33].
Besides the temporal control of protein synthesis and destruction, mammalian Plk1 activity is also regulated by phosphorylation of a conserved threonine in the T-loop. Aurora A and possibly also Aurora B have been proposed to be responsible for the activation of Plk1 [33].
Plk1 binds to its mitotic substrates through two polo box domains, which bind phosphorylated consensus motifs [36]. Thus Plk1 activity towards specific substrates can be modulated by previous phosphorylation of the substrate by other kinases or by Plk1 itself [33].
In mammalian cells Plk1 localizes to the centrosomes, centromeres, kinetochores throughout mitosis and to the midzone of the mitotic spindle in

anaphase. In budding yeast Cdc5 is found on the spindle pole bodies throughout the cell cycle. In mitosis an additional diffuse nuclear signal is observed and during cytokinesis Cdc5 accumulates at the bud neck [33].
Polo like kinases are involved in regulating the entry into mitosis, are required to establish a bipolar spindle, regulate chromosome condensation and cohesion, are required for cytokinesis and mitotic exit [33]. A more detailed description of the role of Plk1/Cdc5 in some of these processes will follow (Sections 2.4., 3.2.)

2. Eukaryotic chromosomes

2.1 Specialized chromosome regions

Eukaryotic DNA is organized into large linear polymers called chromosomes. Specialized domains allow chromosomes to fulfill essential functions.

Centromeres: Centromeres are transcriptionally silenced heterochromatic regions present once on each chromosome. In *S. cerevisiae* the position of the centromere is defined by a short sequence of 125 Bp [37]. In other organisms such a sequence has not been identified. Instead the centromere position is determined by epigenetic marks, including the presence of specialized nucleosomes (see below). These contain a variant form of histone H3 called CENP-A or Cse4 in budding yeast. The centromeric chromatin recruits the components of the kinetochores, through which the chromosome attaches to the mitotic spindle [38].

Telomeres: During DNA replication, synthesis of the lagging strand depends on the generation of a small RNA primer. As a consequence the chromosomes cannot be replicated to the very end and become a few nucleotides shorter after every division. To prevent progressive erosion of chromosome ends cells contain an enzyme called telomerase, which is able

to add short DNA repeats to the end of a chromosome without the need of a DNA template. These specialized chromosomal regions are called telomeres. Their size ranges from several hundred Bp in *S. cerevisiae* to several kb in humans.
The repetitive telomeric sequences recruit a specialized set of proteins to the telomeres. These protect the chromosome ends from being recognized as DNA double strand breaks. Failure to cap telomeres provokes a DNA damage response and results in chromosome end to end fusions [39, 40].

Ribosomal DNA (*rDNA*): The production of the ribosomal RNA (rRNA) makes up a large portion of total transcription, in budding yeast about 60% [41]. To meet this high demand the genes encoding for the precursor rRNAs are present in multiple copies and organized in a way that allows high transcription rates.
In *S. cerevisiae* an array of 100-200 copies of 9.1kb *rDNA* repeats are organized in one locus. In human cells there are 5 *rDNA* clusters, each containing approximately 70 repeats. In *S. cerevisiae* a repeat contains one gene for the 35S and 5S precursor rRNA as well as an origin of replication (**Fig. 4A**). The individual repeats are separated by replication fork barriers, which only allow the passage of the replication fork in one direction (**Fig. 4B**) [42]. The arrangement of replication fork barriers and origins of replication makes sure that transcription of the large 35S precursor rRNA and the replication fork always move in the same direction. Because the *rDNA* is transcribed during S-phase, such an arrangement is important to prevent head to head collisions of replication forks with transcribing RNA Polymerase III. In yeast such collisions were shown to promote recombination within the *rDNA* locus [43] presumably through generating DNA breaks (see below). However, normally not all of the *rDNA* repeats are transcribed and a fraction of them is kept in a heterochromatic state [44]. Having some extra copies of the *rDNA* repeat is beneficial, because it allows inactivation of transcription in some repeats, which is required to repair DNA damage [45].

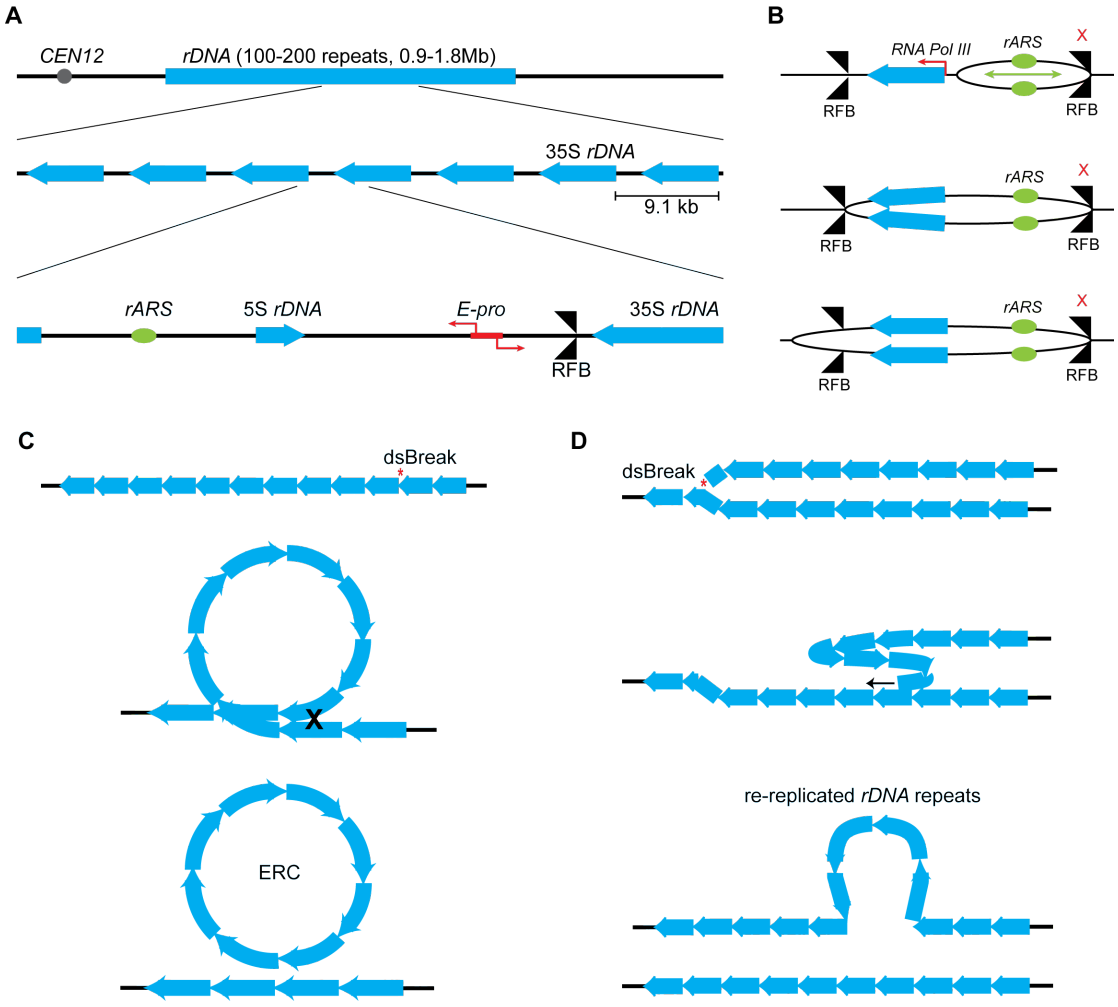

Figure 4: Organization of the yeast ribosomal DNA locus.
(**A**) The *rDNA* array in budding yeast contains 100-200 copies of the 9.1kb *rDNA* locus. The 35S precursor rRNA is produced by RNA polymerase I (Pol I) while the smaller 5S *rDNA* gene is transcribed by RNA Pol III. RNA Pol II transcription of a non-coding RNA takes place at the bidirectional expansion sequence promoter (*E-pro*). Each *rDNA* repeat contains an autonomous replication sequence (*ARS*). Individual *rDNA* repeats are separated by a replication fork barrier (RFB) (**B**) The RFB stalls replication forks that are processing in the opposite direction of RNA Pol III transcription. Like this transcription and DNA replication in the 35S *rDNA* gene always occur in the same direction. This prevents collision of the replication fork with RNA Pol III and allows efficient *rDNA* transcription even during replication. (**C**) Double strand breaks (red asterisk) in the *rDNA* array can lead to intramolecular homologous recombination (black cross), resulting in the excision of extra-chromosomal *rDNA* circles (ERCs) and a reduction in genomic *rDNA* copy number (**D**) DNA double strand breaks at the replication fork can lead to re-replication if the strand anneals on an already replicated repeat. Re-replication results in an expansion of the *rDNA* array. This figure is adapted from [42].

The copy number of *rDNA* repeats can spontaneously increase and decrease [46]. The number of *rDNA* copies is regulated by the relative rates of two opposing processes, which occur in response to DNA double strand breaks in the *rDNA* array. These breaks depend on the presence of the replication fork barrier and transcription by RNA polymerase I [47]. DNA double strand breaks can be repaired by homologous recombination using either the homologous chromosome or the replicated sister chromatid as template [48]. The highly repetitive nature of the *rDNA* region makes this process error prone. Instead of using the replicated sister chromatid as template for DNA repair, the broken site can also pair with another repeat on the same chromosome. Recombination between loci on the same DNA strand leads to the excision of extra-chromosomal *rDNA* circles (ERCs) (**Fig. 4C**). This results in a reduction of genomic *rDNA* copy numbers.

If the DNA breaks during replication and anneals on the already replicated sister chromatid, there is a chance of annealing at the wrong repeat. The gap between the annealing site and the double strand break is then re-replicated, resulting in an amplification of *rDNA* copies (**Fig. 4D**) [49]. This imprecise annealing requires that sister chromatids are not tightly cohesed. Activation of the bidirectional RNA Pol II promoter E-pro, located near the replication fork barrier (**Fig. 4B**), reduces association of cohesin with the *rDNA* and is required for array expansion [50]. Silencing of E-pro requires the histone deacetylase Sir2 [50]. Sir2 dependent silencing of *rDNA* is enhanced under conditions with low metabolic activity like caloric restriction [51] and the size of the *rDNA* array increases when the growth rate is enhanced [46]. Thus *rDNA* expansion can be coupled to the metabolic needs of a cell. When Sir2 is absent in cells with short *rDNA* arrays, the array expands faster and becomes more heterogeneous within a population than in wild type cells [52]. However, the average number of *rDNA* copies in *sir2*Δ mutants is the same as in wild type cells [52]. What limits the expansion of the *rDNA* is therefore still not clear.

2.2. Chromatin Structure

The longest human chromosome is composed of approximately $2.2 \cdot 10^8$ base pairs (Bp) and the complete diploid genome consists of $6 \cdot 10^9$ Bp [53, 54]. As linear B-type DNA molecule this would correspond to a 75mm long thread and 2m total fiber of 2nm width (0.34nm/Bp). The problem of how cells pack such big heavily charged polymers into a nucleus of only a few µm diameter has puzzled biologists ever since the discovery of the DNA double helix in 1953 [55].

The first level of DNA folding is its package into nucleosomes. A complex of 8 positively charged histone proteins, the histone octamer, forms the core of the nucleosome, around which 147 Bp of DNA are wound in 1.7 left-handed super-helical turns [56]. Individual nucleosomes are connected by linker DNA of 10-80Bp length. On electron micrographs this form of chromatin looks like beads on a string. Due to the 10nm diameter of the nucleosome it is also called 10nm fiber. In addition to the histone core, a linker histone H1 binds to the entry and exit site of the DNA and also binds to the linker DNA. Linker histones can influence the position of the nucleosomes on the DNA and the assembly of nucleosomes into higher order chromatin structures. Packaging of the DNA into nucleosomes neutralizes the negative charge of the DNA and introduces a 6 fold axial compaction compared to the B-type DNA helix [57].

The amino (N)-terminal tails of histone proteins are not part of the histone core fold, but extrude from the nucleosome [56]. They can be subjected to a variety of posttranslational modifications, including phosphorylation, acetylation, methylation, ubiquitination and sumoylation**.** These modifications regulate the tightness of DNA/nucleosome interaction but also the interaction between the nucleosome and proteins and can thus influence chromatin composition and structure [58, 59].

An extensively studied example of posttranslational histone tail modification is the phosphorylation of serine10 on histone H3 (H3S10). Across many species

H3S10 gets phosphorylated during mitosis. To a much smaller extent H3S10 phosphorylation is also observed in interphase [59, 60].
H3S10 can be phosphorylated by multiple kinases. In the fungus *Aspergillus nidulans* the NIMA kinase was shown to phosphorylate H3S10 [61]. In mammalian cells the NIMA orthologue Nercc1/Nek9 [62] as well as the vaccinia-related kinase 1 (VRK1) can also phosphorylate H3S10 [63]. Most importantly however, the Aurora B kinase and its orthologues have been found to contribute significantly to mitotic H3S10 phosphorylation among a wide rage of species [64-66]. H3S10 gets dephosphorylated when cells exit mitosis. In S. *cerevisiae* and *C. elegans* the responsible phosphatase is $PP1^{Glc7}$ [64].
The function of this posttranslational histone modification is not well understood. In mammalian cells and *D. melanogaster* histone H3 phosphorylation has been correlated with mitotic chromosome condensation [65, 67-69]. In *Tetrahymena* mutation of the H3S10 to alanine (H3S10A) leads to defects in mitotic chromosome condensation and chromosome segregation [70, 71]. In *D. melanogaster* elevated levels of H3S10 phosphorylation have also been observed at activated loci during a heat shock [72]. Thus H3S10 phosphorylation is paradoxically associated with the highly condensed mitotic chromatin and with transcriptional active open chromatin [67]. Clearly the consequences of H3S10 phosphorylation are not fully understood yet and presumably depend on the context.

In order to pack the DNA into the nucleus it needs to be compacted further than the 10nm fiber. Electron-microscopic observations of isolated rat liver chromatin suggested a DNA fiber of 30nm width [73] and such fibers were also observed in starfish oocytes *in vivo* [74]. Further *in vitro* studies and modeling proposed two different models of how nucleosomes could be packed in a fiber of 30nm diameter with a density between 11-15 nucleosomes/11nm. This corresponds to a 60-fold axial compaction compared to B DNA [75].

Recent evidence however questions the physiological relevance of a 30nm fiber. Cryo-electron microscopy on mitotic chromosomes in HeLa cells did not find evidence for a 30nm folding intermediate [76]. Electron spectroscopic imaging (ESI) of interphasic chromatin in mouse embryonic fibroblasts revealed the 10nm fiber as the prevalent chromatin component that clumped into dense globules without forming 30nm intermediates [57]. These observations are in agreement with results were obtained from chromosome conformation capture based experiments, which suggested a fractal folding of an open chromatin fiber [77, 78]. Thus interphasic chromatin could fold by forming tightly packed globules of 10nm fiber, which together pack into bigger globules to finally form the interphasic chromosome territories. Whether these globules are packed randomly or always organized in the same way and how small globules are organized into bigger domains is still unclear.

2.3. Folding of mitotic chromosomes

As eukaryotic cells enter mitosis chromatin condenses, resulting in the formation of the mitotic chromosomes. Human mitotic chromosomes are axially compacted about 10’000 fold compared to the B-DNA double helix. Mitotic chromosome condensation also helps to organize the chromosomes into individual disentangled units. Both of these steps, axial compaction and disentanglement, are required to segregate chromosomes.

Electron micrographs of purified HeLa metaphase chromosomes depleted from histones showed that DNA is organized in loops of 30-90kb that are connected to a central protein scaffold structure (**Fig. 5A,B**) [79]. Early models of chromosome folding therefore assumed that chromatin gets folded by anchoring DNA loops to a rigid protein scaffold.

Mitotic chromosomes are however not rigid but show a high degree of elasticity. Isolated mitotic chromosomes from amphibians and humans can be stretched reversibly [80, 81]. Chromosome elasticity is completely lost when the chromatin is treated with micrococcal nuclease, which ultimately leads to

fragmentation of the whole chromosome. This shows that the protein scaffold is neither rigid nor continuous.

Because low DNA cutting frequencies do not lead to fragmentation of chromosomes, protein dependent intramolecular links must exist within a chromatin fiber. In amphibian chromosomes these were estimated to occur about every 15kb [82]. Digestion of the protein components of a chromosome using trypsin reduced the mechanical resistance, but chromosomes were still elastic [81]. This suggests that the elastic component of a chromosome is the DNA fiber itself, but the mechanical resistance of the chromosome spring is determined by how frequently intramolecular links are formed. Which proteins are responsible to generate intra-chromosomal crosslinks has not been shown, but most likely they are components of the scaffold.

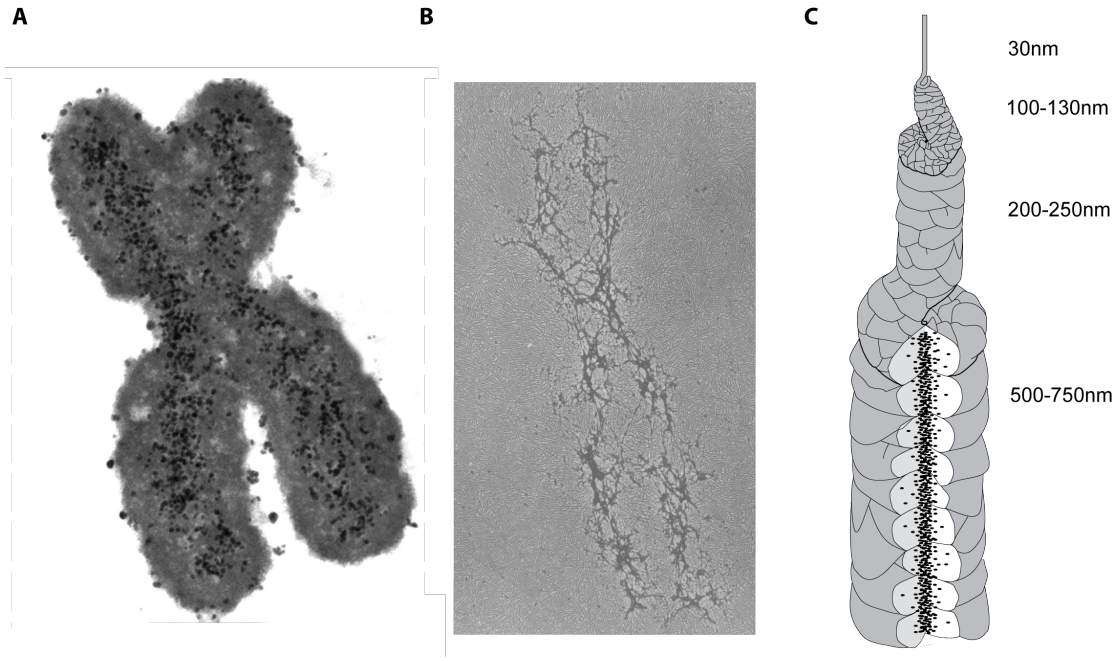

Figure 5: Folding of mitotic chromosomes.
(A) Electro micrograph of a CHO cell metaphase chromosome with immuno gold staining against the condensin subunit SMC2. Image taken from [83]. (B) The protein scaffold of a metaphase chromosome isolated from a HeLa cell after histones were depleted. The thin lines emanating from the scaffold are chromatin loops. Picture taken from [79]. (C) Hierarchical folding axial glue model of chromosome folding. Folding intermediates of the indicated thickness have all be observed in prophase of CHO cells. The black points represent components of the chromosome scaffold. Image adapted from [83].

Light microscopic analysis of chinese hamster ovary (CHO) cells in prophase revealed intermediate folding structures before mitotic chromosomes were fully assembled. The scaffold proteins were already associated with these intermediates, did however not yet form a continuous structure as observed in metaphase chromosomes [83]. This led to the proposal of a hierarchical folding model in which DNA is incorporated into fibers with increasing thickness throughout prophase to finally fold into the metaphase chromosomes. The components of the chromosome scaffold could thus act in small functional units to crosslink the DNA fiber intramolecularly. The apparent existence of a protein scaffold could be explained by accumulation of these small functional units at the center of mature mitotic chromosomes (**Fig. 5C**). How these proteins fold the chromatin and how the scaffold components themselves become assembled at the center of mature metaphase chromosomes however remains elusive.

2.4. Protein components of mitotic chromosomes

Topoisomerase II: The main non-histone components of mitotic chromosomes were identified to be topoisomerase II and structural maintenance of chromosomes (SMC) proteins, which both localize to the protein scaffold [84]. Topoisomerase II (topo II) is an ATP dependent, homodimeric enzyme that introduces transient double strand breaks into DNA and then passes a second double strand through the gap. Like this, topo II can introduce or remove DNA catenanes and supercoils from chromatin. During mitosis, topo II is needed to regulate DNA-mediated sister chromatid cohesion and chromosome condensation [84]. The identification as a component of the chromosome scaffold initially suggested a structural role of topo II for chromosome structure. This view is however challenged by the fact that its association with mitotic chromosomes is dynamic and catalytic activity of topo II is required for chromosome segregation in anaphase from yeast to humans [85-89].

SMC complexes: All structural maintenance of chromosomes (SMC) complexes contain two SMC subunits. SMC proteins contain two 50nm long coiled-coil domains, which connect the hinge region in the middle of the protein with the N- and C-termini, which together form an ATP binding head domain. SMC monomers dimerize through their hinge domains to form a V-shaped structure. The head domains also directly interact in an ATP dependent manner [90].

A variable number of non-SMC subunits are associated with the ATP binding SMC head domains. In all three eukaryotic Smc complexes a member of the kleisin family directly interacts with the head domains and is thought to regulate the head-head interaction (**Fig. 6A**). In eukaryotes there are three different subtypes of SMC complexes: Condensin, Cohesin and the Smc5-Smc6 complex [90].

Condensin: The condensin complex contains the Smc2 and Smc4 subunits. In higher eukaryotes, these SMC subunits form two distinct complexes: condensin I and condensin II. The single condensin complex found in yeast and the mitosis specific condensin I contain the kleisin subunit Brn1 (CAP-H), Ycg1 (CAP-G) and Ycs4 (CAP-D2) [90]. Condensin can bind DNA directly through its hinge region [91]. In addition the kleisin subunit can interact with Histone H2A in human cells and fission yeast [92, 93]. The condensin complex can also entrap DNA by forming a topological ring [94]. Whether condensin can bind one or two DNA strands at the same time is not clear.

In human cell lines, the condensin II complex binds chromatin throughout the cell cycle. In contrast the condensin I complex is excluded from the nucleus through interphase and only gains access to the chromosomes after nuclear envelope break down in mitosis. During anaphase, the levels of condensin I on chromosomes further increase, before it gets removed from the chromosomes in telophase [95, 96]. In budding yeast, the single condensin complex is bound to chromosomes in regular intervals of about 10kb and

stays constant from G1 to metaphase [97]. In anaphase, condensin accumulates on the *rDNA* [98, 99]. This was shown to depend on the temporary down regulation of *rDNA* transcription during anaphase by the phosphatase Cdc14 [100].

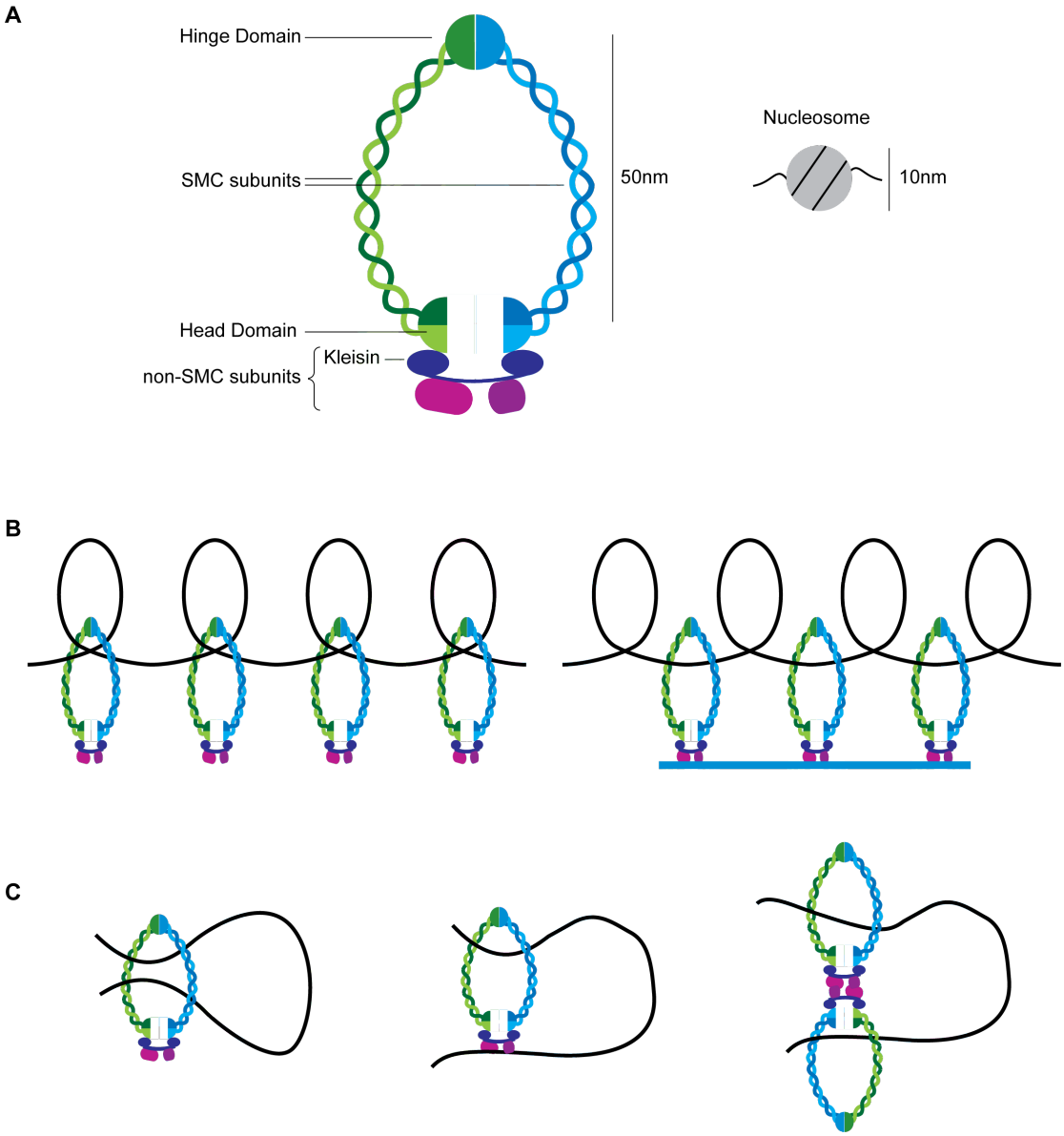

Figure 6: Condensin architecture and possible functions.
(**A**) Cartoon showing the architecture of an SMC complex. A nucleosome is shown to allow size comparison. (**B**) Condensin can stabilize supercoils by binding two strands of the chromatin fiber (black line, left) or by fixing the conformation of the chromosome (right). For this the condensin complex needs to be anchored (blue line). (**C**) DNA loops can be generated by forming intramolecular links on the chromosome. Two sites on the chromosome can be linked through binding of the same condensin complex (left and middle) or through dimerization of two condensin complexes, each bound to one DNA site (right). Figure based on [90, 101].

From yeast to vertebrates condensin is required to condense and segregate chromosomes [102-105]. In the absence of condensin, chromatin becomes less resistant to tension [96]. How condensins induce axial compaction and confer mechanical resistance to chromosomes is not clear. Purified condensin I from frog egg extract is able to axially compact threads of DNA in an ATP dependent manner *in vitro* [106]. The requirement of ATP hydrolysis suggests that repeated cycles of DNA binding and release are involved in the mechanism of condensin action. In human cells association of the mitosis specific condensin I complex is indeed very dynamic [96]. In conjunction with topoisomerase I, *X. laevis* condensin I is able to introduce positive supercoils into plasmid DNA [107]. One role of condensin therefore may be to stabilize supercoils generated by topoisomerase I. Different possibilities of how condensin could stabilize supercoils are shown in (**Fig. 6B**). Condensin can however also introduce axial shortening of naked DNA in the absence of topoisomerase [106], suggesting that condensin itself introduces loops into the DNA fiber. This can be achieved by linking two DNA strands of the same chromatid (**Fig. 6C**). Condensins could in fact mediate the regular intramolecular links in mitotic chromosomes that were suggested by chromosome micromanipulation studies (**Fig. 6B**) [108]. Whether condensin crosslinks DNA strands at all and how ATP driven cycles of condensin binding and release are translated into mechanical movement is however still not known.

During mitosis, condensins get heavily phosphorylated. Purified condensin complexes from frog egg extract were only active when phosphorylated by Cdc2/Cdk [109]. Cdk activity however drops during anaphase when the highest levels of chromosome compaction are reached [110].

More recently in budding yeast it could be demonstrated that phosphorylation of condensin by polo like kinase is sufficient to activate condensin *in vitro* and is required for viability *in vivo* [111]. As polo kinase does not get inactivated until late anaphase [33]**,** this could explain the apparent paradox of increasing condensation levels with decreasing levels of Cdk activity in anaphase.

In yeast and human cells, several subunits of the condensin complex are phosphorylated by the orthologues of the Aurora B kinase *[92, 93, 111, 112]*. Orthologues of the Aurora B kinase have been shown to regulate condensin loading in mitosis in human cells [93, 113], *D. melanogaster* [65], *C. elegans* [114] and *S. pombe* [92, 93, 115]. In budding yeast, condensin accumulation at the *rDNA* locus in anaphase requires Cdc14 activity and inhibition of *rDNA* transcription [100, 116]. Whether Ipl1 is also required for condensin loading in budding yeast is not clear.

Cohesin: The cohesin complex contains the Smc1 and Smc3 proteins, the kleisin subunit Scc1 (Rad21) and Scc3, and forms a circle that can topologically entrap DNA [117, 118].

In budding yeast, cohesin is loaded onto chromosomes during G1 phase. This requires the activity of Scc2 and Scc4 [119]. Cohesin is required for the establishment of sister chromatid cohesion [120], which occurs during S-phase immediately after duplication of the DNA strand [121]. It is proposed that cohesin establishes cohesion by encircling the two replicated sister chromatids, a theory known as the ring model [122]**.**

Stable establishment of cohesion also requires acetylation of the Smc3 head domain by the replication fork associated protein Eco1 [123, 124]. This promotes the dissociation of Wpl1, which counteracts sister chromatid cohesion [125-127]. As Eco1 is only active in S-phase, this mechanism restricts cohesion establishment to the time of chromosome replication [122].

In mammalian cells most cohesin is removed from chromosome arms during prophase [128]. This prophase pathway requires activity of Aurora B kinase and polo like kinase Plk1 [129-131]. Cohesin complexes around the centromere are stabilized until anaphase onset in a process that requires the shugoshin protein Sgo1, which acts antagonistically to polo kinase [132-134]. At anaphase onset the cysteine-protease separase cleaves Scc1. This opens up the cohesin ring and promotes dissociation of cohesin form the chromosomes and thus loss of sister chromatid cohesion [135].

Smc5-Smc6 complex: The Smc5 and Smc6 proteins also form a complex with a number of non Smc proteins. In yeast six interacting proteins have been identified (Nse1-6). Like in cohesin and condensin, a kleisin (Nse4) connects the head domains of Smc5 and Smc6. Another important subunit is the SUMO ligase Nse2, which shows SUMO ligase activity towards Smc5 but also towards components of the cohesin complex [136].

The role of Smc5-Smc6 complex is less understood. It plays a crucial role in the repair of DNA double strand breaks through homologous recombination [136]. The segregation of repetitive chromosomal regions like the rDNA is impaired in the absence of Smc5-Smc6 function due to DNA dependent linkages between sister chromatids [137]. Interestingly, chromatin immuno precipitation of Smc6 showed that the complex is loaded more densely on long than on short chromosomes [138]. Whether the Smc5-Smc6 complex plays a role in shaping mitotic chromosomes is however not clear.

3. Chromosome segregation and mitotic exit: basic mechanism and regulation

3.1. The spindle assembly checkpoint delays anaphase onset until all chromosomes are bipolarly attached to the mitotic spindle

In order to equally partition chromosomes, the two sister-kinetochores of a chromosome need to get attached to microtubules emanating from opposite sides of the mitotic spindle. Such a bipolar attachment is called amphitelic and creates tension between the kinetochores. Tension directly stabilizes the kinetochore-microtubule interaction on purified yeast kinetochores [139]. In addition, kinetochore-microtubule interactions that are not under tension are destabilized through a mechanism that requires the activity of the mitotic kinase Aurora B or its yeast homologue Ipl1 [140, 141]. This creates unattached kinetochores, which are detected by the spindle assembly

checkpoint (SAC). The SAC is able to delay cell cycle progression until all kinetochores are attached to the mitotic spindle [142].

Once all chromosomes are amphytelic attached, no more free kinetochores are generated and the spindle assembly checkpoint is satisfied. This leads to de-repression of Cdc20, which binds and activates the anaphase promoting complex APC/C, a cullin based ubiquitin ligase [143, 144]. Activated APC/C^{Cdc20} ubiquitinates mitotic cyclins (CyclinB) and securin and targets it for degradation by the proteasome [145-147]**.** Securin degradation is required to activate the cysteine protease separase [148, 149].

3.2. Initiation of anaphase and Cdc14 activation in S. cerevisiae

Separase, Esp1 in budding yeast, cleaves the cohesin subunit Scc1 at two specific sites at anaphase onset. This is sufficient to remove cohesin from chromosomes in yeast [135] and in *D. melanogaster* embryos [150]. Cleavage of cohesin is however not sufficient for complete chromosome segregation. In *D. melanogaster* syncytial embryos active topoisomerase II needs to be present to allow complete chromosome separation [150]. In budding yeast full chromosome segregation requires the activation of Cdc14 [98, 99, 151, 152], which allows the accumulation of condensin in the *rDNA* by down-regulating RNA polymerase I transcription in anaphase [100].

Cdc14 is an essential phosphatase, which antagonizes Cdk activity as cells exit mitosis [153]. Throughout most of the cell cycle Cdc14 is sequestered and kept inactive in the nucleolus through binding to Net1. Phosphorylation of Net1 by Cdc28 (Cdk) and Cdc5 (polo kinase) promotes Cdc14 release from the nucleolus. Net1 phosphorylation is counteracted by the phosphatase $PP2A^{Cdc55}$. Separase activation at anaphase onset leads to inhibition of $PP2A^{Cdc55}$ and results in transient release of Cdc14 from the nucleolus. This genetic pathway is termed FEAR (Fourteen Early Anaphase Release). In addition to separase the proteins Slk19, Spo12 and Bns1 also play important, yet not fully understood, roles in the early Cdc14 activation (**Fig. 7**) [154-156].

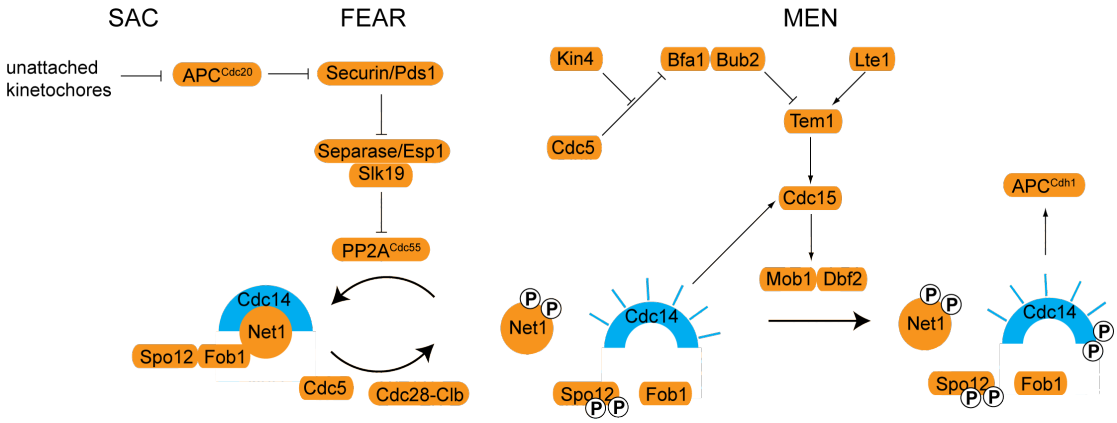

Figure 7: Regulation of mitotic exit in *S. cerevisiae*.
Activation of the Cdc14 phosphatase after satisfaction of the spindle assembly checkpoint (SAC) occurs in two waves. Destruction of securin/Pds1 at the onset of anaphase induces the transient release of Cdc14 from the nucleolus at anaphase onset through the FEAR (Fourteen Early Anaphase Release) pathway. The MEN (Mitotic Exit Network) can be activated after one spindle pole has entered the bud. The small GTPase Tem1 then induces a sustained release of Cdc14 from the nucleus to the cytoplasm. Figure adapted from [156].

A second pathway termed mitotic exit network (MEN) is activated later in anaphase and leads to full Cdc14 activation. A central component of the MEN is the small GTPase Tem1, which is located on the spindle pole body. Tem1 activates a cascade of the downstream kinases Cdc15 and Mob1-Dbf2. Phosphorylation of Cdc14 adjacent to a nuclear localization signal (NLS) by Mob1-Dbf2 allows the release of Cdc14 form to the cytoplasm [157].

Tem1 is negatively regulated by its GAP complex Bub2-Bfa1. Bub2-Bfa1 GAP activity is suppressed by Bfa1 phosphorylation through Cdc5. The mother cell specific kinase Kin4 also phosphorylates Bfa1. This modification activates Bfa1-Bub2 and renders it insensitive to Cdc5 dependent inhibition. As the localization of Kin4 is restricted to the mother cell, polo dependent inhibition of Bfa1-Bub2 becomes relevant as soon as one spindle pole enters the daughter cell. And thus cells delay activation of Tem1 and hence mitotic exit until one spindle pole body has entered the bud, ensuring proper alignment of the mitotic spindle along the polarity axis. This spatial regulation of MEN

activation is referred to as spindle position checkpoint (SPOC) (**Fig. 7**) [158]. Fully active Cdc14 promotes exit from mitosis by dephosphorylating Cdk-substrates and by activating the APC adaptor protein Cdh1. APC^{Cdh1} accelerates the degradation of mitotic cyclins and is responsible for the degradation of the polo kinase Cdc5. Degradation of Cdc5 is essential to inactivate Cdc14 and re-sequester it in the nucleolus at the end of mitosis [159].

Activation of Cdc14 promotes chromosome segregation in anaphase through several mechanisms. First, Cdc14 directly regulates the anaphase spindle. Upon anaphase onset the interpolar microtubules get stabilized in a Cdc14 dependent manner [160]. This correlates with a role of Cdc14 in the maturation of the anaphase spindle, during which a set of proteins concentrates in the region of overlapping interpolar microtubules to form a functional spindle midzone. These proteins include the microtubule bundling protein Ase1, spindle stabilizing protein Fin1, the separase Esp1 and its interaction partner Slk19, as well as the chromosomal passenger complex (CPC) [160-164].
Activation of Cdc14 is also required to disengage the SAC during anaphase by stabilizing microtubule-kinetochore interactions, which are no longer under tension after sister chromatid cohesion has been lost. This requires dephosphorylation of Sli15 by Cdc14, which leads to the removal of the CPC form the kinetochores and thus prevents the destabilizing activity of Ipl1 on microtubule-kinetochore interactions in anaphase [161, 165].

3.3. Segregation of chromosome arms in anaphase

Ectopic cleavage of cohesin in metaphase is not sufficient to segregate repetitive regions like the *rDNA* in budding yeast [151] and in drosophila embryos active topoisomerase is required to fully separate sister chromatids after cohesin cleavage [150]. Thus cohesin independent linkages exist during

anaphase. In budding yeast complete *rDNA* segregation requires activation of Cdc14 and condensin function, which accumulates at the *rDNA* in anaphase [98, 99, 102, 151, 152].

A topological consequence of DNA replication is the formation of DNA intertwines or catenanes, which can be removed by topoisomerase II (topo II). Indeed topo II activity is required for chromosome arm segregation from yeast to human cells [85-89]. Interestingly the *rDNA* separation defects observed in condensin mutants can be overcome by over expression of a small viral topo II but not by over expression of endogenous topo II [166]. This suggests that the observed linkages in condensin mutants are DNA mediated and that the endogenous yeast topoisomerase II activity depends on condensin function. Indeed a recent study showed that catenated plasmids were a better substrate for topoisomerase II when they were positively supercoiled by condensin [167]. Thin threads of unresolved DNA in anaphase have also been observed in human cell lines and their resolution also depends on topo II [89]. Thus DNA catenanes are still present in anaphase and can be removed by the combined action of condensin and topoisomerase II.

In yeast the bud directed sister chromatid arms get extensively stretched during anaphase. By measuring the distance between fluorescently labeled loci in live cells, the DNA density can drop from 225kb/µm in metaphase to as low as 30-40kb/µm in anaphase [168]. This is less than a fourth of the density of a putative 30nm fiber (160-190kb/µm, [169]) and corresponds to a only 10-fold compaction compared to a B-DNA double helix (3kb/µm).

Centromere proximal regions are stretched during several minutes directly after anaphase onset. Rapid recoiling then induces transient stretching of the adjacent chromatin region. Like this stretching and recoiling is propagated along the whole chromosome arm until the chromosome is fully segregated. In condensin mutants, recoiling is not observed or strongly delayed and happens at a slower velocity than in wild type cells [168]. Thus condensins are required to axially compact chromosomes arms during anaphase (**Fig. 8**).

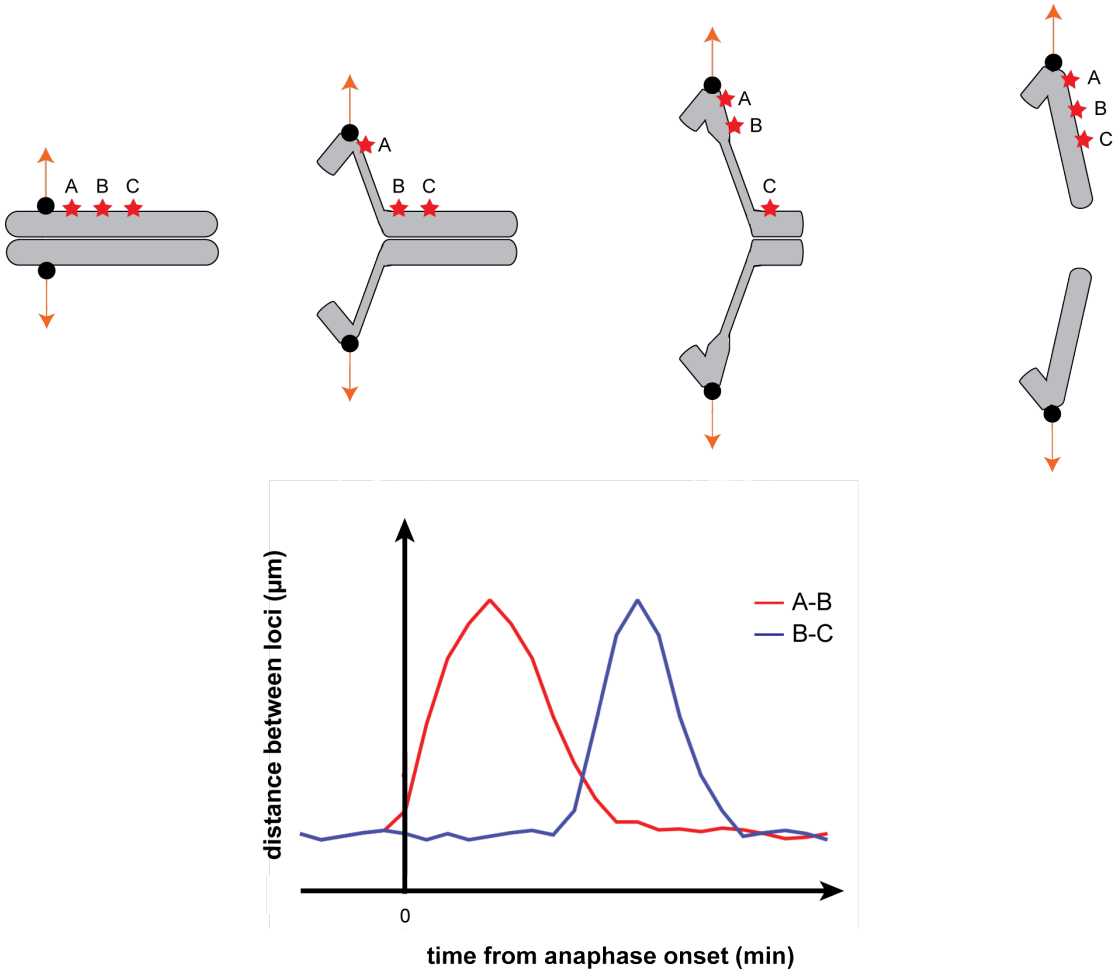

Figure 8: Stretching and recoiling of chromosome arms during anaphase.
(Top) Forces generated by the mitotic spindle (orange arrow) pull the chromosomes on the centromeres (black circles) towards opposite poles. The red stars indicate the position of three hypothetical loci A, B and C. In budding yeast centromere-proximal chromatin (A to B) gets stretched in early anaphase. Subsequent recoiling induces stretching of the adjacent region (B to C). Like this stretching and recoiling is propagated along the entire chromosome arm until the chromosome is fully segregated. (Bottom) The graph shows the hypothetical distance from the loci A to B (A-B) and B to C (B-C) during anaphase as they have been observed in [168].

The anaphase stretching of chromosome arms depends on mechanical linkages between chromosome arms, as no stretching is observed when chromosome replication is prevented [170]. Inactivation of cohesin during anaphase or deletion of shugoshin Sgo1 also reduces the extent of chromosome arm stretching, showing that the mechanical linkages at least in part depend on cohesin [168, 170]. This is in agreement with the observation that the protease activity of separase is still required for timely chromosome

arm segregation during anaphase [168]. Thus both cohesin dependent and independent linkages between sister chromatids are still present in anaphase. As we have seen, how cells delay cohesin removal until all chromosomes are correctly attached to the mitotic spindle is well understood. Also the mechanisms of cohesin removal in prophase and at the metaphase to anaphase transition have been extensively studied. In contrast, much less is known about how cells deal with chromosome segregation errors that become apparent during anaphase. Several studies in yeast and mammalian cells have shown that sister chromatid resolution is not completed at anaphase onset, but that inter-chromatid linkages are still present [89, 98, 151]. Whether and how cells are able to detect incompletely segregated chromosome arms and how they respond to them is still not known.

3.4. Is chromosome size coordinated with spindle length?

In addition to removal of all sister chromatid linkages, chromosome arm segregation can only be completed if the mitotic spindle elongates to at least twice the length of the longest chromosome arm (**Fig. 9**) [171]. Measurements based on fluorescence in situ hybridization (FISH) on yeast metaphase chromosomes estimate a chromatin density in the range of 400kb/µm [172]. More recent studies in non-arrested living cells estimate a metaphase compaction of chromatin density of 225kb/µm [168]. If the chromosomes were compacted to the same level before and after chromosome arm stretching in anaphase, the segregation of the longest chromosome arm (right arm of chromosome XII, 2020kb) would require a mitotic spindle of 10µm or 18µm respectively. A typical mitotic spindle of haploid yeast elongates to maximally 7-9µm [32], in principle too short to segregate the longest chromosome arm. Indeed it was observed that the *rDNA* locus on chromosome XII undergoes a compaction step during anaphase: during metaphase the *rDNA* forms a long loop, which gets extended into threads spanning the whole spindle in early anaphase. In late anaphase these threads segregate without additionally

elongating their spindles by axially compacting the chromatids [173]. Also in human cell lines chromosome arms were shown to shorten during anaphase [110]. This shows that chromosome condensation is not an all or nothing process but rather continuous and it raises the question of how cells ensure that chromosome condensation is sufficient to segregate the longest chromosome arm.

In principle spindle length and the physical length of chromosomes in anaphase could have been adjusted by co-evolution of the two structures. The length of a fully elongated anaphase spindle is however not constant but varies substantially within a population and even more between populations under different environmental conditions. Thus yeast cells need to segregate the same set of chromosomes with spindles ranging from 6-12µm (**Fig. 25A**). Spindle size variability is even bigger during development of multicellular organisms as the size of the elongated anaphase spindle scales with the size of the cell. In the *C. elegans* embryo maximal anaphase spindle extension varies between 5-60µm [174] and a large decrease in spindle size is also observed during the early development of *X. laevis* [175]. We wondered how cells deal with such variability and whether they possess mechanisms to coordinate chromosome arm length with spindle size.

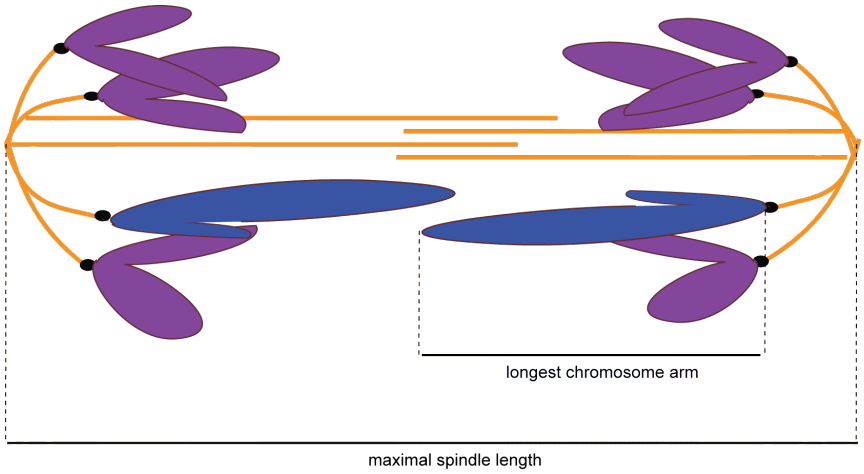

Figure 9: Chromosome size and spindle length must scale.
Scheme illustrating that the mitotic spindle must elongate to at least 2x the size of the longest chromosome arm.

II. Objectives

In order to segregate all chromosomes, the mitotic spindle needs to elongate to at least twice the length of the longest chromosome arm. Maximal spindle extension is however variable as it scales with cell size. We thus wondered whether cells are able to coordinate the size of the chromosomes with the size of the mitotic spindle.

The objectives of the work presented here were to determine:

1) How do cells react to the presence of a highly oversized chromosome

2) What factors are required for a putative adaptive response

3) How can cells spatially regulate chromosome segregation with spindle size

III. Materials and Methods

1. Cell Growth and synchronization

1.1. Growth media

Yeast cells were normally grown on rich YP medium ((1% Yeast Extract (Becton Dickinson, #212720), 2% BactoPeptone (Becton Dickinson, # 211820)), supplemented with 2% sugar (Glucose (Sigma-Aldrich, #G7528), Galactose (Sigma-Aldrich, #48260) or Sucrose (Sigma-Aldrich, #S0389)). Rich medium was supplemented with 0.004% adenine (Sigma-Aldrich, #A9126).

For antibiotic selection rich medium was supplemented with one of the following compounds: 100mg/L nourseothricin (ClonNAT, Werner Bioagents, 51000), 200mg/L Geneticin (G418, Invitrogen, 11811023), 300mg/L hygromycin B (Nucliber, ant-hm-1) or 40mg/L phleomycin (Nucliber, ANT-PH-1)

For selection of auxotrophic markers cells were grown on synthetic minimal medium, lacking the amino acid of choice. Complete synthetic minimal medium was composed of 0.67% Yeast Nitrogen Base w/o ammonium sulfate (Becton Dickinson, #291920), 0.004% adenine (Sigma-Aldrich, #A9126), 0.002% uracil (Sigma-Aldrich, #U0750), 0.002% tryptophan (Sigma-Aldrich, #T0254), 0.002% histidine (Sigma-Aldrich, #53319), 0.003% lysine (Sigma-Aldrich, #62840), 0.003% leucine (Sigma-Aldrich, #61820) and 0.002% methionine (Sigma-Aldrich, #M9625).

Solid medium contained 2% agar (Becton Dickinson, # 214510). Agar, Peptone and yeast extract were mixed with water and autoclaved, all other components were filter sterilized.

To induce sporulation of diploid yeast, cells were inoculated in minimal sporulation medium (1% potassium acetate (Sigma-Aldrich, #P1190)) supplemented with 0.002% of each of the 5 amino acid added to synthetic minimal medium.

To stock strains, cells were scraped directly from 2-3 day old rich solid medium and resuspended in 30% glycerol/70% liquid rich medium. Stocks were kept at -80 °C.

1.2. Cell Growth analysis

For spotting assays, cells were grown on liquid rich medium to exponential phase ($0.4 \leq OD_{600} \leq 0.6$). Serial dilutions were carried out from a stock solution of $OD_{600}=0.01$ (ca. $1.7 \bullet 10^5$ cells/ml) in rich medium. 10µl of each dilution were spotted on rich plates, which were inoculated at the indicated temperatures and growth was scored after 48h and 72h.

1.3. Cell synchronization

For synchronization ion G1, cells were arrested in 10µg/ml α-factor for 2h at room temperature (1mg/ml stock in methanol stored at -20 °C, α-factor was purified by the in house proteomics facility). To release cells from the α-factor arrest, cells were washed three times with rich medium.

For synchronization in metaphase by Cdc20 depletion (Fig. 21E) the endogenous CDC20 promoter was replaced by *pMET3.* To arrest in metaphase, exponentially growing cells were transferred to rich medium containing 0.02% (10x) methionine for 3 hours. Cdc20 expression and anaphase was induced by washing the cells with minimal synthetic medium lacking methionine.

2. Yeast strains

2.1. Strain background

Saccharomyces cerevisiae strains are derivatives of S288c background. The *ipl1-321* allele was derived from W303 background. The strains carrying the TetO and LacI arrays on chromosome IV were derived from a previously described strain [176] of a BF264-15 15D background [177]. All haploid strains carrying the TetO and LacI arrays (derived from YMM409) used in this study have genomic contributions corresponding to 1/2 S288c, 1/4 W303 and 1/4 BF264-15D, with the exception of the *cdc5-1* (60% S888c, 20%W303, 20% BF264-15D, Fig. 17) and *smc2-8* (30% S888c, 60%W303, 10% BF264-15D, Fig. 18) mutants. As compound chromosomes were generated by transformation, they are always isogenic to the corresponding mutant strain with normal karyotype, except for the subtelomeric genes that were lost during chromosome fusion.

All diploid cells were obtained form crosses between strains derived from YMM409 and pure S288c background.

2.2. Yeast crosses

1.2.1. Isolation of diploid cells

Haploid yeast cells of opposite mating type were mixed on YPD plates. 6-8h after mating zygotes were isolated using a dissection microscope (axioskop 40, Zeiss). The diploid state of cells was confirmed by 1) morphologic analysis: diploid cells are bigger and more elongated than haploids, 2) absence of a mating response and 3) the ability to sporulate.

1.2.2. Sporulation and tetrad dissection

Diploid cells grown for 1 day on YPD plates were inoculated in minimal sporulation medium. After 3 days tetrads were digested with 0.05mg/ml Zymolyase 100T (Seikagaku Biobusiness, #120493) at room temperature for

5 minutes. Digested tetrads were plated on YPD plates and dissected using a dissection microscope (axioskop 40, Zeiss). Spores of the relevant genotype were selected based on growth on selective media.

2.3. Strain generation and plasmids

2.3.1. Yeast Transformation

DNA insertion, gene deletions and gene fusions were generated by transformation of PCR products or linearized plasmids essentially as described in [178]: Yeast cells were inoculated over night in liquid medium and diluted to an optical density of OD_{600}=0.1 in 10ml rich medium in the morning. Cells were harvested when the cultures reached an optical density of OD_{600}=0.6 by centrifugation at 400g for 5min at room temperature in a 15ml tube. Cells were washed in 1ml transformation buffer (100mM Li acetate, 10mM Tris, 1mM EDTA, pH 8) and resuspended in 72µl transformation buffer. 8µl of freshly denatured, chilled salmon sperm DNA (10mg/ml salmon sperm DNA (Sigma-Aldrich, #D1626); 10min denatured at 95 °C, cooled on ice) were added to the cells. 1-10µl of PCR product or plasmid were added to the cells, followed by 500µl of PEG buffer (as transformation buffer, but containing 40% PEG-3350 (Sigma-Aldrich, #P4338) and incubated on a rotating wheel for 30min. After addition of 65µl of DMSO (Sigma-Aldrich, #D2650) cells were heat-shocked for 15min at 42 °C. Cells were harvested by centrifugation at 400g for 2min, resuspended in 100*µ*l medium and plated. Selection for auxotrophic markers was carried out directly on synthetic minimal medium lacking the amino acid of choice. For selection of antibiotic resistances, cells were first plated on rich medium and replicated onto plates containing the antibiotic after 1-2 days. Genomic DNA of transformants was isolated for analysis by PCR essentially as described in [179].

2.3.2. Generation of chromosome fusions

To fuse chromosomes IV and XII, haploid *pGAL1-CEN4* cells were grown on rich sucrose based medium and transformed with a PCR fragment encoding the *natNT2* cassette [178] flanked by sequences with homology to chromosomal coordinates 1058973-1059025 on chr XII and 1516925-1517001 on chr IV (for primer sequences see **Table 1**). Recombinants were grown on galactose plates for 2-3 days and subsequently replicated onto galactose plates supplemented with nourseothricin. Positive clones were confirmed by PCR and growth defects on glucose media, presumably as a consequence of dicentric formation on (Fig. 10). Chromosome fusion was also confirmed by pulsed field gel electrophoresis (PFGE). Agarose inserts were prepared as described in [180]. The chromosomes were run in a 0.8% Agarose in 0.5x TBE gel. The gel was run on a BioRad CHEF (Clamped Homogenous Electric Field) Mapper system for 48h, with the auto-algorithm set to separate fragments from 1-2.5Mb.

Table 1 – Primers used for chromosome fusion

Product	Forward primer	Reverse primer
1 pGAL:CEN4	GGTAATGAAATGAGATGATACTTGCTTAT CTCATAGTTAACTGGCATAAAGAATTCGA GCTCGTTTAAAC	GGTTTTATCGTCACAGTTTTACAGTAAATAAG TATCACCTCTTAGAGTTACATTTTGAGATCCG GGTTTT
2 XII:IV fusion	GCTTTATCATTAACGGACGAAGAAAGAAT GTGTATCGCGTATTTTTAGACTATCGCGT ACGCTGCAGGTCGAC	GCTATGGTAAGCGTAAGAGAGTTTTGTCTTTA TACTGCTGTACATTATATGAGGTTTTGTTAAAT TGACTCATAATAATCGATGAATTCGAGCTCG
3 cen4Δ	ACATTCTTATAAAAAAGAAAAAAATTACTG CAAAACAGTACTAGCTTTTAACTTGTATCC ATCTGTTTAGCTTGCCTCGTC	TTTACTCGACTTCAGGTAATGAAATGAGATGA TACTTGCTTATCTCATAGTTAACTGGCATAAAT CGATGAATTCGAGCTCGTT
4 cen12Δ	ATTAAGCAATTGAACAAAATAACGTTCGTT TTAAGTTTTGTGGTTATTTTCAAGTTTCTG ATCTGTTTAGCTTGCCTCGTC	TTTTGTTTACCAGCGAATGCTCTTATTTATCTT CTGCGCCTTTCCAATAATCTAATTATCTCGAT GAATTCGAGCTCGTT
Check A	ATGCCAATTTCTTTCCCACC	GCAGATCCAAATATGTAGAACC
Check B	ATGCCAATTTCTTTCCCACC	GCTTAAAGGTAGCGTATAGTAAGG
Check C	ATAGTGGTTGACATGCTGGCTAGT	TACTCCAGGTACAGTCCTCTAGGT
Check D	GCAATTGAACAAAATAACGTTCG	AAGCGTAGTCCATAGGTACGATCA

2.3.3. Mutagenesis of histone H3 and SLI15

To generate histone H3 mutants, *HHT1* and *HHT2* loci (including 5' and 3' UTR) were PCR amplified with mutagenic primers to introduce the S10A mutations, and cloned by gap repair into pRS316-derived vectors [181]. Replacement of the endogenous copies of *HHT1* and *HHT2* was obtained by successive transformations with a restriction fragment spanning the mutant allele and a selection marker (details available upon request). Positive clones were confirmed by sequencing.

Endogenous *SLI15* was mutated to *SLI15-6A* (mutations: 6A: S335A, S427A, S437A, S448A, S462A and T474A) by transformation [178] of plasmid pMM34 digested with XbaI (Fermentas, #ER0681). Correct gene replacement was confirmed by digestion of a SLI15 PCR product (Primers: OMM184 and OMM249) with PauI (Fermentas, ER1091), which only cuts the *SLI15-6A*, but not *SLI15*. In addition the strains were confirmed by sequencing of the SLI15 locus. Diploid strains heterozygous for *SLI15/SLI15-6A* were generated by mating of *SLI15* and *SLI15-6A* cells and subsequent clonal isolation of diploids. Heterozygosity of the diploids was confirmed by digestion of a SLI15 PCR product with PauI. The *SLI15-6A* plasmid was a gift from Frank Uhlmann (London Research Institute, London).

2.3.4. Promoter replacement at the CDC20 locus

To replace the endogenous promoter of Cdc20 with *pMET3*, cells were transformed with MscI digested pMM179. Transformants were selected on synthetic minimal medium lacking both methionine (to allow *CDC20* expression) and leucine (to select for positive transformants). Positive clones were confirmed by the accumulation of large budded cells after 5 hours of growth on rich plates supplemented with extra methionine (500µl of 0.2% methionine stock solution soaked into the plate surface). *pMET3:CDC20* cells were stocked in minimal synthetic medium lacking methionine/30% glycerol.

The plasmid for CDC20 promoter exchange was a gift from Ethel Queralt (Bellvitge Institute of Biomedical Research, Barcelona).

2.3.5. Origin of further plasmids and mutants

Template plasmids for PCR mediated deletions and fusion protein generation were all from [178] except for the fluorescent proteins mCherry and tdTomato which were amplified from plasmids provided by the lab of Karsten Weiss (University of California, Berkeley). The pGal:Esp1-GFP plasmid, was a gift from Steven Reed (The Scripps Research Institute, California) [163].
Temperature sensitive mutant alleles were crossed into the used strains. The *smc2-8* strain was provided by Luis Aragon (Imperial College, London). The mutant alleles of *ipl1-321, cdc15-1* and *cdc5-1* were provided by Yves Barral (ETH Zurich, Switzerland).

3. Genome analysis of strains carrying the compound chromosome

3.1. Sequencing and de-novo assembly of the whole yeast genome

Whole genome sequencing was performed at the CRG Ultra-sequencing facility. Sequences of 40 bp, paired-end reads, with an average insert size of 320 bp, were obtained using an Illumina GAIIx sequencer, and preprocessed with the SCS 2.5 software. Genome assembly was performed with the AMOS package [182], using as a reference the S288c sequence downloaded from SGD [183]. A minimum region of overlap of 16 nucleotides and a maximum of two mismatches were required to assemble two reads. The final coverage obtained was 50x and 38x for chromosomes IV and XII in the wild type strain and the mutant compound chromosome, respectively. Blast searches [184] (99% identity cut-off) from the reference genome sequence were used to identify the location of genes encoded in the assembled chromosomes.

Chromosome alignments and dot-plots were generated as described [185], with the Perl scripts provided within that project and using a windows size of 20 and a word size of 100. Custom Python scripts were used to facilitate the automation of the Blast searches and the filtering of low-quality reads.

3.2. Analysis of rDNA copy number by qPCR

Quantitative real-time PCR analysis was performed on genomic DNA isolated from log phase cultures by Phenol:Chloroform:Isoamyl alcohol (Sigma-Aldrich, #P2069) extraction, and treated with RNase as described [186]. Primers were designed to amplify a 160 bp fragment on the ITS2 element in *RDN1* (5'-TCGCCTAGACGCTCTCTTC-3' and 5'-GCCTTTTCATTGGATGTT-3') and a 188 bp fragment on *SLI15* (5'- AGGCTCTACCCGTTCAATCA-3' and 5'-TATGCGTATTTTCGGGGCTA-3'). For each qRT-PCR reaction (10µl), 0.1 ng of genomic DNA was added into a PCR master mix containing 0.4 µM of each primer and 1× of SYBR Green I Master (Roche). qRT-PCR reactions were performed in 384-well plates on a LightCycler 480 system (Roche) using the following program: 1) 95°/10min; 2) 45x 95°/15s, 60°/15s, 72°/10s. Primer efficiency for both primer pairs was determined as described [187] using the slope from the LightCycler software (E_{rDNA}=1.814; E_{SLI15}=1.868) from dilution series (1-0.01ng/reaction). Cp values were calculated with the same software. Copy number of *rDNA* repeats was calculated relative to the single copy gene *SLI15* using the following formula:

$$\frac{[rDNA]}{[SLI15]} = \frac{E_{SLI15}{}^{Cp_{SLI15}}}{E_{rDNA}{}^{Cp_{rDNA}}}$$

The [rDNA]/[SLI15] ratio was determined for three technical replicates. This was repeated in three independent experiments (biological replicates). Student t-test was performed on the results of the biological replicates.

4. Microscopy

Except where noted, time-lapse analysis of chromosome segregation was performed on cells synchronized with alpha-factor (10 mg ml^{-1}; Sigma) for 2h, released in fresh YPD medium for 1 hour at 25 ºC, and placed in a pre-equilibrated temperature-controlled microscope chamber 15 min prior to imaging.

Cells were plated in minimal synthetic medium lacking tryptophan in 8 well Lab-Tek chambers (Nunc). Prior to plating, chambers were coated with concanavalin A (Sigma-Aldrich, #C7275) by incubation of 250µl of an 1mg/ml (in PBS) solution for 20min. Before use, the chambers were washed 3x with 0.75ml minimal synthetic medium. Except for figures 16, 19 and 23, where cells were placed on minimal synthetic medium agar pads.

Imaging was performed using an Andor Revolution XD spinning disc confocal microscope equipped with an Andor Ixon 897E Dual Mode EM-CCD camera, except for figures 16, 19 and 23, where cells were imaged using an Olympus IX8 wide-field fluorescent microscope with a Hamamatsu Orca ER camera (Fig. 19) or an applied Precision DeltaVision wide-field fluorescent microscope with a Roper CoolSnap HQ2 camera (Fig. 16 and 23). Time-lapse series of 4-5 µm stacks spaced 0.5-0.68 µm were acquired every 1.5-2min.

5. Image analysis and statistics

Images were analyzed on 2D maximum projections (except Fig 23) or 3D (Fig 23) stacks using ImageJ (http://rsb.info.nih.gov/ij/) and Microsoft Excel. Distances between signals were measured between local maxima.

Nucleolar localization of Cdc14 was quantified essentially as described in [188]. Cells were outlined manually and the mean signal and standard deviation were measured for each channel and frame. The coefficient of variation (CV) was calculated by dividing the standard deviation by the mean.

The CV of Cdc14-tdTomato was finally normalized to the CV of GFP (Net1-GFP and Spc42-GFP).

Graphs and statistical analysis (*t*-test allowing for unequal variance) were performed with Prism software (GraphPad) and Excel (Microsoft). On figures, Asterisks indicate $p<0.02$ (*) or $p<0.001$ (**). To illustrate the data point distribution, measurements are represented in box-plots (i.e. Fig. 13E and others). The boxes include 50% of data points, whiskers 95%. The median is indicated by a line and the mean by a cross. The standard error of the mean on figures 19C and 23B were calculated based on the data in Fig 19B and 23A using error propagation.

6. Protein analysis

To fix cells, 1ml of liquid yeast cultures were mixed with 300µl of 85% trichloracetic acid (TCA, Sigma-Aldrich, #T6399) to a final concentration of 20%. After 10-60 minutes of fixation (RT), cells were collected by centrifugaion at 13'000g for 1min, the supernatant was discarded. Centrifugation was repeated to remove most of the supernatant. Cells fixed like this can be stored at -80 °C.

Add 100µl of 1x TCA Sample Buffer (350mM Tris, 0.1M dithiotheritol (DTT), 2% SDS, 4% Glycerol, 0.1% Bromophenolblue, pH 8.8,) and approximately 300µl of acid washed glass beads (Sigma-Aldrich, #G8772). Cells were broken by shaking for 2x45s in a FastPrep FP120 (Thermo Savant). To reduce foam, tubes were centrifuged at maximum speed for 1 minute. Samples were denatured at 95 °C for 10 minutes. To collect cell lysates, 1.5ml tubes were perforated with a hot needle and placed in a fresh 1.5ml tube for centrifugation. 20µl of this lysate were run on a 10% acrylamide gel and transferred onto a nitrocellulose membrane using a semi-dry system (BioRad).

Membranes were blocked with 5% milk in TBST (TBS with 0.05% Tween20) for 1h at room temperature (RT) or over night at 4 °C. Primary antibodies were diluted in 5% milk/TBST and incubated for 1h at RT or over night at 4 °C. The mouse-α-HA antibody (Roche, #11666606001) was used at 1/2000 dilution. The rabbit-α-Clb2 antibody (TEBU-BIO, #SC9071) was used at 1/2000 dilution. The gaot-α-Cdc5 (Santa Cruz, #sc-6733) was used at 1/2000 dilution. The goat-α-Hog1 antibody (a gift from Francesc Posas) was used at 1/7000 dilution. Primary antibodies were washed away with TBST (6 washes over the course of 30minutes).

Secondary antibodies were used all used at 1/10’000 dillution in TBST: goat-α-rabbit-Alexa680 (Invitrogen, #A21109), donkey-α-mouse-IRDye800 (Bonsai Technologies, #610732124). Secondary antibodies were incubated for 1h at room temperature. After 4x washing with TBST, the membranes were analyzed using an Odyssey LI-COR System (Biosciences).

IV. Results

1. Generation of a long compound chromosome

1.1 Fusing two chromosomes

To address how cells cope with a highly oversized chromosome, we generated an exceptionally long chromosome arm by fusing the two longest chromosomes IV and XII. Fusion was accomplished through homologous recombination of a bridging PCR fragment with the subtelomeric regions of the two chromosomes. This led to the formation of the long compound chromosome *LC(XII:IV)* (**Fig. 10A**) and to loss of the subtelomeric regions and telomeres of the right arms of chromosomes IV and XII. As a consequence of this, several subtelomeric genes were lost. Because deletion of these genes had no reported severe phenotypes, they were not further considered in this study. A list of open reading frames within the lost regions can be found in **Table 2**.

To prevent dicentric chromosome formation, the centromere *CEN4* was inactivated in galactose-containing medium by the *GAL1* promoter (*pGAL1*) [189]. Before chromosome fusion, cells with *pGAL1:CEN4* grew poorly in galactose due to chromosome IV instability. Cells carrying the fused chromosome *LC(XII:IV)pGAL1:CEN4* did not show this growth defect, consistent with it being segregated through *CEN12*. These cells showed impaired growth on glucose due to dicentric chromosome formation (**Fig. 10B)**. Subsequent deletion of *CEN4* and *CEN12* generated the stable monocentric compound chromosomes, *LC(XII:IV)cen4*Δ *and LC(XII:IV)cen12*Δ (**Fig. 10A**). Using this method, we expected chromosome arms that are 3.5 and 3.2 Mb long, representing a 75% and 60% increase in

length of the longest wild type chromosome arm (2Mb, assuming 120 *rDNA* repeats) (**Fig. 10E**).

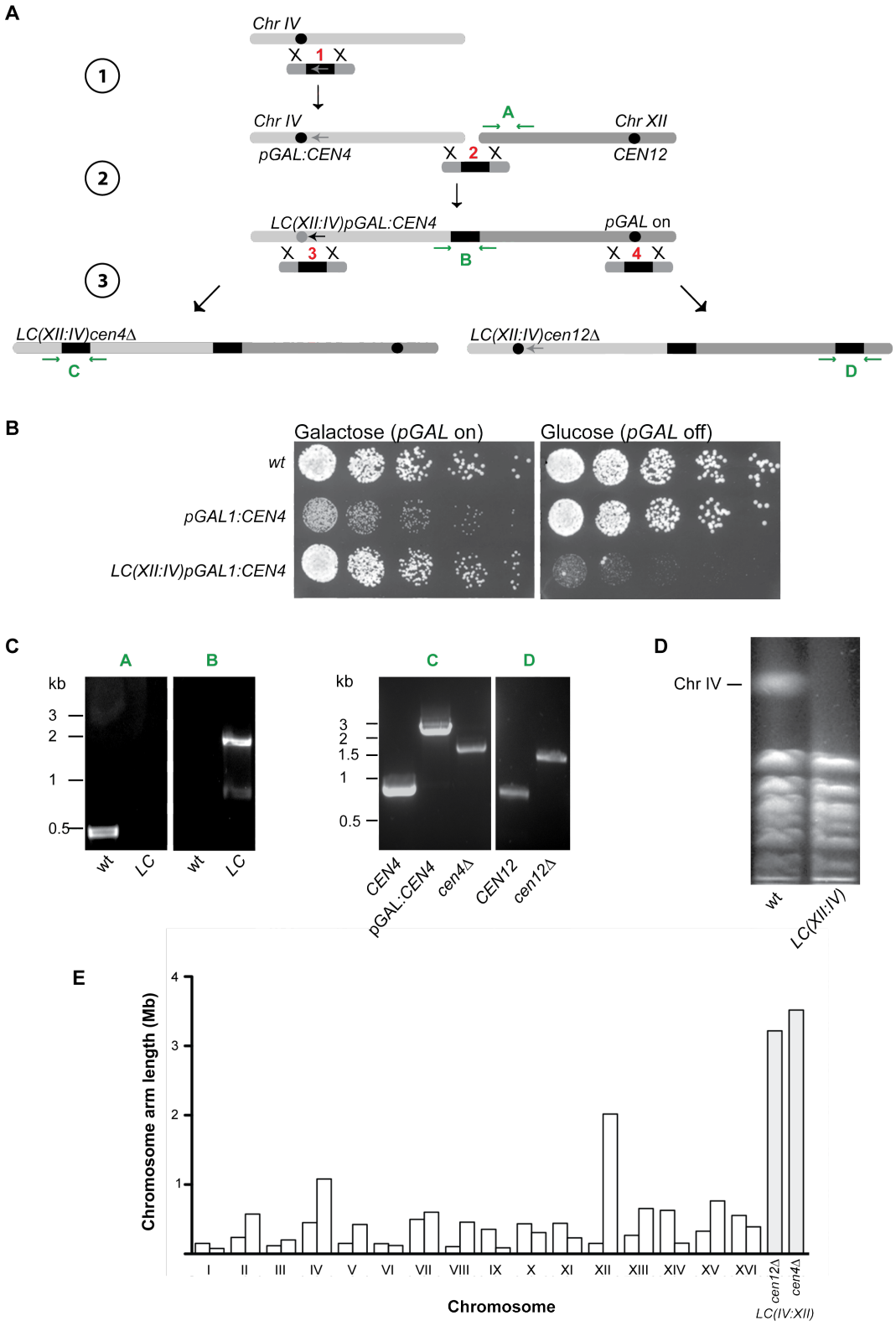

Figure 10: Generation of the long chromosome LC(XII:IV)
(**A**) Step 1: Integration of *pGAL1* upstream of *CEN4*. Step 2: Homologous recombination between a PCR-generated „bridging" fragment and chromosomes IV and XII. Step 3: Deletion of *CEN4* or *CEN12*. (**B**) Serial dilutions of wild type (YMM409), *pGAL1:CEN4* (YMM413) and *LC(XII:IV)pGAL1:CEN4* (YMM520) log-phase cultures grown for 48h (glucose) or 72h (galactose) at 30 °C . Galactose (*pGAL1 on*) inactivates the conditional centromere. (**C**) Agarose gel electrophoresis of PCR products to confirm chromosome fusion (using primer pairs A and B) and *CEN4* and *CEN12* modifications (primers C and D). The position of the primer pairs is indicated in (A). Primer sequences used in the generation of the bridging fragment, gene insertions and deletions (in red), and for checking primers used to verify chromosome fusion (in green) are listed in **Table 1**. **(D)** Pulsed field gel electrophoresis (PFGE) of digested wild type and *LC(XII:IV)* cells. The putative position of chromosome IV is indicated. (**E**) Chromosome length of all yeast chromosomes and the long arm of the compound chromosome after either *CEN4* or *CEN12* deletion. Arm length for chromosome XII and the fused chromosomes was calculated assuming 120 copies of the 9.1kb *rDNA* repeat, as measured for wild type cells in this study (see Fig. 13)

Table 2: Genes lost upon fusion of chromosomes XII and IV (excluding genes in telomeres)

Chromosome	Gene	Function	Mutant phenotype[1]
IV	IRC4	unknown	Increased levels of spontaneous Rad52 foci [190], increased sensitivity to Irradiation [191] MMS, and Rapamycin [192]
IV	YDR541C	dihydrokaempferol 4-reductase (putative)	Increased chronological lifespan [193]
IV	PAU10	unknown	unknown
XII	YLR460C	unknown	Slightly decreased competitive fitness in minimal medium [194]
XII	PAU4	unknown	Slightly decreased competitive fitness in minimal medium [194]

[1]Information about mutant phenotypes was taken from: "Saccharomyces Genome Database", http://www.yeastgenome.org

1.2 Verification of correct chromosome fusion

First, fused chromosomes were analyzed by PCR. Primer position and PCR reactions to detect loss of the subtelomeric region downstream of the recombination site (A), chromosome fusion (B) and modification of CEN4 (C) and CEN12 (D) are indicated in (**Fig. 10A, C**). Primer sequences for generation of the transformed PCR fragments and for analyzing the fused

chromosomes are listed in **Table 1**. To visualize the individual chromosomes directly on a gel we used pulsed field gel electrophoresis (PFGE) [195]. Unfortunately we were not able to see the fused chromosomes directly, but we saw one band disappearing after chromosome fusion (**Fig. 10D**). We assume that this band corresponds to chromosome IV because the same band changed its position when we fused chromosome IV to another chromosome (data not shown). Why we were not able to detect chromosome XII or the compound chromosome is not clear.

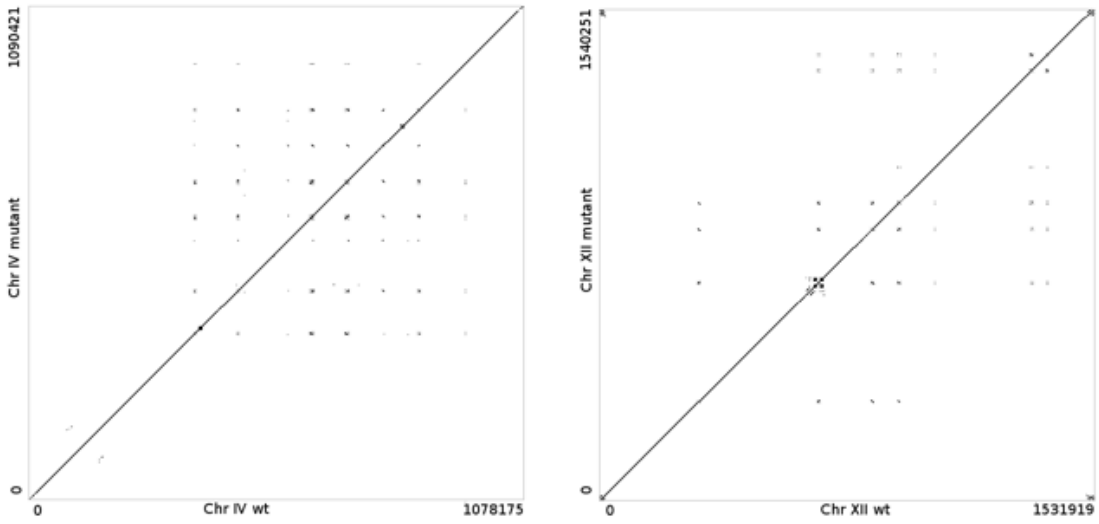

Figure 11: Whole genome sequencing
Dot-plot showing the alignment between chromosomes IV and XII of the *wild type* strain (*wt,* YMM409) and the corresponding regions of the compound chromosome in the *LC(XII:IV)cen4*Δ strain (mutant, YMM524). The lines represent exact matches between the two strains. Positions of the matches on the two genomes (in base pairs) are shown along the axes. The absence of significant gaps along the diagonal indicates lack of large (>3 Kb) genomic re-arrangements or deletions outside of repetitive regions. Lines and dots outside the diagonal are due to the existence of stretches of identical sequences along the chromosome. As expected, this is most apparent for the highly repetitive region containing a cluster of ribosomal DNA genes located in the long arm of chromosome XII (X-like structure on the diagonal).

1.3 Genome sequencing does not reveal large chromosomal rearrangements

Whole genome sequencing of wt and fusion chromosome strains was performed on an Illumina GAIIx sequencer. Analysis of the reads showed that gene order and intergenic distances were conserved between wild type and *LC(XII:IV)* strains, and identified no genomic rearrangements other than the fusion of chromosomes IV and XII (**Fig. 11**). Together this shows that we have succeeded in generating an extra long chromosome without additional or unwanted chromosome rearrangements. Cells coped surprisingly well with the oversized chromosome arm displaying no growth defect (**Fig. 10B**).

2. The long chromosome segregates without altering the mitotic spindle

2.1 Spindle dynamics are undistinguishable between wild type and LC(XII:IV)cen4△ cells

We next examined how cells segregate *LC(XII:IV)* chromosomes. Anaphase spindle elongation, visualized by fusing the spindle pole body (SPB) component Spc42 to green fluorescent protein (Spc42-GFP), progressed with identical kinetics in wild type and *LC(XII:IV)cen4*△ cells, to reach identical lengths (**Fig. 12D**). Thus, to segregate this long chromosome cells did not need to elongate the spindle more or prolong anaphase.

2.2 Long chromosome arms segregate efficiently

Chromosome IV was next visualized using Tet- and Lac- operator arrays integrated at the *TRP1* and *LYS4* loci, and TetR-mRFP and LacI-GFP reporters [176]. Position of these loci and their relative distance to the active centromere on the different chromosomes are indicated in (**Fig. 12A-B**).

Segregation of the *TRP1* and *LYS4* loci in *LC(XII:IV)cen4Δ* cells occurred in inverse order than in wild type, consistent with inversion of chromosome IV

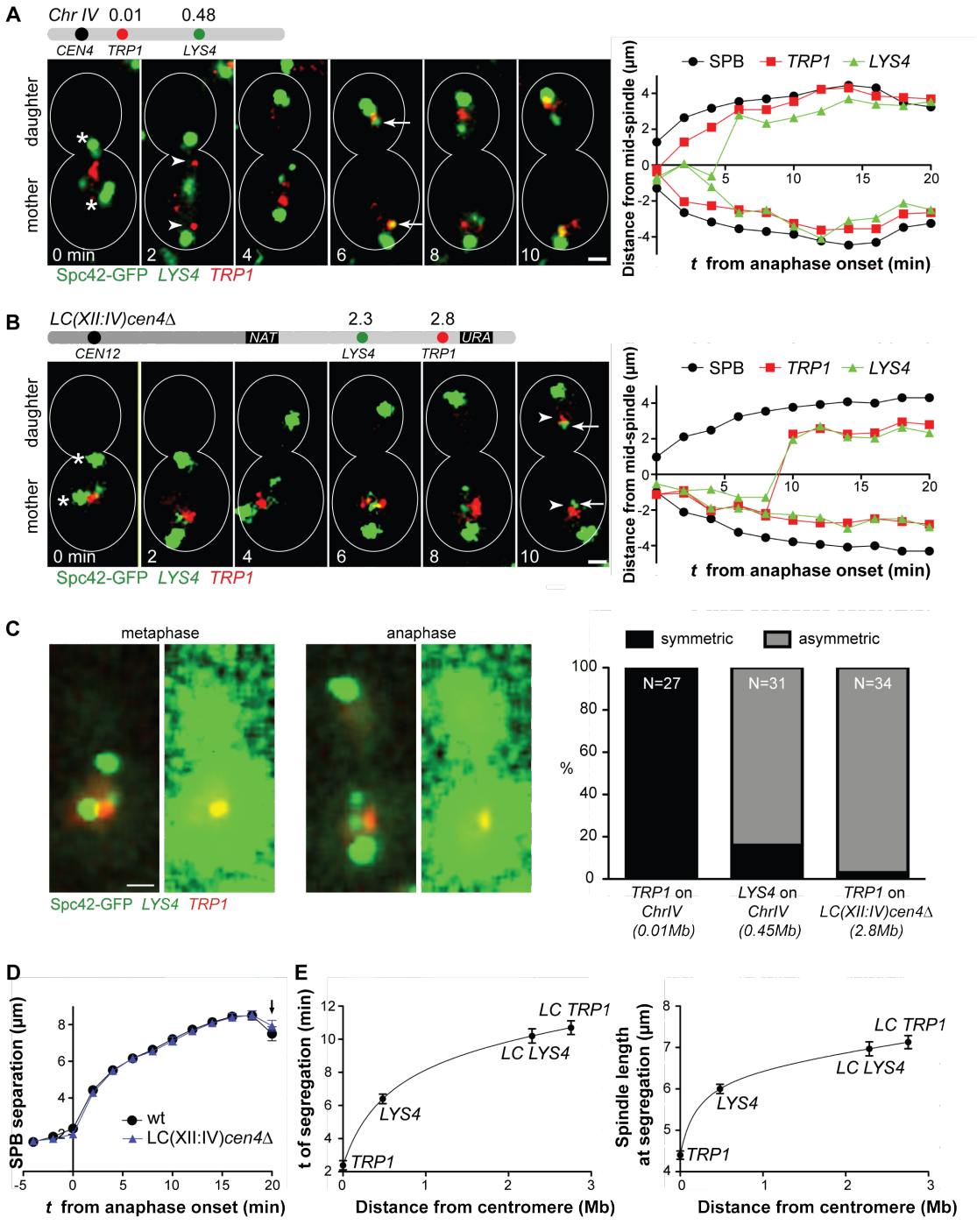

Figure 12: Efficient segregation of the fusion chromosome
(**A-B**) Analysis of SPBs (green, Spc42-GFP, asterisks), *LYS4* (green) and *TRP1* (red) trajectories in time lapse series of *wild type* (YMM409) and *LC* (YMM524) cells. The cartoons show the position of the *TRP1* and *LYS4* and indicate the distance of the loci

relative to the active centromere are in Mb (numbers based on results from (Fig. 13)). Arrowheads and arrows indicate segregation of *TRP1* and *LYS4*, respectively. Time 0=anaphase onset. Scale bars=1µm. (**C**) Quantification of asymmetric locus segregation: Segregation of a locus was considered asymmetric when both decohesed sister-loci appeared on the mother half of the mitotic spindle, as shown on the right image, at least once during anaphase. Mother and daughter cells were distinguished based on background fluorescence. (**D**) Spindle elongation dynamics (distance between SPB) in wild type and *LC(XII:IV)cen4*Δ cells (n=20). The arrow marks spindle breakdown. (**F**) Time of segregation (sister spots are separated by >2µm) relative to anaphase onset (left), or corresponding spindle length (right), for loci on the indicated chromosome, plotted against the distance to the centromere. Nonlinear fit shows an asymptotic relationship (n>25). In E-F, data points are mean ±SEM.

sequences relative to the active centromere (**Fig. 12A-B**). Chromosome arms segregated asymmetrically, with the bud directed chromatid being stretched across the spindle midzone during anaphase. This asymmetry became more evident for loci with increasing distance form the active centromere (**Fig. 12C**). To assess the efficiency of chromosome segregation we measured the time required to segregate a given locus relative to anaphase onset and the length of the mitotic spindle at the time of locus segregation. Interestingly segregation timing and the spindle length at segregation did not increase linearly with increasing distance of a locus to the active centromere (**Fig. 12E**). This suggests that with increasing chromosome arm length, the segregation is more efficient and becomes more dependent on mechanisms other than spindle elongation.

3. The rDNA array is shortened on the compound chromosome

A big part of chromosome XII and consequently of *LC(XII:IV)cen4*Δ is made up of the only ribosomal DNA (*rDNA*) locus in the yeast genome (**Fig. 13A**). The *rDNA* locus is a highly repetitive region consisting of 9.1kb repeats. The copy number of *rDNA* repeats is dynamic within a given population and normally varies between 100-200 copies, depending on the strain background [46, 47]. The segregation of the *rDNA* locus has been shown to depend on an additional condensation step during anaphase [98, 112, 151]. We first

considered the possibility that cells adapt to the increase in chromosome arm length by shortening the *rDNA* locus, by either increasing its compaction or by reducing the number of *rDNA* copies.

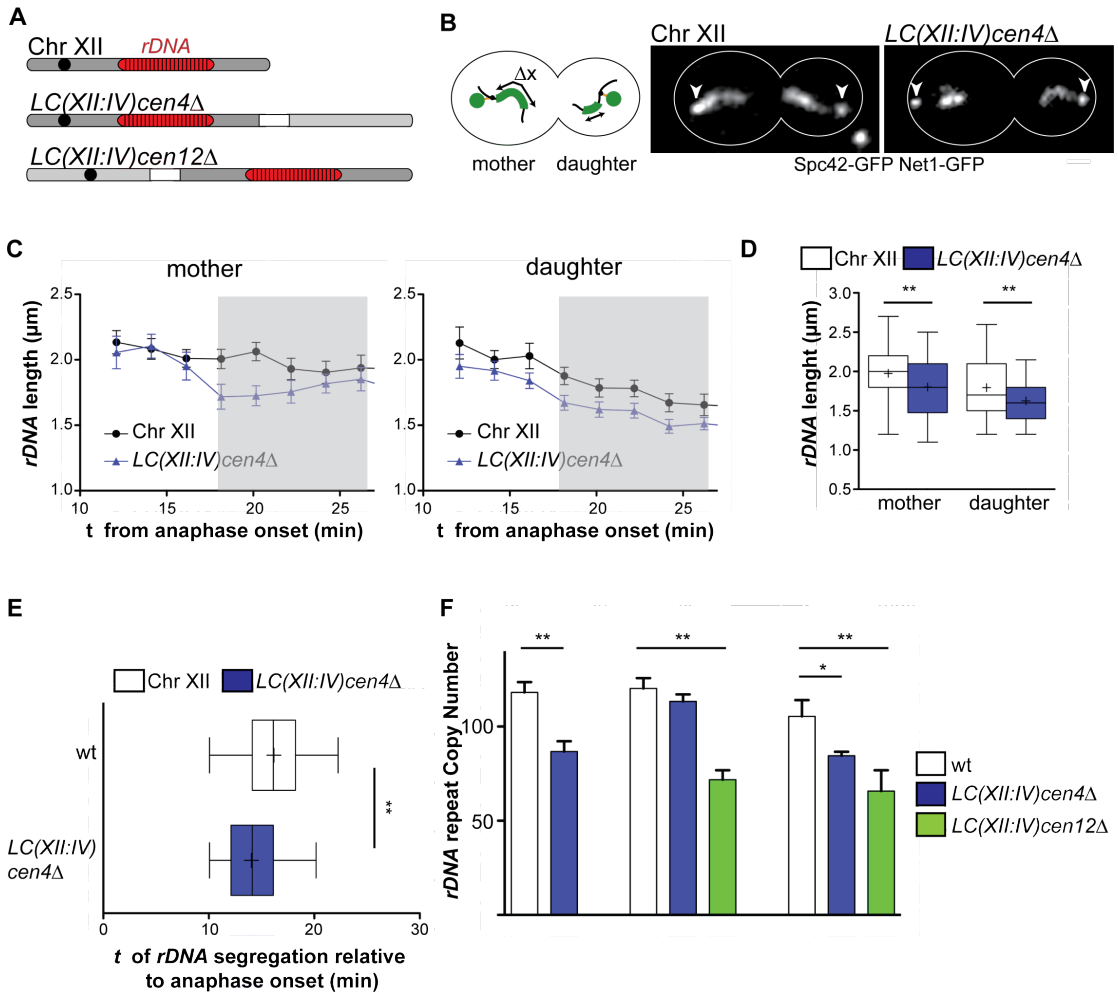

Figure 13: The *rDNA* array is shortened on *LC(XII:IV)*
(**A**) Schematic representation showing the positions of the *rDNA* array on the indicated chromosomes. (**B**) Representative images from cells with labeled SPBs (arrowheads) and *rDNA* (Net1-GFP) on chromosome XII (YMM564) and *LC(XII:IV)cen12*Δ (YMM599). (**C-E**) Analysis of time series (Δt=2min): (**C**) The length of the Net1-GFP signal (*rDNA*) was measured after sister-chromatid separation by more than 2µm in the indicated compartments (n=27). (**D**) *rDNA* length in anaphase (shaded region in (C)). In these and following graphs, boxes include 50% of data points, whiskers 95%. Median (lines) and mean (crosses) are shown. Asterisks indicate p<0.02 (*) or p<0.001 (**). (**E**) Timing of the Net1-GFP separation by more than 2µm measured relative to onset of spindle elongation (n>100). (**F**) *rDNA* copy number (relative to a single copy gene) determined by qPCR in three independent wild type (YMM1, YMM409, YMM564) and corresponding *LC(XII:IV)cen4*Δ (YMM569, YMM524, YMM599) and *LC(XII:IV)cen12*Δ (YMM527, YMM917) strains. Primers were designed to amplify fragments of similar sizes in the ITS2 element of the repeated *RDN1* locus and on the single copy gene *SLI15*. Error bars represent the standard deviation of three independent experiments.

3.1. The rDNA array on the compound chromosome is shorter and segregates earlier than on chromosome XII

To analyze *rDNA* compaction in vivo we expressed a fusion of green fluorescent protein (GFP) with Net1, which is part of the *rDNA* associated RENT complex [196]. In addition to Net1 we expressed Spc42-GFP to label the SPBs, which allowed us to follow anaphase progression (**Fig. 13B**). First we estimated the length of the *rDNA* array by measuring the length of the Net1-GFP signal in time lapse images between completed sister chromatid resolution and spindle breakdown. Indeed the *rDNA* was shorter when measured on *LC(XII:IV)cen4*Δ than on chromosome XII, on both the mother and the daughter directed chromatid (**Fig. 13C-D**). Consistent with this was the observation that the *rDNA* array on *LC(XII:IV)cen4*Δ segregated earlier than on chromosome XII (**Fig. 13E**). Thus cells adapt to the increase in chromosome length by shortening the *rDNA*.

3.2. The number of rDNA repeats is reduced on the compound chromosome

To determine the *rDNA* copy number we performed quantitative PCR analysis on genomic DNA isolated from different strains carrying either a wild type karyotype, *LC(XII:IV)cen4*Δ or *LC(XII:IV)cen12*Δ. The number of *rDNA* repeats was reduced by 6-25% in *LC(XII:IV)cen4*Δ strains relative to wild type chromosome XII (87-110 repeats vs. 110-120) (**Fig. 13F**). Interestingly on *LC(XII:IV)cen12*Δ the reduction was even stronger with around 40% in both strains analyzed (66-72 repeats) (**Fig. 13F**). Together this shows that the big increase in chromosome arm length poses a pressure on the cells, forcing them to adapt by reducing the *rDNA* copy number and possibly by additional mechanisms that increase axial compaction.

4. The distal region of the compound chromosome is hyper-compacted

The reduction in *rDNA* copy numbers led to a substantial shortening of the fused chromosome arms from the estimated 3.5Mb on *LC(XII:IV)cen4*Δ and 3.2Mb on *LC(XII:IV)cen12*Δ (120 *rDNA* repeats) to 3.2Mb (87 repeats) and 2.7Mb (66 repeats) respectively. This however still represents an increase of 60% and 35% in length compared to the longest wt chromosome arm and thus the reduction in *rDNA* copy number cannot fully explain the cellular adaptation to the fused chromosomes.

*4.1 The TRP1-LYS4 distance is reduced on the LC(XII:IV)cen4*Δ

We therefore set out to analyze chromosome compaction outside the *rDNA* locus by comparing the distance between the *TRP1-LYS4* loci on chromosome IV and *LC(XII:IV)cen4*Δ (**Fig. 14A**). This system has previously been used to measure chromosome condensation during mitosis [176]. Time lapse imaging showed that in wild type cells, the *TRP1-LYS4* distance decreased after segregation (**Fig. 14B-C**) to about 75% of its metaphase value, indicating that chromosome IV compaction still increased in late anaphase. Anaphase compaction was systematically highest for the bud-directed chromatid (**Fig. 14C**). On *LC(XII:IV)cen4*Δ the *TRP1-LYS4* distance was smaller than on chromosome IV. Consistent with this chromosome region being more compacted, we observed chromosome arm stretching less frequent on *LC(XII:IV)cen4*Δ than on chromosome IV (not shown). By decreasing the time interval between frames from 2min to 15s we could see that the *TRP1-LYS4* region on *LC(XII:IV)cen4*Δ also gets stretched during anaphase, but for a shorter period and to a smaller extent than on chromosome IV (**Fig. 14D-E**). Therefore hyper-compaction of the *TRP1-LYS4* region occurs in the compound chromosome and could facilitate its segregation. Thus the chromosome context influences the compaction state

of a chromosomal region. It is however not clear whether the hyper-compaction on the compound chromosome is caused by the increased length of the chromosome arm, by its vicinity to the *rDNA* or whether it is a consequence of the different position relative to the active centromere. Indeed, such a position effect has been reported for centromere proximal and centromere distal regions using the same reporter system in live cells: While the centromere proximal region between *TRP1* and *LYS4* only condensed during mitosis, fluorescent reporters integrated in the *LYS4* locus and in the telomere of chromosome IV showed that the centromere distal region was compacted throughout the cell cycle [176]. We thus wanted to examine the influence of an active centromere on chromosome arm compaction.

4.2 The presence of an active centromere influences compaction of neighboring chromatin regions

In order to analyze the influence of the centromere on chromosome compaction, we inactivated *CEN4* on chromosome IV by placing *pGAL1:CEN4* cells in galactose. *TRP1-LYS4* distance in metaphase was reduced to the same extent on chromosome IV with inactivated *CEN4* and on *LC(XII:IV)pGAL1:CEN4* relative to wild type chromosome IV (**Fig. 14F**). One possible explanation for this phenomenon is that forces exerted from microtubule attachments to the kinetochore continuously stretch the region around the centromere. This can however be excluded as depolymerization of the mitotic spindle with nocodazole does not significantly decrease *TRP1-LYS4* distance on chromosome IV (**Fig. 14G**). We can therefore conclude that, at least in metaphase, most of the hyper-compaction observed on *LC(XII:IV)cen4*Δ is caused by the absence of an active centromere, but is independent of microtubule forces.

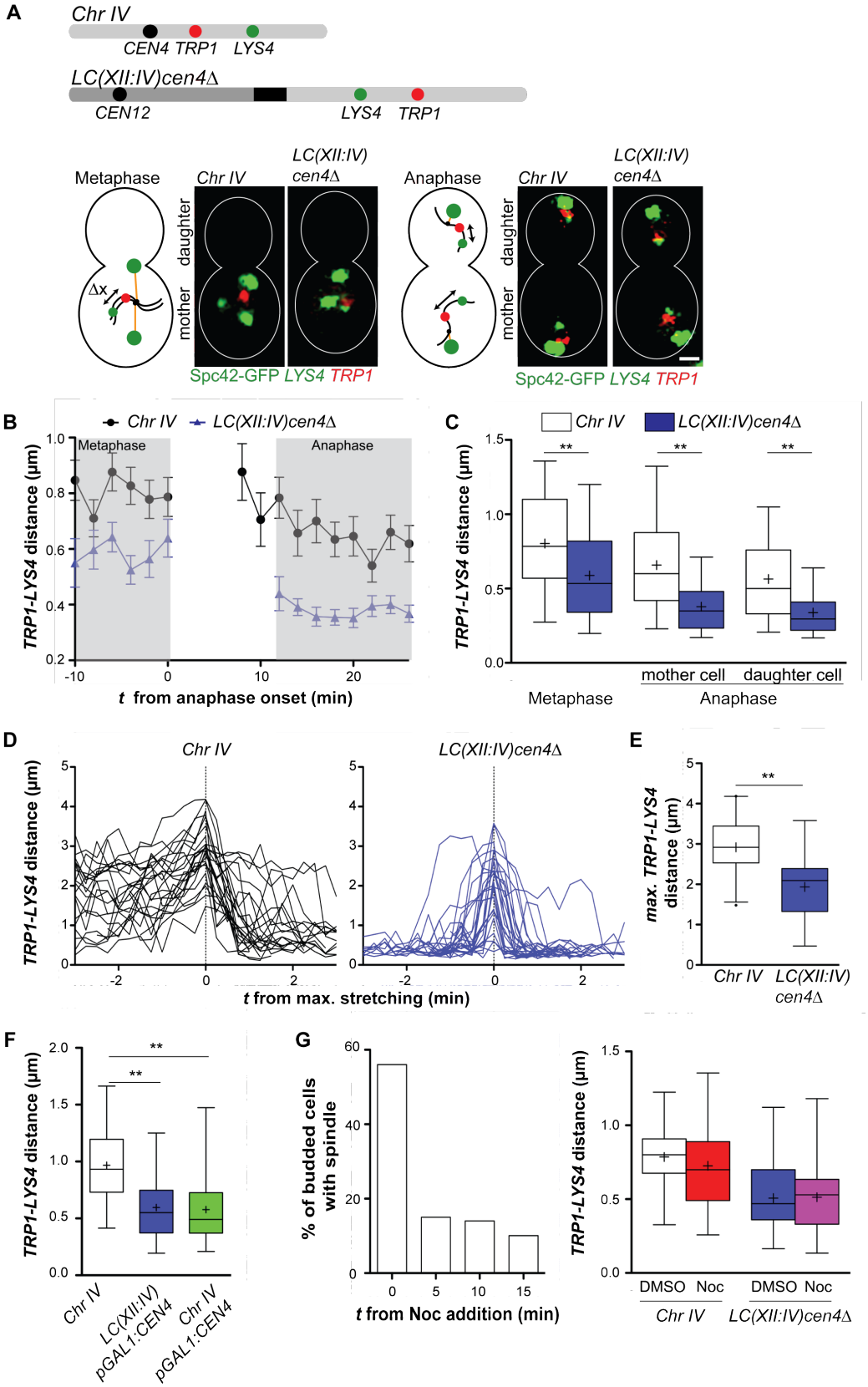
A
Chr IV
CEN4 TRP1 LYS4
LC(XII:IV)cen4Δ
CEN12 LYS4 TRP1
Metaphase
Chr IV
LC(XII:IV) cen4Δ
Anaphase
daughter
mother
Δx
Spc42-GFP LYS4 TRP1
B
Chr IV
LC(XII:IV)cen4Δ
Metaphase
Anaphase
TRP1-LYS4 distance (μm)
t from anaphase onset (min)
C
Chr IV
LC(XII:IV)cen4Δ
TRP1-LYS4 distance (μm)
mother cell
daughter cell
Metaphase
Anaphase
D
Chr IV
LC(XII:IV)cen4Δ
TRP1-LYS4 distance (μm)
t from max. stretching (min)
E
max. TRP1-LYS4 distance (μm)
Chr IV
LC(XII:IV) cen4Δ
F
TRP1-LYS4 distance (μm)
Chr IV
LC(XII:IV) pGAL1:CEN4
Chr IV pGAL1:CEN4
G
% of budded cells with spindle
t from Noc addition (min)
TRP1-LYS4 distance (μm)
DMSO Noc
DMSO Noc
Chr IV
LC(XII:IV)cen4Δ

Figure 14: Chromosome Compaction is increased on *LC(XII:IV)cen4*Δ
(**A**) *Top*, Schematic representation showing the positions of fluorescent marks (Lac and Tet operator repeats) in chromosome IV (YMM409) and *LC(XII:IV)cen4*Δ (YMM524). *Bottom***,** Representative metaphase (*left*) and anaphase (*right*) cells with labeled SPBs (large green dot), *TRP1* (red) and *LYS4* (green) loci. (**B-C**) The distance between *TRP1-LYS4* was measured in time series (Δt=2min, 23 °C) during metaphase (0-10 min prior to spindle elongation) and in anaphase (complete locus segregation-spindle breakdown) (**B**) in the mother compartment. (**C**) Data points from the shaded area in (B) are pooled in the box plot. (**D-E**) *TRP1-LYS4* distances were measured in time series (Δt=15s, 30 °C) and (**D**) aligned at the point of maximal chromosome stretching (t_0). (**E**) Box-plot showing the maximal *TRP1-LYS4* distance measured on chromosome IV and *LC(XII:IV)cen4*Δ during anaphase (n≥24). (**F**) Cells were shifted from sucrose to galactose based medium upon release from G1 arrest (alpha factor), except for *LC(XII:IV)pGal:CEN4*, which was always kept on galactose. *TRP1-LYS4* distance was measured in time series (Δt=2min, 25 °C) from 0-5 min prior to spindle elongation (n≥20). (**G**) Mitotic spindles were depolymerized using nocodazole (Noc, 50µg/ml) in exponential cultures. Images were acquired at the indicated times to determine depolymerization efficiency (left). *TRP1-LYS4* distances were measured 10min after nocodazole addition in large budded cells with a single nucleus (metaphase, right).

5. The centromere-proximal region of the compound chromosome hyper-compacts specifically during anaphase

*5.1 The TRP1-LYS4 distance is reduced on the LC(XII:IV)cen12*Δ *specifically during anaphase*

To analyze chromosome compaction on the compound chromosome independently of effects from the centromere we compared the *TRP1-LYS4* distance on chromosome IV to *LC(XII:IV)cen12*Δ, in which the position relative to the active centromere is not altered (**Fig. 15A**). Time lapse series showed, in contrast to *LC(XII:IV)cen4*Δ, that *TRP1-LYS4* distance is the same on both chromosomes during metaphase, but increases more on *LC(XII:IV)cen12*Δ than on chromosome IV during anaphase (**Fig 15B-C**). Consistent with hyper-compaction being established during late anaphase, we were not able to detect a difference in the maximal stretching of the *TRP1-LYS4* chromatin region during early anaphase (**Fig. 15D**) nor a significant advancement of *LYS4* segregation (**Fig. 15E**). As this hyper-compaction is independent from centromere effects, this shows that cells are able to measure chromosome arm length during late anaphase and respond to it.

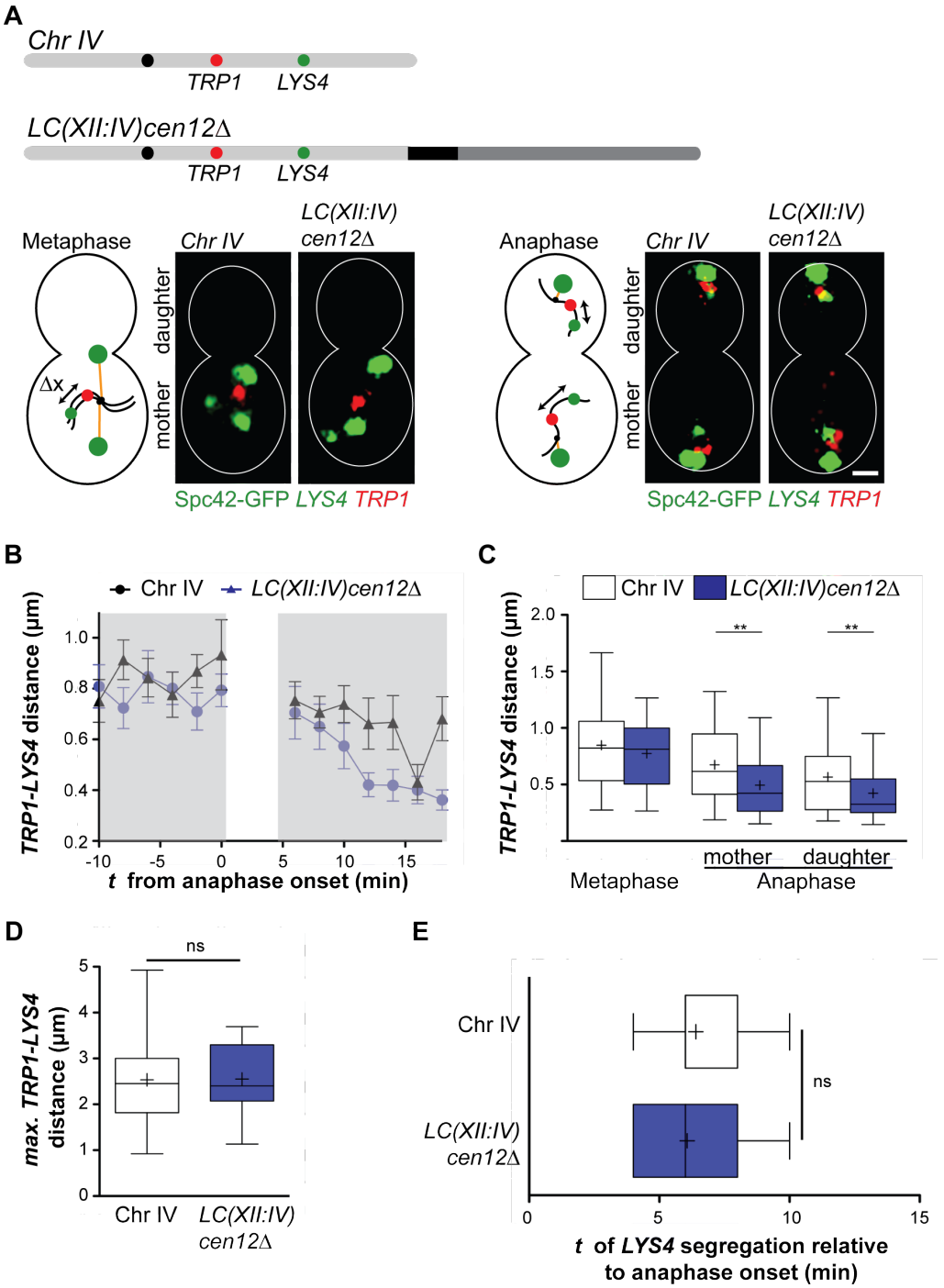

Figure 15: Anaphase chromosome compaction is increased on *LC(XII:IV)cen12*Δ
(**A**) *Top*, Schematic representation showing the positions of fluorescent marks (Lac and Tet operator repeats) in chromosome IV (YMM409) and *LC(XII:IV)cen12*Δ (YMM527). *Bottom*, Representative metaphase (*left*) and anaphase (*right*) cells with labeled SPBs (large green dot), *TRP1* (red) and *LYS4* (green) loci. (**B-E**) Time-lapse series (Δt=2min, 30 °C) (**B**) The distance between *TRP1-LYS4* was measured during metaphase (0-10 min prior to spindle elongation) and in anaphase (complete locus segregation-spindle

breakdown) in the mother compartment. (**C**) Data points from the shaded area in (B) are pooled in the box plot. (**D**) Maximal *TRP1-LYS4* distance during anaphase. (**E**) Timing of the *LYS4* separation by more than 2µm measured relative to onset of spindle elongation (n≥28).

5.2 Hyper-condensation is specific for the long chromosome

Next we wondered whether hyper-compaction affected all chromosomes or whether this reaction was specific for the *LC(XII:IV).* For this we analyzed the *TRP1-LYS4* region in diploids where only one copy each of chromosomes IV and XII were fused (**Fig. 16**). The compaction of the *TRP1-LYS4* reporter increased, like in haploid cells, when it was placed on *LC(XII:IV)cen12*Δ and *LC(XII:IV)cen4*Δ. A non-labelled long chromosome was however not able to induce hyper-compaction on a labeled, wild type chromosome IV (**Fig. 16**). Thus, cells appear to have a “chromosome ruler” to assess the length of the LC and adapt its compaction individually.

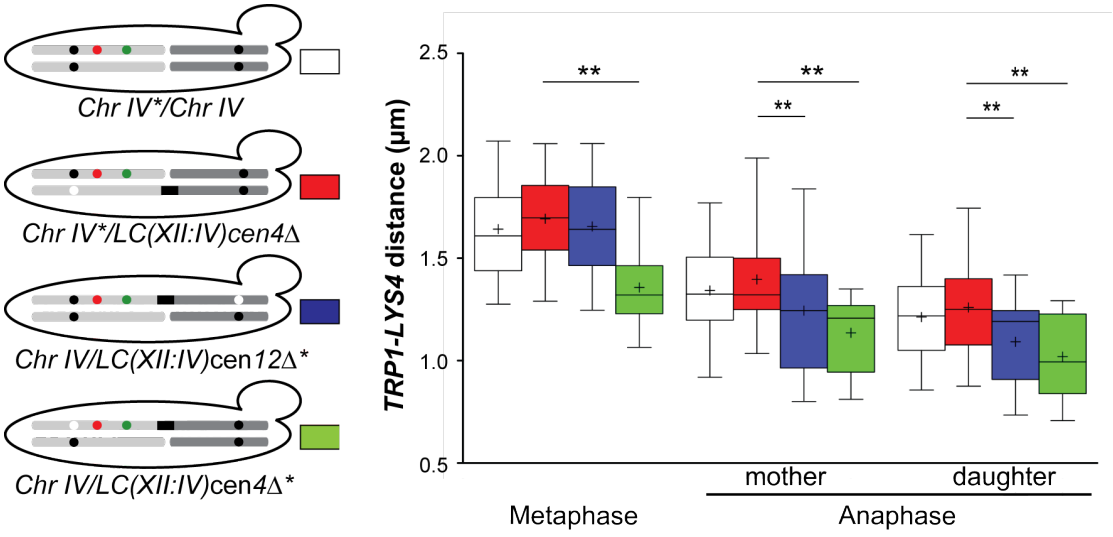

Figure 16: Hyper-compaction is specific to the *LC(XII:IV)* chromosome
Left, Schematic representation of diploid cells showing the two copies of chromosomes IV and XII. Chromosome fusions (black rectangle) and labelled *TRP1* and *LYS4* loci (red and green circles) are indicated. *Right,* Quantification of the *TRP1-LYS4* distance from time-lapse images during metaphase and anaphase in the depicted diploid strains.

So far we have shown that the fusion of chromosomes IV and XII triggered several changes on the chromosomes that all decrease its physical length. First, chromosome fusion led to a decrease in the number of *rDNA* copies, substantially reducing the DNA content on the fusion chromosome. When chromosome IV was placed at the tip of chromosome XII, the TRP1-LYS4 region was more compact, presumably because centromere architecture or kinetochore assembly can decrease compaction in centromere associated chromatin regions. Next we showed that centromere proximal regions on the LC are hyper-compacted specifically during late anaphase. Whether this response depends on the increase in chromosome arm length or on its vicinity to the *rDNA* on the LC is not clear and we will return to this question at the end of chapter 8 and in the discussion. Finally we have shown that increased compaction in both, centromere proximal and centromere distal regions, is not a global response but is specific for the compound chromosome. In the following sections we will focus on how the anaphase specific hyper-compaction in the centromere proximal region is regulated.

6. Hyper-compaction depends on chromosome condensation

6.1 Polo kinase Cdc5 is required to adapt to the fusion chromosome

To identify the molecular players involved in the observed hyper-compaction response, we started looking for genetic interactions between the long chromosome and genes with a function in chromosome segregation. As the compound chromosome was more compacted we hypothesized that adaptation to the increased chromosome arm length depended on chromosome condensation. One of the main activators of condensin in budding yeast is the polo kinase Cdc5 [168]. We found that strains carrying the chromosome fusion were hypersensitive to decreased levels of Cdc5 activity (**Fig. 17A**). Cdc5 kinase plays important roles in both spindle elongation [197] and chromosome condensation [111]. A partial inactivation of

the temperature sensitive *cdc5-1* allele led to decreased rates of spindle elongation (**Fig. 17B**) and to decondensed chromosome arms in anaphase (**Fig. 17C**). Consequently the segregation of long chromosome arms was heavily impaired: at semi-permissive temperature (30 °C), *LYS4* on chromosome IV was only segregated in 80% of cells before spindle breakdown and only 20% of cells were able so segregate *TRP1, located at* the end of the long arm of *LC(XII:IV)cen4*Δ (**Fig. 17D**). This explains the genetic interaction between *cdc5-1* and the long chromosome and suggests that cells rely on chromosome condensation and spindle elongation to adapt to the increased chromosome arm length.

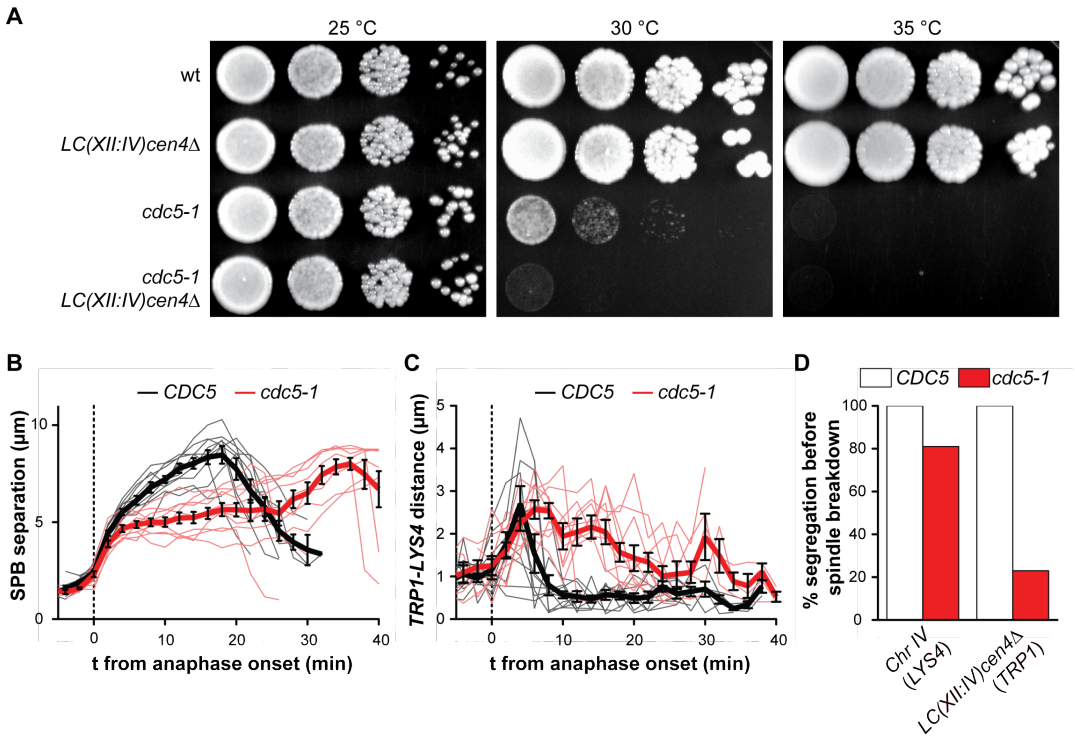

Figure 17: Polo kinase is required for adaptation to the *LC(XII:IV)*
(**A**) 10x serial dilutions of *wild type* (YMM409), *LC(XII:IV)cen4*Δ (YMM524), *cdc5-1* (YMM713), *cdc5-1 LC(XII:IV)cen4*Δ (YMM761) cells. Exponentially growing cells were grown for 2 days at 25, 30 or 35 °C. (**B-D**) Data from time lapse (Δt=2min) images of wild type and *cdc5-1* cells with labelled SPBs, *TRP1*- and *LYS4* loci. Cells were arrested in G1 (α-factor) and released at room temperature for 75min. 15min prior to image acquisition cells were shifted to 30 °C. (**B**) spindle length and (**C**) *TRP1-LYS4* distances measured on daughter directed chromatid from 5min prior to onset of spindle elongation until spindle breakdown. (**D**) shows the percentage of cells that segregate the indicated loci prior to spindle breakdown (n≥26).

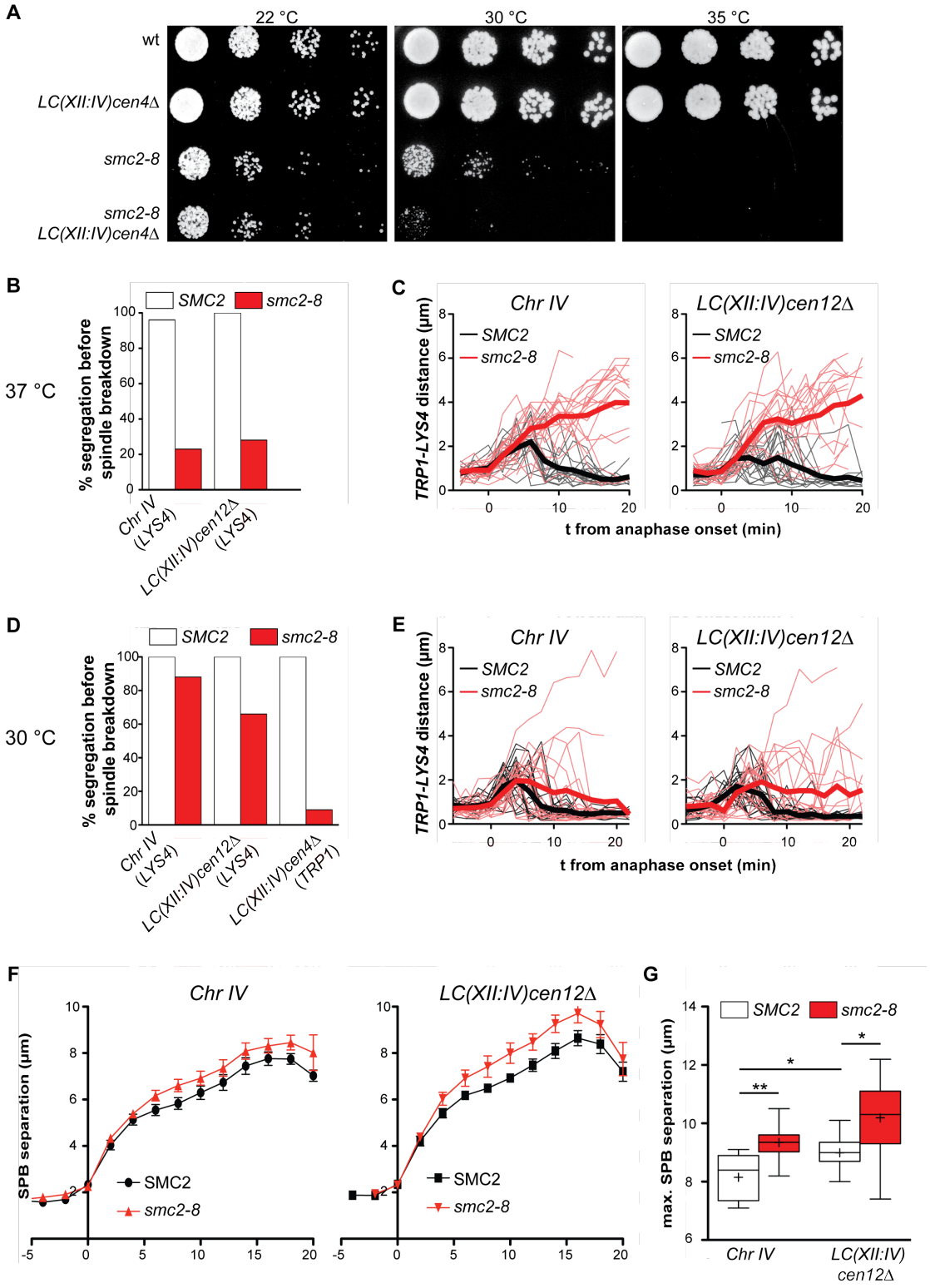

Figure 18: Hyper-compaction of *LC(XII:IV)* depends on condensin
(**A**) 5x serial dilutions of *wild type* (YMM409), *LC(XII:IV)cen4Δ* (YMM524), *smc2-8* (YMM1210), *smc2-8 LC(XII:IV)cen4Δ* (YMM1248) were spotted on rich glucose

medium and grown for 2 days at 22, 30 or 35 °C (**B, D**). Quantification of the segregation efficiency of the indicated loci at 37 °C (B, n≥18) and 30 °C (D, n≥50). (**C, E**) *TRP1-LYS4* distances of daughter-directed chromatids were measured on *ChrIV* and *LC(XII:IV)cen12*Δ (YMM527, YMM1263) of the indicated genotype until spindle breakdown (followed through Spc42-GFP trajectories) at 37 °C (C, n≥10) and 30 °C (E, n=20). Thin lines represent individual cells, thick lines show the mean. (**F**) Spindle elongation dynamics (distance between SPB) in cells of the indicated genotype carrying either *wild type* chromosome IV or *LC(XII:IV)cen12*Δ at 37 °C (n≥10). (**G**) Box plot of the maximal spindle length measured in (F) (n≥10). In **(**B-C) and (F-G) alpha factor arrested cells were released from G1 at 25 °C and shifted to 37 °C 20 minutes prior to image acquisition, in **D-E** cells were released from alpha factor at 30 °C.

6.2 Condensin activity is required for efficient segregation of long chromosome arms

As we did not observe changes in spindle dynamics in *LC(XII:IV)* cells (**Fig. 12D**) and polo kinase is an essential activator of the condensin complex [111], we next tested whether condensin activity is required for the adaptation to the fusion chromosome. Indeed *LC(XII:IV)* cells carrying the conditional condensin mutation *smc2-8* showed reduced viability at semi-permissive temperature (**Fig. 18A**). In smc2-8 mutant cells at 37 °C spindle breakdown preceded *LYS4* segregation in 80% of the cells, independently of the whether it was measured on chromosome IV or *LC(XII:IV)cen12*Δ (**Fig. 18B)**. This was reflected by a complete lack of compaction of the *TRP1-LYS4* region during anaphase (**Fig. 18C**). As expected from the genetic interaction the segregation defects were stronger when measured on *LC(XII:IV)* at 30 °C: While *LYS4* on chromosome IV segregated prior so spindle breakdown in 90% of the cells, this number dropped to 60% when measured on *LC(XII:IV)cen12*Δ and the very distal *TRP1* locus on *LC(XII:IV)cen4*Δ only segregated in 10% (**Fig. 18D**). Consistent with this at 30 °C the compaction of the *TRP1-LYS4* region was more strongly impaired on *LC(XII:IV)cen12*Δ than on chromosome IV. (**Fig. 18E**). Thus compaction and segregation of the *LC(XII:IV)* requires more Cdc5 and condensin activity than chromosome IV and we therefore termed the observed increase in axial compaction on *LC(XII:IV)* “adaptive hyper-condensation”.

6.3 Mitotic spindles hyper-elongate in the absence of condensin activity

Even though we did not observe a change in spindle dynamics when initially characterizing *LC(XII:IV)cen12*Δ cells, we observed that at 37 °C, spindles from LC(XII:IV)cen12Δ cells became longer than wild type spindles (**Fig. 18G**). Surprisingly, when chromosome condensation was inactivated using the *smc2-8* mutant allele, the spindles grew even bigger, with the spindles of cells carrying the compound chromosome being more affected (**Fig. 18F-G**), consistent with [198]. This suggested that, if chromosome condensation is not sufficient to fully segregate chromosome arms, the mitotic spindle can hyper-elongate and promote chromosome segregation.

7. Anaphase hyper-condensation depends on Ipl1 activity

The most striking aspect of the adaptive hyper-condensation is the fact that cells are able to adjust chromosome condensation for each chromosome individually during anaphase. From the mitotic kinases known to regulate condensin activity [199] only the Aurora kinase Ipl1 shows a localization pattern compatible with a chromosome ruler function: As part of the chromosomal passenger complex (CPC) Ipl1 localizes to the mitotic spindle during anaphase [32] and could thus adjust chromosome condensation to the size of the anaphase spindle. Such a model could also account for the observation that the bud directed chromatid, which gets stretched extensively across the spindle midzone, ends up to be more compacted in anaphase than the mother directed chromatid (**Fig. 14C, 15C**).

We therefore asked whether Ipl1 mediated the adaptive response. We characterized chromatin compaction in temperature-sensitive *ipl1-321* mutants shifted to 35ºC at anaphase onset. This treatment did not perturb spindle dynamics [32] (**Fig. 19A**) and only mildly kinetochore biorientation [140] (*TRP1* sister-dots on chromosome IV segregated correctly in 100% of

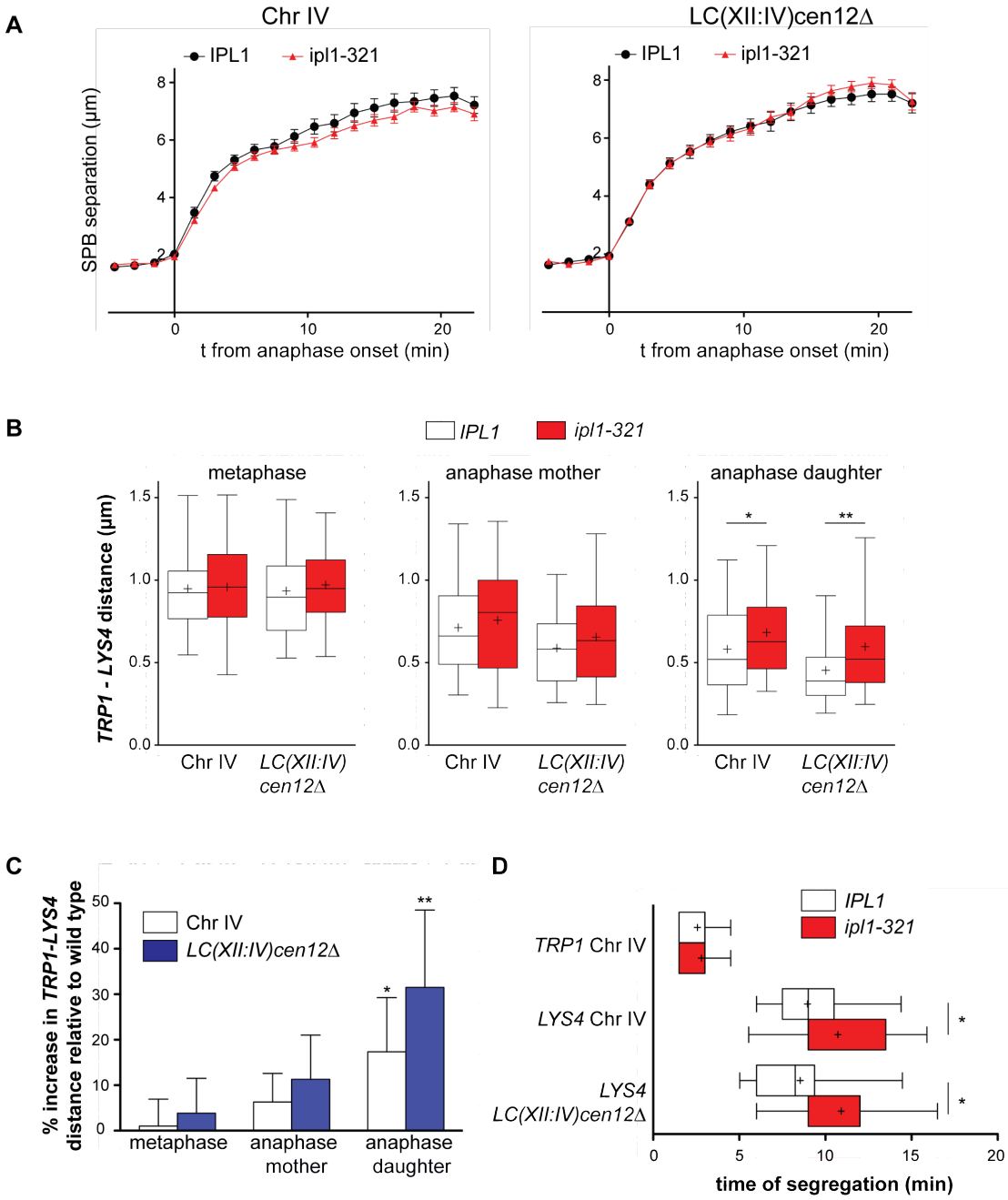

Figure 19: Hyper-condensation of LC(XII:IV)cen12Δ depends on Ipl1 activity.
Cells (*wild type* (YMM409), *LC(XII:IV)cen12Δ* (YMM527), *ipl1-321* (YMM410), *LC(XII:IV)cen12Δ ipl1-321* (YMM529)) were arrested in G1, released for 75 minutes at room temperature and shifted to 35 ºC 15minutes prior to image acquisition (N>25). (**A**) Distance between the spindle pole bodies in anaphase for the indicated strains (mean ± SEM) (**B**) *TRP1-LYS4* distances of the same cells were determined as in (Fig. 14 E). (**C**) Relative loss of condensation upon Ipl1 inactivation was calculated as the ratio of the mean distance between *TRP1-LYS4* shown in (B). Standard error of the mean was calculated using error propagation. (**D**) The time of segregation of the indicated loci relative to anaphase onset was determined as in (Fig. 12F). Note that segregation of *LYS4* in the *LC(XII:IV)cen12Δ* chromosome is slightly advanced in *IPL1* cells. t_0=onset of spindle elongation, N>25.

wild type cells and 93% of *ipl1-321* cells; N>100). However, Ipl1 inactivation affected *TRP1-LYS4* compaction, particularly in *LC(XII:IV)cen12*Δ and the bud-directed chromatids (**Fig. 19B-C**), resulting in a segregation delay of long chromosome arms (**Fig. 19D**). Yet, Ipl1 inactivation did not abolish anaphase condensation in general (**Fig. 19B**). Thus, Ipl1 contributed little to the bulk of anaphase condensation, but was required for hyper-condensation of chromosome arms, proportionally to their length.

8. Ipl1 localization to the mitotic spindle is required to induce condensation

8.1 Ipl1 must localize to the spindle midzone to adapt chromosome condensation to spindle length

As hyper-condensation depended on Ipl1 (**Fig. 19**) we hypothesized that spindle-localized Ipl1 directly adjusts chromosome condensation to the size of the mitotic spindle. To directly test this model we asked whether adaptive hyper-condensation required Ipl1 localization to the spindle midzone.

The midzone protein Slk19 mediates timely activation of the Cdc14 phosphatase [155], CPC and separase spindle recruitment [161, 200] and midzone focusing [162]. Loss of Slk19 caused a decrease in anaphase compaction of *TRP1-LYS4* on chromosome IV (**Fig. 20A**), the second longest yeast chromosome, and delayed *LYS4* segregation (p<0.02) **(Fig. 20B)**. Proper Ipl1 localization is recovered in *slk19*Δ and *cdc14* mutant cells when replacing Sli15 with its constitutively dephosphorylated form, *Sli15-6A* [161]. Expression of *SLI15-6A* in *slk19*Δ cells restored chromosome compaction and segregation to near wild type levels (**Fig. 20A-B**). Thus, Ipl1 must be on the midzone to adapt condensation of endogenous long chromosomes.

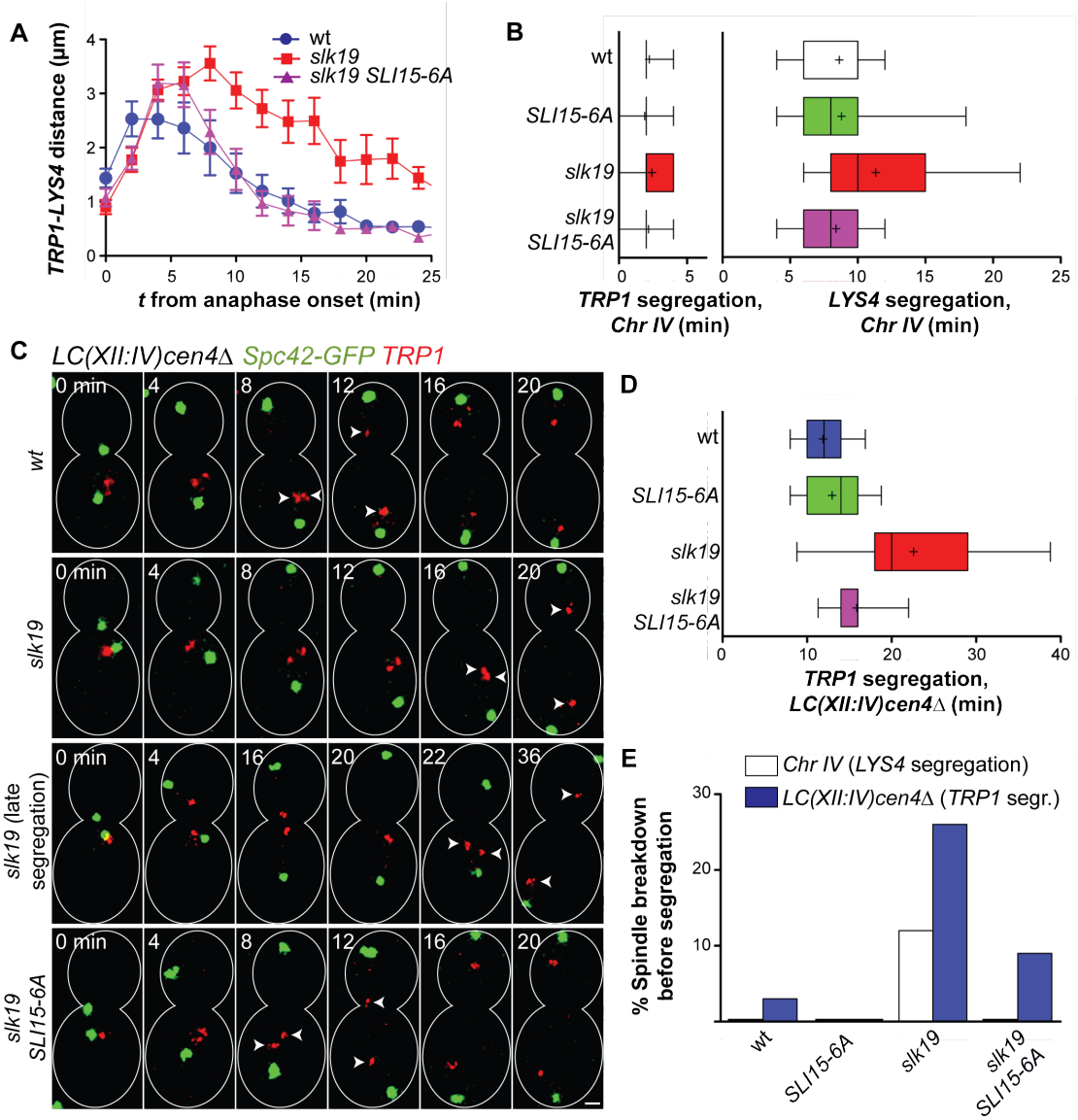

Figure 20: Ipl1 targeting to the spindle midzone is required for segregation of long chromosome arms.
Time-lapse series of exponentially growing diploid cells were acquired at 30 ºC. (N>18 for *ChrIV*; N>30 for LC). (**A**) *TRP1-LYS4* distance in chromosome IV throughout anaphase, in cells of indicated genotype (mean ± SEM). (**B**) Segregation time of *TRP1* and *LYS4* on *ChrIV* relative to anaphase onset. (**C**) Representative image series showing segregation of the *TRP1* locus, located at the distal tip of the long arm of *LC(XII:IV)cen4*Δ. Arrowheads mark *TRP1* before and after segregation. (**D**) Segregation time of *TRP1* in *LC(XII:IV)cen4*Δ cells of the indicated genotype. (**E**) Percentage of cells in which the spindle breaks prior to chromosome segregation in the same cells as in (C, D). All cells are diploid strains carrying one chromosome with labeled *TRP1* and *LYS4*: *wild type* (*SLK19/SLK19 SLI15/SLI15; YMM772 and YMM771)*; *SLI15-6A* (*SLK19/SLK19 SLI15/SLI15-6A; YMM773 and YMM770*); *slk19* (*slk19Δ/slk19Δ SLI15/SLI15; YMM780 and YMM779*); *slk19 SLI15-6A* (*slk19Δ/slk19Δ SLI15/SLI15-6A;YMM1045 and YMM1046).*

8.2 Segregation of long chromosome arms depends on Ipl1 localization to the mitotic spindle

To examine the effects of midzone-bound Ipl1 on the segregation of long chromosomes, we visualized the distal region of *LC(XII:IV)cen4*Δ, marked by the *TRP1* locus (2.8 Mb from *CEN12*), in *slk19*Δ mutants. Separation of the distal *TRP1* locus, but not that of a centromere-proximal one, was delayed in *slk19*Δ mutants (p<0.001) (**Fig. 20B-D**). As a consequence of this delay, spindle breakdown preceded *TRP1* segregation in 27% of *LC(XII:IV)cen4*Δ *slk19*Δ mutant cells (**Fig. 20C-E**). Expression of *SLI15-6A* largely suppressed these defects (**Fig. 20E**). Thus, Slk19 affected segregation mainly through targeting of Ipl1/Aurora B to the spindle midzone, which was especially important for the segregation of long chromosomes.

We have previously raised the question of whether the increased compaction on *LC(XII:IV)cen12*Δ is caused by the increased length of the chromosome or by the close proximity of the *rDNA* to the *TRP1-LYS4* region on the compound chromosome. We showed that Ipl1 activity and it's localization to the mitotic spindle is required for hyper-condensation and segregation of the *LC(XII:IV)*. The same machinery however also affects the *rDNA*-free chromosome IV, showing that Ipl1 induced chromosome condensation does not depend on the presence of the r*DNA*. This suggests that the Ipl1 dependent hyper-condensation of *LC(XII:IV)cen12*Δ is caused by the increased length of the chromosome arm and not by the vicinity of the *rDNA*.

9. Ipl1 is not required for condensin loading onto rDNA in budding yeast

So far we have demonstrated that long chromosomes hyper-condense their centromere-proximal region in an Ipl1 dependent manner. Next we wanted to

identify the relevant Ipl1 targets that mediate this response. We will consider the following candidates: condensins, histone H3, and cohesins.

As shown earlier, activity of condensins is rate limiting for survival of long chromosome cells. Condensins are phosphorylated in an Ipl1-dependent

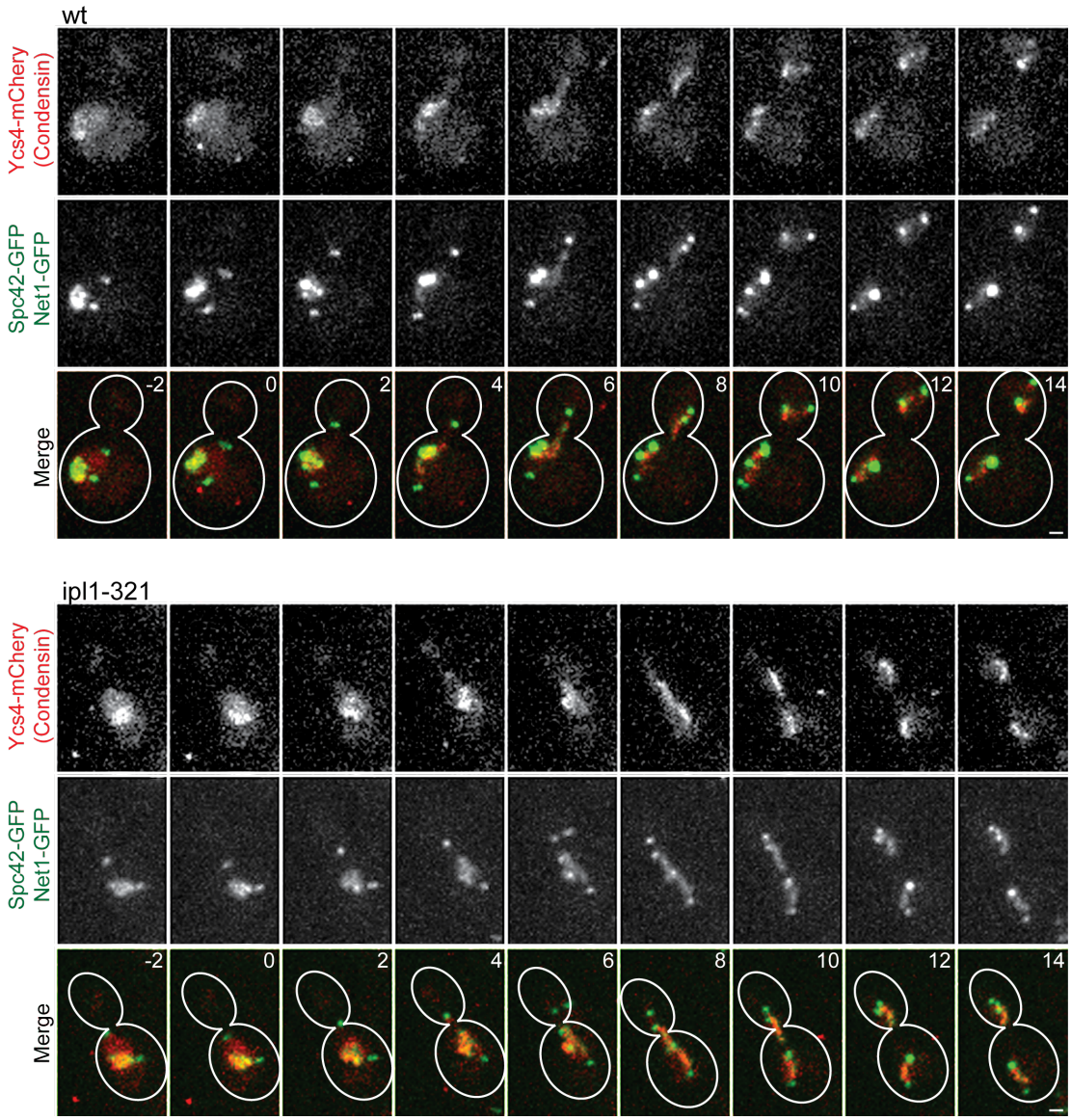

Figure 21: Ipl1 activity is not required to accumulate condensin at the *rDNA*
Cells expressing the fusion proteins Ycs4-mCherry (condensin subunit) Net1-GFP (nucleolar protein), and Spc42-GFP (spindle pole component) under the endogenous promoter were arrested in G1 at room temperature and released at 37 °C. Representative images of a time series of the indicated strains are shown: *wild type* (YMM1431) and *ipl1-321* (YMM1432).

manner during mitosis in budding and fission yeast [111, 112]. In addition condensin recruitment to mitotic chromosomes has been shown to depend on orthologues of the Aurora B kinase in species from fission yeast to humans [65, 92, 93, 113-115]. To test whether Ipl1 directly regulates condensin association with chromatin in *S. cerevisiae*, we fused the condensin subunit Ycs4 with mCherry and analyzed its recruitment to chromatin using time-lapse microscopy. In anaphase Ycs4-mCherry accumulates with the *rDNA* marker Net1-GFP [98], this localization did not require Ipl1 activity (**Fig 21**). Thus Ipl1 dependent phosphorylation of condensin in *S. cerevisiae* does not play a crucial role for condensin loading to the *rDNA.* We can however not rule out a role of Ipl1 in regulating condensin activity or its targeting to non-*rDNA* regions.

10. Hyper-condensation depends on phosphorylation of histone H3 serine 10

Another well-known chromatin substrate of Ipl1 during mitosis is Serine 10 on the N-terminal tail of histone H3. Mostly correlative evidence suggested this phosphorylation to regulate chromosome condensation [201]. Mutation of Ser10 to Alanine in the two histone H3 genes *HHT1* and *HHT2* (*H3S10A* mutant) phenocopied Ipl1 inactivation, reducing condensation of *LC(XII:IV)cen12*Δ more than of chromosome IV, specifically in anaphase, and most strongly in the bud (**Fig. 22A-B**). In contrast to *ipl1-321* mutants, segregation of the *LYS4* locus was however not significantly delayed (**Fig. 22C**). Phosphorylation of H3S10 can have various consequences, including the eviction of the heterochromatin specific chromodomain protein HP1 in mammalian cells [202]. Although HP1 homologues are not known in yeast, we cannot rule out that the mutation of H3 on serine 10 has general effects on gene expression, which could indirectly affect chromosome compaction. However, the fact that the *H3S10A* phenotype closely resembles the

phenotype of *ipl1-321* mutants supports the idea that Aurora-dependent phosphorylation of histone H3 at serine 10 mediates, at least in part, adaptive hyper-condensation in anaphase.

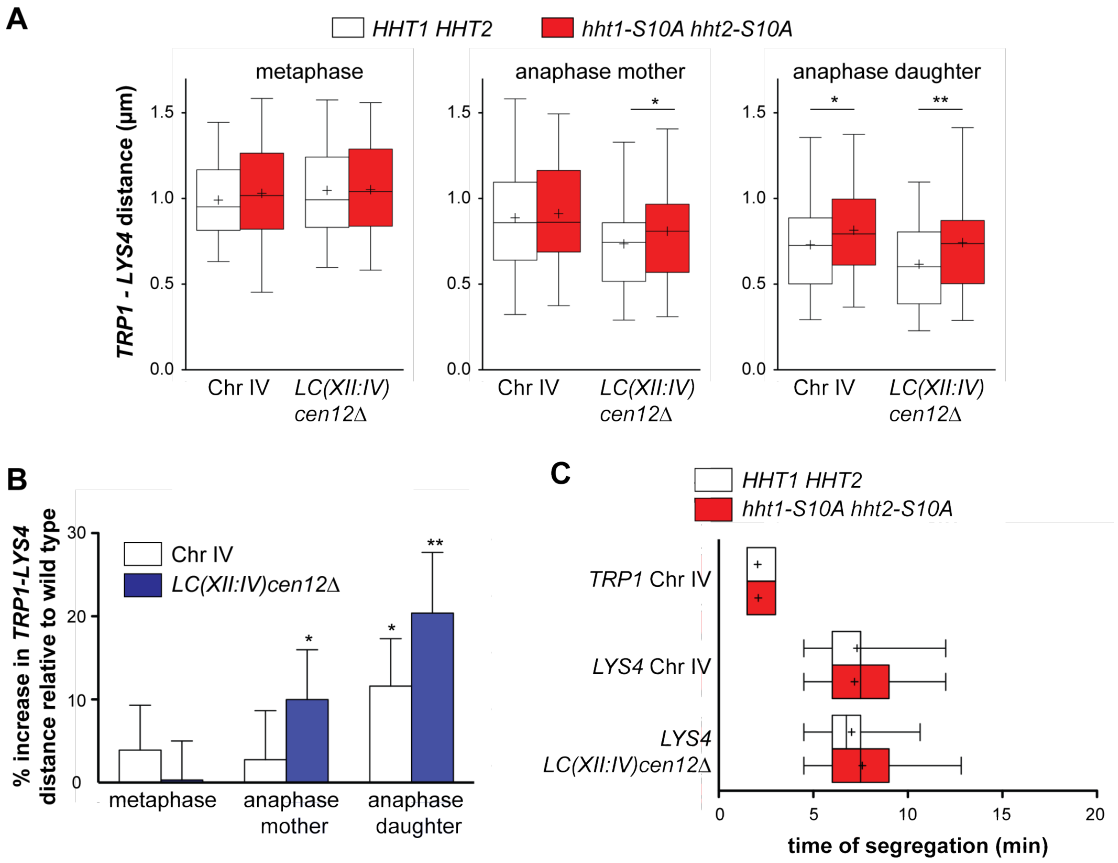

Figure 22: Hyper-condensation of *LC(XII:IV)cen12*Δ depends on phosphorylation of histone H3 on serine 10.
Cells were arrested in G1, released for 1h at room temperature and equilibrated at 30 ºC 15minutes prior to image acquisition. (**A**) *TRP1-LYS4* distances of the indicated strains were determined as in (Fig. 14 E). (**B**) Relative loss of condensation upon Ipl1 inactivation was calculated as the ratio of the mean distance between *TRP1-LYS4* shown in (A). Error bars show standard error of the mean, which was calculated using error propagation (**C**) The time of segregation of the indicated loci relative to anaphase onset was determined as in (Fig. 12F). Used strains: *wild type* (YMM409), *LC(XII:IV)cen12*Δ (YMM527), *hht1-S10A hht2-S10A* (YMM947), *hht1-S10A hht2-S10A LC(XII:IV)cen12*Δ (YMM948), t_0=onset of spindle elongation, N>35.

11. Ipl1 helps to remove cohesin dependent linkages during anaphase

Even though the *H3S10A* and *ipl1-321* mutants show very similar phenotypes regarding anaphase hyper-condensation, only *ipl1-321* mutants show a delay in segregation of the *LYS4* (**Fig. 19C, 22C**). H3 serine10 therefore might not be the only relevant Ipl1 target promoting chromosome arm segregation during anaphase.

11.1. Segregation errors in ipl1-321 mutants suggest sister chromatid linkages during anaphase

Analysis of the segregation trajectories of *LYS4* in *ipl1-321* mutants showed that after initial segregation, the daughter directed locus was often pulled back into the mother cell (**Fig. 23A-C**). Such back-and forth movements have been observed on dicentric chromosomes and in topoisomerase II mutants [168]. We therefore hypothesized that mechanical linkages between sister chromatids persisted in anaphases without Ipl1 activity.

11.2. Separase localization is aberrant in slk19∆ mutants and cannot be rescued by SLI15-6A expression

Sister chromatid cohesion is mainly regulated through the cohesin complex, which is cleaved and inactivated by separase [122]. A recent study showed that the protease activity of separase is still required during late anaphase [168]. Interestingly the spindle-localization of the budding yeast separase Esp1 is aberrant in *slk19∆* mutants, which show a severe delay in chromosome arm segregation. Targeting of Ipl1 to the spindle by expressing *SLI15-6A* in *slk19∆* mutants restores chromosome segregation but not Esp1 localization (**Fig. 20B, 23D**). It is possible that targeting of Ipl1 to the spindle midzone can compensate for the mis-localized separase in *slk19∆* mutants, possibly through removal of cohesin from chromosome arms in anaphase.

11.3 Ipl1 may contribute to removal of cohesin during anaphase

To directly test whether Ipl1 is needed to remove cohesin during anaphase we inactivated the conditional allele of a cohesin subunit, *scc1-73*, in the absence of Ipl1 activity. Because inactivation of cohesin led to an increase in the size of the metaphase spindle, we could not use onset of spindle elongation to define entry into anaphase. As mentioned in the introduction, the Cdc14 phosphatase gets activated and released from the nucleolus at anaphase onset. This depends on the activation of separase after satisfaction of the spindle assembly checkpoint (SAC). We therefore defined anaphase onset as the time when the fusion protein Cdc14-tdTomato was released from the nucleolus. The *scc1-73* single mutant cells were excluded from the analysis because they showed aberrant anaphases: cells elongated their spindles without releasing Cdc14-tdTomato from the nucleolus (data not shown), indicating that *scc1-73* cells attempted to segregate their chromosomes in the presence of an activated SAC. In the *scc1-73 ipl1-321* double mutant however, Cdc14 activation occurred normally (**Fig. 23E**), presumably because Ipl1 itself is required for SAC activation [203]. Importantly, the time required to completely segregate the *rDNA* array was increased in an *ipl1-321* mutant and this was reversed when cohesin was inactivated simultaneously in an *scc1-73 ipl1-321* double mutant (**Fig. 23E-F**). This suggests that Ipl1 helps to remove residual cohesin during anaphase. It is however not clear whether Ipl1 directly targets cohesin or whether this is an indirect effect. Chromosome condensation was suggested to promote removal of cohesin during anaphase [168], and therefore Ipl1 could indirectly help to remove cohesin by promoting condensation.

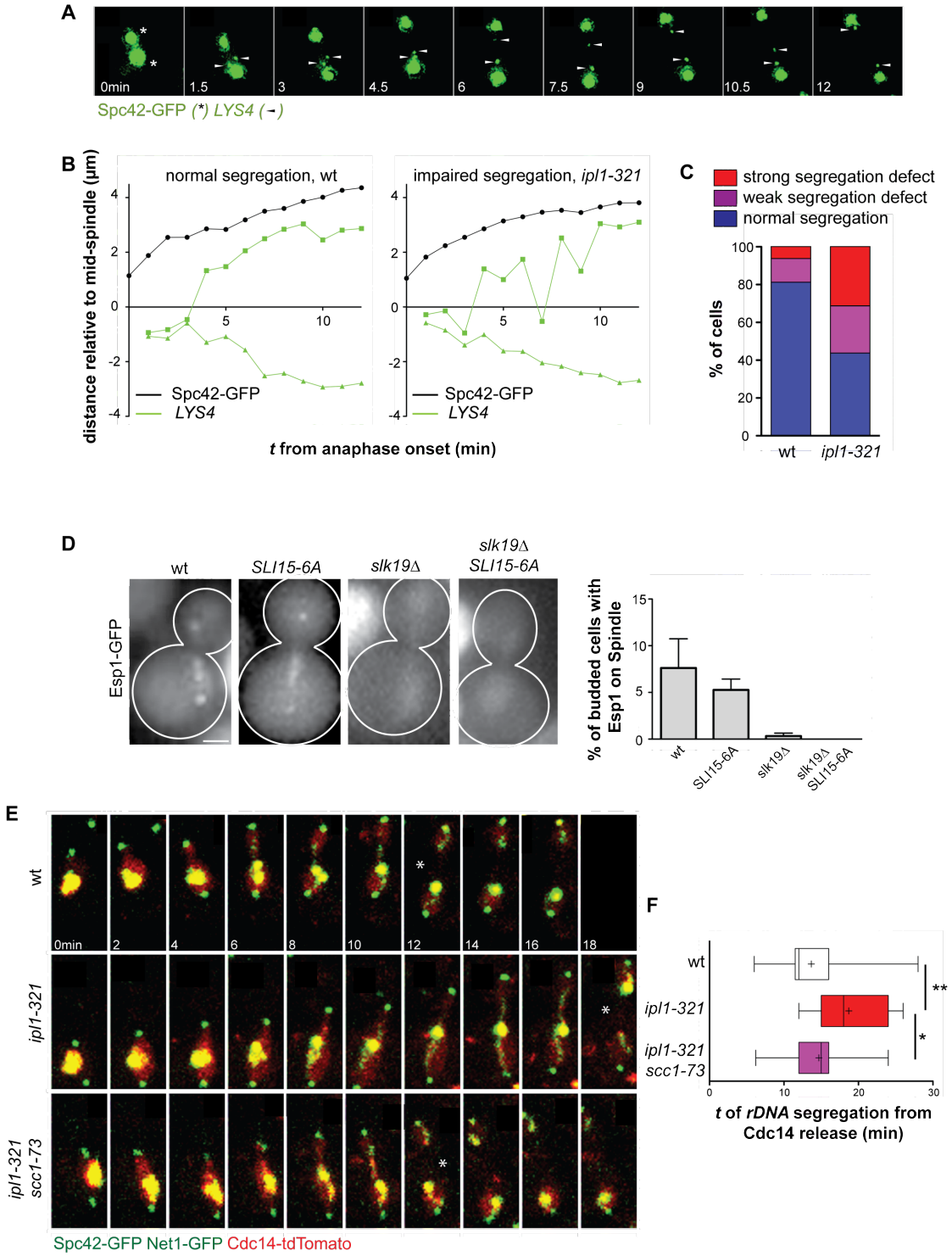

Figure 23: Ipl1 promotes the resolution of cohesin dependent linkages between sister chromatids.
(**A-C**) Analysis of the segregation defects of in *ipl1-321* mutant cells expressing Spc42-GFP and with a fluorescently tagged LYS4 locus (the same data as used for (Fig. 19)) (**A**) The image series shows an anaphase of an *ipl1-321* mutant cell, in which an already segregated *LYS4* locus moves temporarily back into the mother cell. (**B**) The

position of the spindle pole bodies and the *LYS4* loci was determined relative to the middle of the spindle in two representative cells of the indicated genotype (*wt*: YMM409; *ipl1-321*: YMM410). (**C**) Quantification of the observed segregation defects. Segregation was classified as impaired, when the *LYS4* locus showed back- and forth movement in anaphase. This was considered to be strong when the locus crossed the middle of the spindle as seen in (A) and (B). (**D**) *pGAL1:ESP1-GFP* bearing integrative plasmids were transformed into the indicated backgrounds (*wild type* (YMM1302), *slk19*Δ (YMM1303), *SLI15-6A* (YMM1304), *slk19*Δ *SLI15-6A* (YMM1305)). Cells were grown to exponential phase in rich (YP) raffinose medium at 30 °C. Esp1-GFP expression was induced by adding 2% galactose for 1h before image acquisition. For each condition >100 large budded cells were selected using the DIC channel and scored for Esp1-GFP localization to the spindle. The graph shows mean ± SEM of three independent clones analyzed for each genotype. The scale bar is 1 µm. (**E-F**) Cells expressing the fusion proteins Cdc14-tdTomato, Net1-GFP (nucleolar protein), and Spc42-GFP (spindle pole component): *wild type* (YMM564), *ipl1-321* (YMM639), *ipl1-321 scc1-73* (YMM1374). Cells were arrested in G1 and released at room temperature. After 45 min cells were shifted for another 45min to 37 °C prior to image acquisition. (**E**) Representative image series of cells of the indicated genotype. Release of Cdc14-tdTomato from the nucleolus can be observed in the second frame. Asterisks indicate the frame in which *rDNA* segregation is completed. (**F**) Segregation of the *rDNA* was measured relative to release of Cdc14-tdTomato from the nucleolus. In *ipl1-321* and *ipl1-321 scc1-73* mutants, about 60% of the cells had to be excluded form the analysis because the *rDNA* did not segregate at all in anaphase.

12. The level of anaphase condensation scales with the size of the mitotic spindle

So far we have shown that increasing chromosome arm length leads to increased chromosome condensation. We propose that the mitotic spindle acts as a molecular ruler, which measures chromosome arm length and adjusts its condensation state to the length of the spindle (**Fig. 28**). One prediction of this model is that cells with smaller spindles will compact their chromosomes more than cells with larger spindles. To test this prediction, we analyzed the *TRP1-LYS4* distance on chromosome IV under different growth conditions, which affected the size of the mitotic spindle. Indeed the *TRP1-LYS4* distance was smaller under growth conditions, which promoted smaller spindles (**Fig. 24A**). A decrease in *TRP1-LYS4* distance was also observed when spindle size was reduced by introducing the *whi3*Δ mutation (**Fig 24B**), which leads to decreased cell size due to premature entry into the cell cycle

[204]. This shows that spindle size scales with chromosome condensation under physiologically relevant conditions.

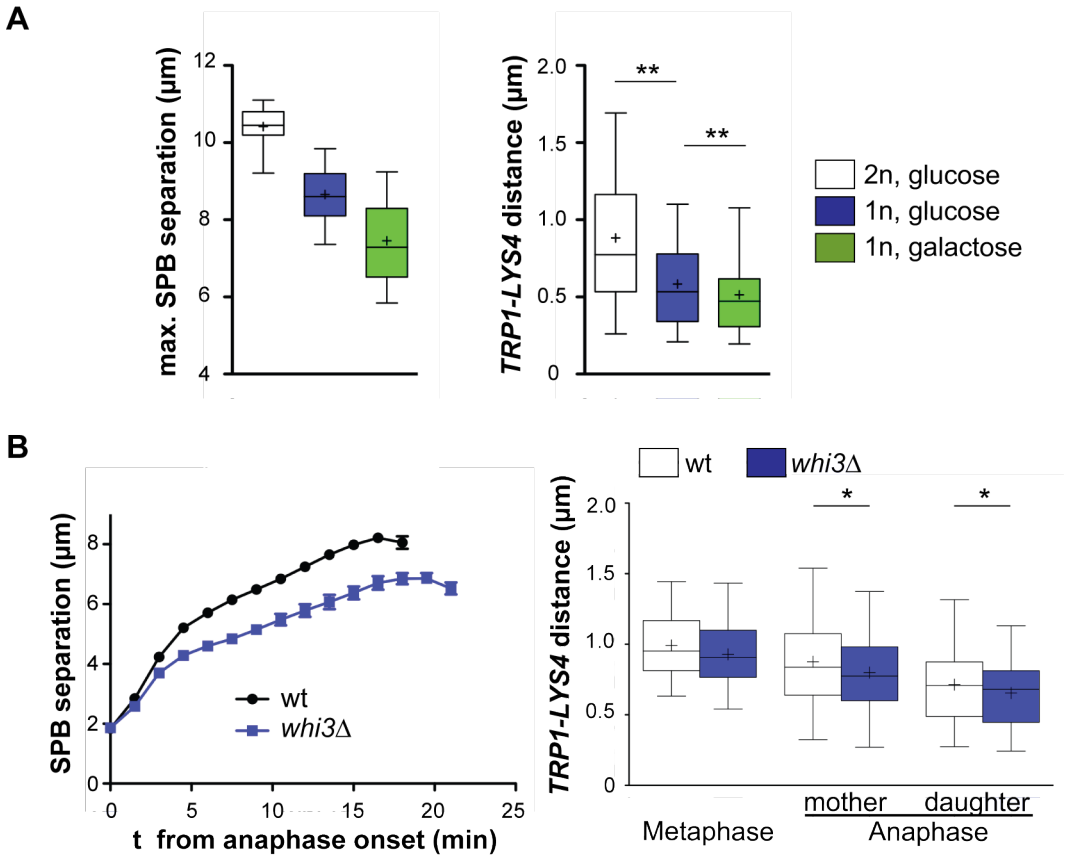

Figure 24: Chromosome compaction scales with the size of the anapahse spindle.
(**A**) *Left* Quantification of the maximal anaphase spindle size of a diploid (2n) (YMM772) and a haploid (1n) *wild type* yeast strain (YMM409) imaged under the indicated growth conditions at room temperature. *Right* The *TRP1-LYS4* distance determined as in (Fig. 14 E) in anaphase after complete chromosome segregation on the bud directed sister chromatid. (**B**) *Left* Spindle dynamics (mean ± SEM) and *right* *TRP1-LYS4* distances in wild type (YMM409) and *whi3*Δ (YMM 1389) cells (N=24). *TRP1-LYS4* distances was determined from segregation of *LYS4* until maximal spindle elongation (7.5-18min for wt, 10.5-21min for *whi3*Δ).

13. Ipl1 is not required for timely activation of Cdc14, but for its inactivation in telophase

13.1 Cdc14 activity is needed for Ipl1 induced segregation of chromosome arms

We have previously shown that expression of non-phosphorylatable *SLI15-6A* rescues delayed chromosome arm segregation of *slk19*Δ mutants (Chapter 8). Our interpretation of this result was that Ipl1 at the spindle midzone directly induces chromosome arm compaction and thus circumvents the defects caused by delayed Cdc14 activation in an *slk19*Δ mutant. This predicts that *SLI15-6A* expression should have the same effect when expressed in a *cdc14-1* mutant. Cdc14 is known to be required for the complete segregation of chromosome XII due to its role in repression of *rDNA* transcription [98, 99, 102, 151, 152] We found here that the *cdc14-1* mutant also delayed segregation of *rDNA*-free chromosome arms (**Fig. 25A**). In contrast to *slk19*Δ mutants however, *SLI15-6A* expression did not rescue the delay in *cdc14-1* cells (**Fig. 25A**). Thus, Ipl1 requires Cdc14 activity in order to induce chromosome compaction. This raised two possible scenarios: 1) Ipl1 and Cdc14 act in parallel pathways, which are both essential to promote chromosome condensation or 2) Ipl1 targeting to the spindle midzone could promote Cdc14 activation.

13.2 Ipl1 activity is not needed for timely release of Cdc14 from the nucleolus but for timely re-import

To test whether Ipl1 is involved in activation of Cdc14 in anaphase, we monitored Cdc14 activation by measuring Cdc14-tdTomato release from the nucleolus in time lapse series (**Fig. 25B**). This method readily detected Cdc14 activation delays in the known mutants *slk19*Δ, affecting early stages of Cdc14 release [155], and *cdc15-1*, which is needed for sustained Cdc14 release in late anaphase [205] (**Fig. 25C**). In *ipl1-321* mutants release of

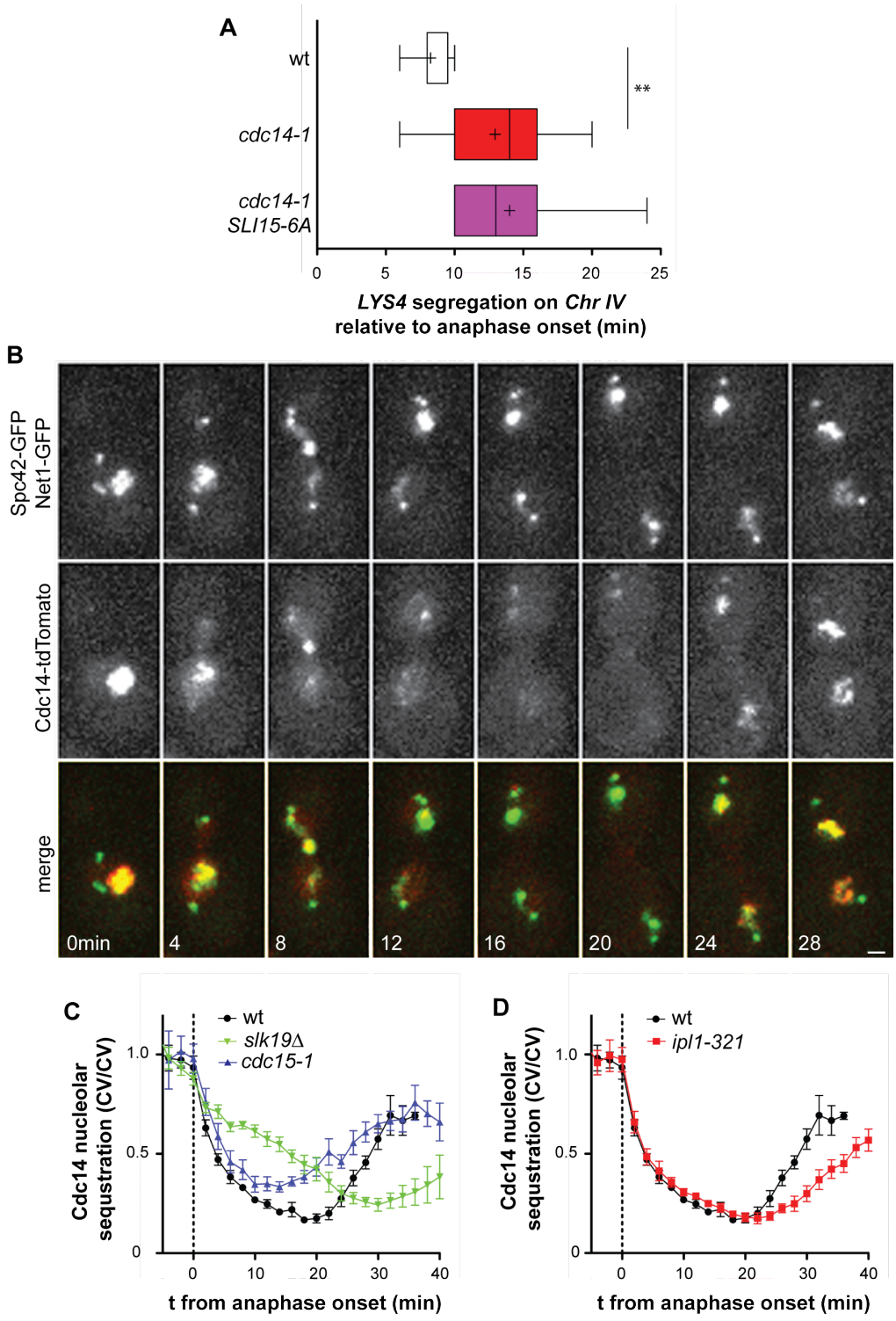

Figure 25: Ipl1 is required for timely Cdc14 inactivation
(**A**) Data from the analysis of image series of exponentially growing diploid cells, shifted to 37 °C 15min before image acquisition: *wild type (CDC14/CDC14 SLI15/SLI15; YMM772); cdc14-1 (cdc14-1/cdc14-1 SLI15/SLI15; YMM1209); cdc14-1 SLI15-6A (cdc14-1/cdc14-1 SLI15/SLI15-6A; YMM1226).* (**B-D**) Data from time lapse image

series of cells arrested in G1 and released at 37 °C for 2h prior to image acquisition. (**B**) Representative image series of a wild type cell expressing Cdc14-tdTomato, the spindle pole body marker Spc42-GFP and the nucleolar marker Net1-GFP. (**C-D**) Quantification of Cdc14 release from the nucleolus for *wild type* (YMM564), *slk19*Δ (YMM1129), *cdc15-1* (YMM641), *ipl1-321* (YMM639). The graph shows the coefficient of variation (CV=standard deviation/mean, see methods section) of Cdc14-tdTomato normalized by the CV of the GFP signal. t_0=onset of spindle elongation.

Cdc14-tdTomato occurred like in wilt type cells. The re-import of Cdc14 to the nucleolus happened however later and at a lower rate (**Fig. 25D**). Thus Ipl1 is not required for Cdc14 activation but plays a role in its re-sequestration into the nucleolus in telophase.

13.3 Clb2 and Cdc5 are degraded with wild type kinetics in the absence of Ipl1 activity

Re-sequestration of Cdc14 at the end of anaphase depends on Bub2-Bfa1 and requires degradation of the polo kinase Cdc5 by APC^{Cdh1} [159]. To test whether activation of APC^{Cdh1} was impaired in *ipl1-321* mutants, we followed the degradation kinetics of the APC^{Cdh1} substrates Cdc5 and the mitotic cyclin Clb2 in cells released from a Cdc20-depletion metaphase arrest (**Fig. 26A)**. By western blot analysis however *ipl1-321* mutants and wild type cells degraded Clb2 and Cdc5 with identical kinetics. Also when *ipl1-321* mutant cells were arrested in G1 using α-factor and released at restrictive temperature, no delayed degradation of Clb2 could be detected (**Fig. 26B**). Thus Ipl1 does not seem to be involved in activating APC^{Cdh1} and we still do not understand why Cdc14 re-import is delayed in *ipl1-321* mutants. Possible scenarios are that Ipl1 helps to inactivate Tem1, for example by activating Bub2-Bfa1, or that Ipl1 increases the binding of Cdc14 to Net1 in the nucleolus directly through chromatin modifications. We also do not understand yet the consequences of delayed re-import of Cdc14 and should be further investigated.

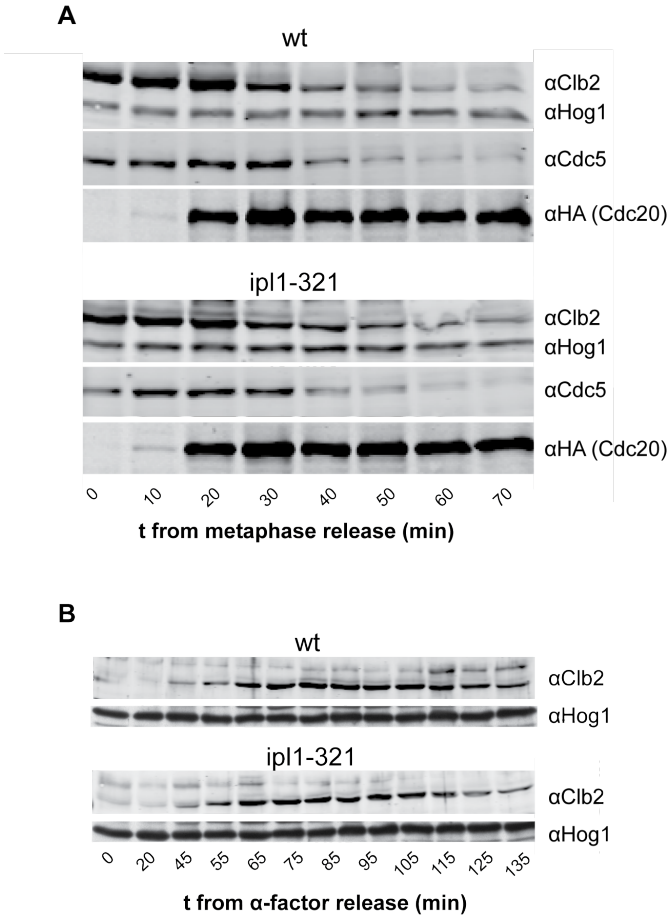

Figure 26: Ipl1 is not required for timely degradation of APC^{Cdh1} substrates
(**A**) *IPL1* (YMM1050) and *ipl1-321* (YMM1051) cells were arrested in metaphase by transcriptional repression of Cdc20 (see methods section). After 2h arrest at room temperature, cells were shifted for 1h to 37 °C before release at 37 °C. Samples were taken at the indicated time points following the induction of Cdc20 expression. (**B**) IPL1 (YMM1148) and *ipl1-321* (YMM1149) cells were arrested for 2h at room temperature in α-factor and released at 37 °C, samples were taken at the indicated time points. After 60min α-factor was added to prevent cells from entering the next cycle. Samples were fixed immediately and processed for western blot analysis (see methods section).

Concerning the condensation of chromosome arms, we conclude that Aurora induced chromosome arm compaction is dependent on Cdc14 activity. The reason why *SLI15-6A* expression is able to induce chromosome arm compaction in *slk19*Δ but not in *cdc14-1* mutants however remains unclear. Two scenarios could explain the apparent paradox. In *slk19*Δ mutants there could be some residual Cdc14 activity in early anapahse as compared to complete inactivation in *cdc14-1* mutants. This small amount of Cdc14 activity could be sufficient to down regulate transcription and allow the accumulation

of condensin on the DNA, but insufficient for Ipl1 targeting to the mitotic spindle. If this scenario, artificial targeting of Ipl1 to the mitotic spindle could induce chromosome condensation only in *slk19*Δ mutants but not in *cdc14* mutants.

Alternatively *slk19*Δ cells could, on top of delaying Cdc14 activation, have additional Cdc14 independent defects, which could be rescued by targeting Ipl1 to the mitotic spindle. Indeed, the separase Esp1 localizes to the anaphase spindle in *cdc14-2* mutants [162], but not in *slk19*Δ mutants (our study). Expression of *SLI15-6A* does not rescue the localization of Esp1 in *slk19*Δ mutants (**Fig. 23D**). Instead, targeting of Ipl1 to the mitotic spindle may compensate for the lack of separase. In fact we have presented evidence here that Ipl1 helps to remove cohesin form chromosome arms in anaphase (**Fig. 23E-F**). This view is supported from preliminary results of *bns1*Δ *spo12*Δ mutants, in which Cdc14 activation is similarly delayed as in *slk19*Δ mutants [155] but which are not known to affect Esp1 localization to the spindle. In *slk19*Δ cells chromosome arm segregation is more severely delayed than in *spo12*Δ*bns1*Δ cells (data not shown). This suggests that at least a part of the segregation delay in *slk19*Δ mutants is caused by the absence of Esp1 form the mitotic spindle. Expression of SLI15-6A can rescue chromosome arm segregation in *slk19*Δ but not in *spo12*Δ*bns1*Δ mutants (data not shown), suggesting that Ipl1 targeting to the anaphase spindle may indeed compensate for the lack of separase.

V. Discussion

To address the question whether chromosome size is coordinated with the length of the mitotic spindle, we have generated largely oversized chromosome arms by means of chromosome fusion. The fused chromosomes were well tolerated during mitosis. Adaptation to the increased chromosome arm length required DNA condensation, as it depended on the activity of condensin and Cdc5.

Analysis of the DNA content and structure of the compound chromosomes revealed that cells reduced the physical length of the fused chromosomes through different mechanisms:

The *rDNA* array on the LC(XII:IV) decreased in size relative to when located on chromosome XII by reducing the number of *rDNA* repeat copy number.

Condensation of the *TRP1-LYS4* region normally found on chromosome IV increased when placed on the compound chromosome. This response did not affect all chromosomes in the nucleus, but was specific for the long chromosome. When *TRP1-LYS4* was placed distally from the active centromere, hyper-condensation was observed throughout mitosis. We showed evidence that centromeres are able to reduce compaction in centromere proximal regions independently of their attachment to mitotic spindles. This suggests that centromere distal regions are more condensed than centromere proximal regions due to the increased distance to an active centromere.

If the *TRP1-LYS4* region was placed centromere proximal on the fusion chromosome hyper-condensation was detected specifically in late anaphase. Anaphase hyper-condensation depended on the Aurora kinase Ipl1, it's localization on the spindle midzone and on phosphorylation of histone H3 on

serine 10. We suggest that the level of chromosome condensation in anaphase is adjusted to the length of the mitotic spindle. Consistent with this, the level of chromosome condensation inversely correlates with the length of anaphase spindles.
Furthermore we suggest that Ipl1 might be involved in removing cohesin dependent inter-chromatin linkages during anaphase and we propose a new role for Ipl1 in promoting the reimport of Cdc14 to the nucleolus in telophase.

1. The rDNA array on compound chromosomes is smaller than on chromosome XII

In order to understand how cells adapted to the increased chromosome arm size we analyzed the DNA sequence of compound chromosome carrying cells. Whole genome sequencing of the yeast strains carrying the compound chromosomes did not reveal any major alteration in the genome besides the chromosome fusion, showing that the compound chromosome can be maintained stably. However, using quantitative real-time PCR we found a decrease in the size of the *rDNA* array located on the compound chromosome compared to wild type chromosome XII. The number of copies was lower on *LC(XII:IV)cen12*Δ compared to *LC(XII:IV)cen4*Δ*.* What could be responsible for this reduction?

Two different processes can lead to a reduced *rDNA* copy number on the long chromosomes. Since the number of *rDNA* repeats varies naturally from cell to cell [46], when generating the compound chromosome, fusion could occur preferentially in cells with relatively small *rDNA* arrays. Alternatively, the reduced size of the *rDNA* array can be the result of selection after chromosome fusion. We cannot easily distinguish between the two possibilities because analysis of the copy number occurred at least 50 generations after chromosome fusion. To test whether *rDNA* copy number

was already reduced at the time of chromosome fusion, expansion and retraction of the *rDNA* array could be prevented through deletion of the replication fork blocking protein Fob1 [47] prior to chromosome fusion.

One trait influenced by the *rDNA* copy number is the length of the chromosome arm. Oversized chromosomes could for example more frequently mis-segregate and thus be selected against. Reducing the number of *rDNA* repeats would then be an advantage. This hypothesis is especially attractive because in budding yeast the only *rDNA* array is located on the longest naturally occurring chromosome arm. This raises the possibility that in wild type cells the maximal tolerated length of the chromosome arm determines the maximal possible number of *rDNA* copies by limiting expansion of the array. Interestingly most other eukaryotes have several *rDNA* arrays distributed on different chromosomes. If chromosome arm length can become limiting to *rDNA* array expansion, such an organization would allow a much bigger maximal number of *rDNA* copies.

Indeed, one observation suggests that the reduction in *rDNA* copy number on the compound chromosome is related to difficulties in segregating the *rDNA* locus during anaphase. We have found that the *rDNA* array is shorter on *LC(XII:IV)cen12*Δ than on *LC(XII:IV)cen4*Δ. On *LC(XII:IV)cen12*Δ the *rDNA* locus is 1.5Mb away from the active centromere compared to 0.3Mb on *LC(XII:IV)cen4*Δ. The *rDNA* on *LC(XII:IV)cen12*Δ therefore segregates later in anaphase and has less time to fully resolve. Reducing the number of *rDNA* repeats could therefore be especially beneficial on *LC(XII:IV)cen12*Δ. To further test whether the length of the chromosome arm limits the expansion of the *rDNA* array one could reduce the size of chromosome XII instead of making it longer as we did. This has actually been done by fragmenting chromosome XII into two individual chromosomes. Removal of the 650kb region between the rDNA and the telomere of chromosome XII was well tolerated. It would be interesting to know whether the size of the *rDNA* array was increased in these cells but this has not been systematically addressed in that study [205].

Changing the position relative to the active centromere is however not only important during anaphase, but may also affect the subnuclear localization of a chromatin region [206]. Tethering of the *rDNA* to the nuclear periphery has been shown to be crucial to stabilize *rDNA* copy numbers by suppressing recombination within the *rDNA* array [207]. Loss of perinuclear tethering led to an increase of rDNA repeats [207]. Thus if the observed lower number in *rDNA* copies on *LC(XII:IV)cen12*Δ compared to *LC(XII:IV)cen4*Δ is a result of changed subnuclear position, the *rDNA* on *LC(XII:IV)cen12*Δ would be expected to be more closely associated with the nuclear periphery.
The stability of the *rDNA* array, namely the accumulation of ERCs, has also been implicated to play an important role in replicative senescence [208]. It would be interesting to find out whether fusing chromosomes IV and XII also affects replicative life span.

Independently of what is causing the decrease in *rDNA* copy number one would expect direct consequences on cell physiology. Under conditions where ribosome production is limiting, a reduction of *rDNA* copies should result in decreased growth rates. We were however not able to detect any difference in growth rates between wild type cells and cells carrying the *LC(XII:IV)cen12*Δ, on which the number of rDNA copies was reduced by almost 50%. In rich glucose based medium at 30 °C *wild type* strains had a generation time of 129±8 min while cells carrying *LC(XII:IV)cen12*Δ had a generation time of 129±3 min (±SEM, N=3; Francesca Di Giovanni and Manuel Mendoza, unpublished observations). This suggests that the same number of *rDNA* repeats are being transcribed in both cell types. This means that the number of silenced repeats must be reduced on the *LC(XII:IV)cen12*Δ. A reduction in silent *rDNA* copies was shown to confer increased sensitivity to the DNA damaging agents MMS and UV irradiation [45]. We would thus expect that chromosome fusion increases cellular sensitivity to DNA damage. Cells carrying the fusion chromosome were however not more sensitive to hydroxy urea. We did however detect a synthetic interaction between cells carrying a

compound chromosomes and the temperature sensitive *smc6-9* mutation (Iris Titos and Manuel Mendoza, unpublished observations). The Smc5-6 complex is required to establish DNA-cohesion for homologous recombination during DNA double strand break repair [136] but is also needed for the segregation of the *rDNA* locus in anaphase [137]. Interestingly, the Smc5-6 complex was shown to be enriched on long chromosome arms [138]. *LC(XII:IV)cen4*Δ*,* the compound chromosome with the longer chromosome arm and with more *rDNA* repeats, was more sensitive to loss of SMC6 activity. We therefore believe that the synthetic interaction is caused by a failure to fully resolve the long chromosome arms in anaphase or by other problems that result from increased chromosome arm length but that we do not understand yet.

2. Centromere distal chromatin is hyper-compacted

Outside of the *rDNA* locus we did not detect any major changes in DNA content of the compound chromosome. Using live cell microscopy we observed increased axial compaction between the *TRP1* and *LYS4* loci on *LC(XII:IV)cen4*Δ when compared to chromosome IV. This increased compaction was observed throughout mitosis. During metaphase the different compaction on chromosome IV and *LC(XII:IV)cen4*Δ could be attributed to the changed position of the analyzed region relative to the active centromere.

The increased compaction of the *TRP1-LYS4* region on *LC(XII:IV)cen4*Δ shows that centromere distal chromatin is more compacted than centromere proximal chromatin. A similar observation has been made when comparing a centromere proximal with a centromere distal region on wild type chromosome IV using the LacO/LacI reporter system in live cells [176]. This observation helps to explain that centromere distal loci segregate more efficiently than centromere proximal loci: The length of the mitotic spindle

required to segregate a given locus does not need to increase linearly with the distance of that locus relative to the active centromere because distal regions are more compacted.

The observed increased compaction is most likely a result of several processes. In metaphase, we could show that inactivation of *CEN4* on chromosome IV leads to the same increase in compaction as placing the whole chromosome IV at the tip of chromosome XII. One possibility is that attachment of the kinetochores to the mitotic spindle and their alignment at the metaphase plate forces the centromere proximal chromatin into a more extended conformation. 3D models of the haploid yeast genome based on chromosome conformation capture data support a role of the mitotic spindle in shaping chromosome conformation: The position of each chromosome seems to be dictated by the way the chromosomes were segregated in mitosis. Centromeres are clustered at one end of the nucleus, creating a zone with high DNA density. Possibly as a consequence of this, the centromere proximal regions all adapt an extended conformation. The tips of the long chromosome arms extend to the opposite end of the nucleus, where the concentration of chromatin is lower. These chromatin regions tend to fold onto themselves and take on a more compacted chromosome conformation (**Fig. 27**) [206].

From these observations it seems plausible that spindle forces help to shape mitotic chromosomes. Disrupting the kinetochore-microtubule attachment by treating the cells with nocodazole did however not induce the same increase in compaction as observed for inactivation of the centromere. These experiments are however not fully comparable: While centromeres were inactivated directly when released from G1, depolymerization of the spindle microtubules was performed in metaphase. It is possible that centromere-microtubule attachment prior to metaphase is sufficient to force centromere proximal regions into an extended conformation. To directly compare the two

experiments, microtubules should be depolymerized when cells are released from G1, at the same time as the centromere is inactivated with the *pGAL1* promoter. This would allow distinguishing between a direct effect of the centromere on the structure of the adjacent chromatin or a more indirect effect through attachment to the mitotic spindle.

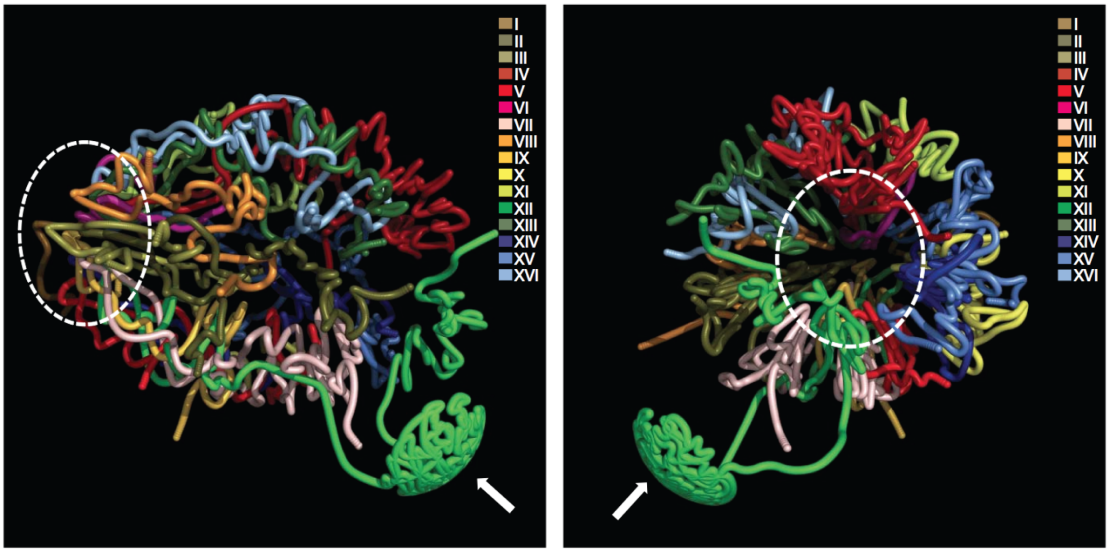

Figure 27: 3D model of the yeast genome
This image was taken from [206]. It shows a model of the yeast genome that was calculated based on chromosome conformation capture data form exponentially growing yeast cultures. The position of the chromosomes in the nucleus reflects the expected position of chromosomes in telophase with the centromeres clustering at one end and the chromosome arms extending in the other direction. Color labels for the individual chromosomes are indicated in the top right corner.

3. Chromosome condensation and spindle length are coordinated

Both increasing the length of chromosome arms and decreasing the size of the anaphase spindle induces increased chromosome compaction, and thus spindle size is coordinated with chromosome compaction. One prediction of this is that smaller chromosomes are less condensed than larger chromosomes. Indeed this is the case when comparing our data with other studies that measured chromosome compaction in live cells using the TetO/LacO-system. The distance between two loci spaced by 180kb on the

long arm of chromosome VII was measured to be around 0.8µm from G1 to metaphase [168]. On the right arm of chromosome IV, which is about twice the size of the arm of chromosome VII, we measured the same distance for a 450kb region in metaphase. The bigger chromosome IV therefore seems to be compacted twice as much as chromosome VII. Unfortunately no comparable data for anaphase condensation is available for chromosome VII.

The coordination between spindle length and chromosome size could be crucial during the early development of multicellular organisms, during which spindle size changes dramatically [174, 175]. In *X. laevis* chromosome condensation can be reconstituted in vitro. A recent study showed that the relative abundance of the condensin I and condensin II complexes influence the level of axial compaction of chromosomes. In meiotic egg extract, the condensin I:condensin II ratio is 5:1. If this ratio was brought to 1:1 by reducing the amount of condensin I, chromosome length became smaller. If the ratio stayed constant and both complexes were reduced 5-fold, the length of the chromosome arms was the same as before dilution of the extract [209]. In another study chromosomes were isolated from G2 arrested embryos of different developmental stages and condensation was induced by placing them in metaphase egg extract. Chromosomes isolated from older embryos (stage20, small cells) condensed more than chromosomes isolated from young embryos (stage 6, big cells) [210]. Epigenetic information on those chromosomes therefore defines how much they need to condense. To change this information, a passage through the cell cycle is required [210]. While condensin II already binds to chromosomes before mitosis, condensin I is not loaded until after nuclear envelope breakdown [96]. In the in vitro condensation system, condensin I therefore must stem from the same metaphase extract for all chromosomes, while condensin II was probably loaded onto chromosomes before their isolation from differently staged cells of origin. One explanation for the increased axial compaction could therefore be a higher level of condensin II on chromosomes of older and smaller cells. This would predict that the levels of condensin II on chromosomes increase

during development and that changing the levels of condensin II requires a passage through the cell cycle.
It is however also tempting to speculate that midzone mediated chromosome condensation, as we have described it here, adjusts chromosome size to anaphase spindle length in *X. laevis.* It would therefore be interesting to know when in the cell cycle the condensation information on a chromosome is changed. Aurora-dependent anaphase chromosome condensation has been observed in *S. pombe* and human cells [92, 93, 110], suggesting that adaptive anaphase condensation is conserved. As controlled manipulation of chromosome size is difficult to achieve in higher eukaryotes, interfering with spindle size and monitoring the effect on anaphase compaction would be the experiment of choice to test whether the coordination of spindle size with chromosome compaction is conserved.

Interestingly, condensin inactivation not only prevented chromosome arm segregation in anaphase but also caused the anaphase spindles to elongate further than under wild type conditions. This suggests bidirectional signaling between chromatin and the elongating anaphase spindle: the spindle promotes chromatin condensation while unsegregated chromatin fosters spindle elongation. As the yeast polo like kinase Cdc5 is required for both, chromosome condensation [111] and anaphase spindle elongation [197], the clear genetic interaction between Cdc5 and the compound chromosome is not surprising.
A possible mechanism for the observed hyper-elongation of the anaphase spindle could include the Aurora kinase Ipl1. In wild type yeast cells Ipl1 accumulates on the mitotic spindle during anaphase, but this does not happen in the condensin mutant *smc2-8* [198]. Because Ipl1 is required for timely disassembly of the mitotic spindle [32], Ipl1-mislocalization could lead to spindle stabilization in *smc2-8* mutants. However, when a mutant allele of another subunit of the condensin complex, *ycg1-2*, was used, mis-localization of Ipl1 in anaphase was not observed when but the anaphase spindles still

increased their elongation (Iris Titos and Manuel Mendoza, unpublished observations). This suggests that the increase in anaphase spindle length happens independently of Ipl1.

Alternatively the increased elongation of the anaphase spindle could be the result of a change in the balance of forces within the mitotic spindle. Altering chromatin structure can indeed influence the dynamics of the mitotic spindle. In budding yeast for example cleavage of cohesin is sufficient to trigger spindle elongation [211]. In Drosophila S2 cells knockdown of the cohesin subunit Rad21 increases the size of the metaphase spindle [212]. The condensin complex is able to linearly compact DNA molecules against a force [106] and in budding yeast is required to recoil stretched chromatids in anaphase [168]. Condensin could therefore oppose anaphase forces that drive the spindle poles apart. Its inactivation could thus change the balance of forces within the spindle and lead to increased spindle elongation. If this were true, hyper-activation of condensin, for example through overexpression of condensin or condensin activators, should decrease anaphase spindle length.

4. Spindle midzone localized Aurora ensures complete chromosome arm segregation

Anaphase specific hyper-condensation of the compound chromosome depended on the Aurora kinase Ipl1 and its localization to the spindle midzone and phosphorylation of histone H3 on serine 10. In HeLa cells a gradient of Aurora B activity centering around the spindle midzone was clearly demonstrated in anaphase [213]. Fixation of cells in anaphase and immuno-labeling of phosphorylated H3S10 resembles the Aurora B activity gradient: H3S10 on tips of chromosome arms and on chromosomes lagging at the spindle midzone is highly phosphorylated [214]. We therefore propose a model in which spindle-midzone localized Ipl1 induces compaction of

chromatin that has not been segregated away from the middle of the spindle, and like this acts as a molecular ruler (**Fig. 28**).

How phosphorylation of H3S10 leads to the observed change in chromosome condensation is not clear. Mitotic phosphorylation of histone H3 has been correlated with a conformational change of the amino terminal tail of histone H3 in breast cancer cells. UV-crosslinking showed that the tail is closely associated with DNA during interphase, while the phosphorylated tail is more loosely associated with DNA during mitosis [215]. The conformational change of the N-terminal tail of histone H3 could influence higher order chromatin structure on several levels. The more loosely associated tail of histone H3 could for example weaken the DNA-histone interaction and like this facilitate remodeling of chromatin through repositioning of nucleosomes. Whether H3S10 phosphorylation influences nucleosome position can be tested using chromatin immuno precipitation (ChIP) or MNase digestion in combination with deep sequencing [216]**.**

Another way how histone modification can influence higher order chromatin structure is by influencing the binding affinity between histone tails and non-histone proteins. In mammalian cells phosphorylation of H3S10 was shown to inhibit methylation of histone H3 lysine 9 (H3K9) [217, 218] and blocks binding of the chromodomain protein HP1 to methylated H3K9 [202]. Methylated H3K9 in turn inhibits H3S10 phosphorylation [218]. However, in budding yeast no homologues of HP1 are known and a H3K9 methylation has not been detected [219]. To test whether phosphoryltion of H3S10 alters chromatin composition in budding yeast, H3S10A mutants could be analyzed by mass spectrometry of purified chromatin [220] or by microscopy or ChIP of candidate proteins**.**

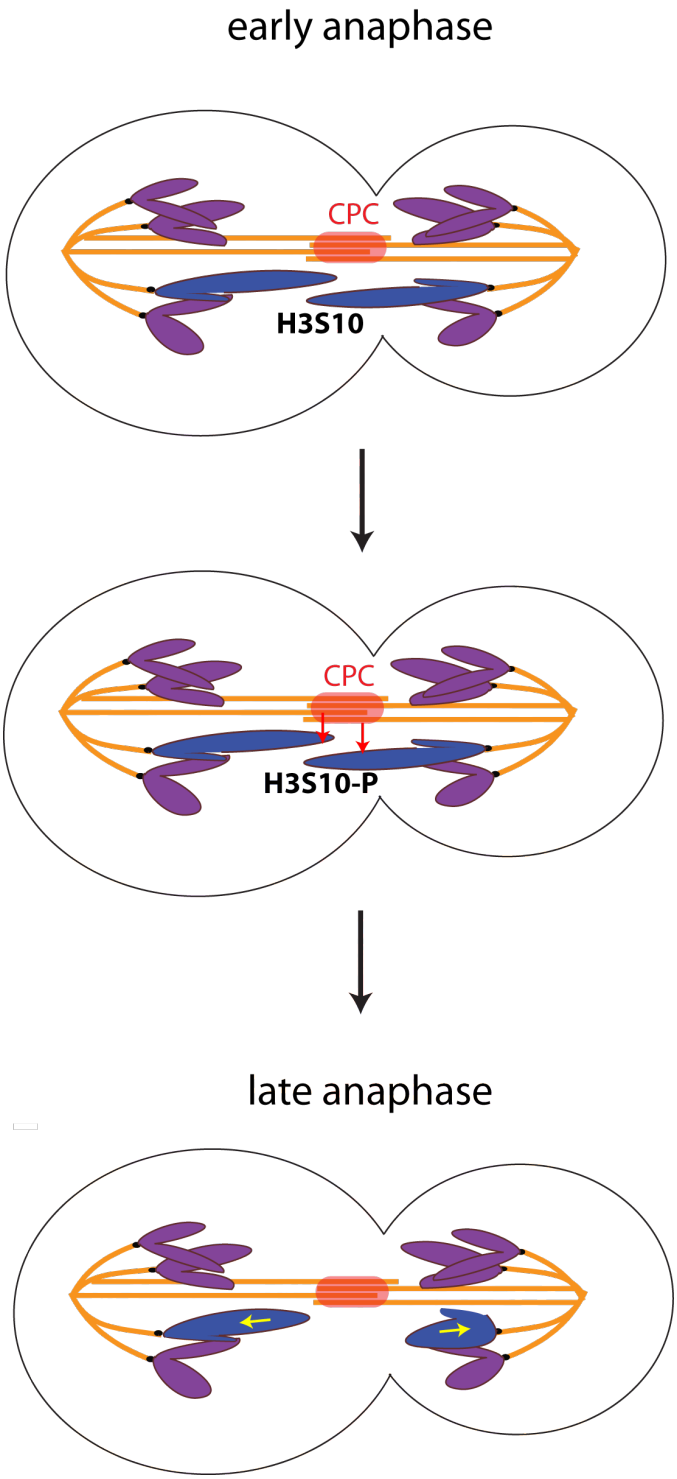

Figure 27: Model for how an Ipl1-dependent signal generated at the spindle midzone induces chromosome condensation.
(CPC: chromosome passenger complex, in red) adjusts the level of condensation of long chromosome arms (in blue) to the length of the mitotic spindle, through phosphorylation of histone H3 on chromosome arms.

While *ipl1-321* mutant cells showed delayed segregation of chromosome arms, such a phenotype was not observed in H3S10A mutants, suggesting that Ipl1 has other targets relevant for chromosome segregation in anaphase. Because several subunits of the yeast condensin complex are phosphorylated in an Ipl1 dependent manner [111, 112] and condensin is essential for chromosome segregation [102-105], we tested whether Ipl1 plays a role in the anaphase accumulation of condensin in the *rDNA*. Using fluorescent microscopy we however observed that condensin was recruited normally to the *rDNA* after inactivation of Ipl1.

Condensin recruitment to mitotic chromosomes was shown to depend on orthologues of Aurora B kinase in a wide range of species [65, 92, 93, 113-115]. Phosphorylation of the barren orthologues by Aurora kinase in *S. pombe* (Cnd2) and *H. sapiens* (CAP-H) was shown to be required for the association of condensin with the amino terminal tail of histone H2A. In *S. pombe* mutation of the phosphorylated residues to alanine is lethal and completely prevents chromosome arm segregation in anaphase [92, 93]. It was therefore surprising that recruitment of Ycs4 to the *rDNA* in anaphase did not depend on Ipl1. It is however also possible that condensin binding outside the *rDNA* is regulated differently and does depend on Ipl1. Because the nucleolar Ycs4-mCherry signal is quite strong in anaphase, binding of condensin to non-rDNA regions is difficult to analyze by microscopy. To circumvent this problem chromatin immuno-precipitation (ChIP) could be used instead.

The observation that condensin loading was only affected in *S. pombe* and not in *S. cerevisiae* is however in agreement with the phenotypic difference between the used Aurora mutants. In *S. pombe* inhibition of the analogue sensitive allele *ark1-as2* led to a complete inhibition of chromosome arm segregation in anaphase, while inactivation of *S. cerevisiae* temperature sensitive allele *ipl1-321* in anaphase only caused a mild chromosome arm segregation delay. Thus either *ipl1-321* is not a null allele or the role of Ipl1 in condensin loading is not conserved in *S. cerevisiae*. In fact the N-terminal

region, in which the human and fission yeast barren orthologues are phosphorylated by Aurora, is not present in *S. cerevisiae*.

In the light of the well-conserved role of Aurora B kinase to regulate condensin localization from fission yeast to humans it appears however unlikely that this mode of regulation should not be present in budding yeast. To further investigate the possibility that Ipl1 directly regulates condensins in *S. cerevisiae*, I have mutated all serines and threonines to alanine in the Ipl1 consensus motives on all condensin subunits. Preliminary results suggest that the generated mutant alleles *ycs4-6A*, *brn1-6A*, *ycg1-3A* and *smc2-7A* (*smc4-7A* was not tested) can still fulfill their essential function, as they can replace temperature sensitive condensin alleles when integrated ectopically into the genome (Gabriel Neurohr and Manuel Mendoza, unpublished). I have however not tested yet whether Ipl1 dependent phosphorylation was fully abolished in these mutants. It is therefore possible that I have missed one or more important phosphorylation sites.

Together we have not found any evidence for an important role of Ipl1 in condensin loading. But even if Ipl1 is not required to load condensin onto chromosomes, it could still play an important role in regulating its activity. For example by locally activating Cdc5 or by priming condensins for phosphorylation by Cdc5. Further experiments using different *IPL1* mutant alleles and a more thorough analysis of the non-phosphorylatable condensin alleles will help to interpret our current observations on the role of Aurora in activating condensin in *S. cerevisiae*.

Interestingly, the delay in *rDNA* segregation observed in *ipl1-321* mutants could be reversed when the cohesin mutant allele *scc1-73* was inactivated simultaneously. This suggested that the segregation delays observed in *ipl1-321* are at least in part caused by residual cohesin that connects the sister chromatid arms in anaphase.

In budding yeast the bulk of cohesin gets removed from chromosome arms at anaphase onset through proteolytic cleavage of Scc1 by separase [135]. A

recent study however suggested that the proteolytic function of separase is still required during anaphase for timely segregation of chromosome arms. When anaphase is prevented through nocodazole addition in a *mad2*Δ mutant, most cohesin is degraded. Anaphase can then be induced by nocodazole removal. In such anaphases the proteolytic function of separase is still required for timely chromosome arm segregation [168], suggesting that cohesin needs to be actively removed from chromosome arms during anaphase. This was supported by the fact that inactivation of cohesin in anaphase reduced chromosome arm stretching [168]. Our results are in agreement with the observation that residual cohesin needs to be removed from the chromosome arms in anaphase.

But how could Ipl1 promote the removal of cohesin form chromosome arms in anaphase? In higher eukaryotes most of the cohesin is removed from the chromosome arms before anaphase [128]. This so called prophase pathway requires Aurora B and polo like kinase and is antagonized by shugoshin [129-134]. In principle an analogous pathway could help to remove cohesin form chromosome arms in *S. cerevisiae* anaphase.

In mammalian cells removal of cohesin from chromosome arms in prophase depends on phosphorylation of the cohesin subunit SA2 (Scc3) [221]. In the frog *X. laevis* polo kinase Plx1 could directly phosphorylate cohesin in vitro, while Aurora B could not [131]. In vivo data however suggest that at least one other kinase than polo like kinase phosphorylates SA2 [134]. In prophase centromeric cohesin is protected by shugoshin, which counteracts SA2 phosphorylation [134]. Inhibition of Aurora B in HeLa allowed shugoshin binding along the chromosome arms [222]. Even though a direct phosphorylation of SA2 by Aurora B cannot be excluded, the evidence suggests that Aurora B in anaphase most likely affects cohesin indirectly through regulating shugoshin localization. In budding yeast however, shugoshin is not required for sister chromatid cohesion in mitosis [223]. It is thus unlikely, that Ipl1 counteracts cohesin in anaphase through inactivating shugoshin analogous to the prophase pathway in mammals.

Resolution of sister chromatids and chromosome condensation are however not independent processes, but they are functionally coupled. Catenated plasmids for example have been shown to be a better substrate for topo II when previously supercoiled by condensin [167]. And overexpression of a viral topo II in yeast can rescue chromosome arm segregation defects of condensin mutants [166]. Condensin does not only help to remove catenanes between sister chromatids, but also cohesin dependent linkages were proposed to be removed in a condensin dependent manner in anaphase [168]. It is thus possible that Ipl1 indirectly promotes cohesin removal by promoting chromosome condensation through either phosphorylation of histone H3 on serine 10 and possibly by activating condensin. Whether Ipl1 directly removes cohesin or indirectly by stimulating condensation is however still not clear.

5. How can the spindle midzone induce condensation in centromere proximal regions?

Spindle midzone induced chromosome condensation can explain why chromosome regions that are exposed for longer to the spindle midzone are more compacted. However, our model (**Fig. 27**) does not explain why the centromere proximal region on the compound chromosome is hyper-condensed during anaphase, because this region segregates with the same kinetics on both chromosomes. A prolonged exposure to the midzone bound Ipl1 can thus not be the explanation for the observed anaphase hyper-condensation. The role of Ipl1 in adaptive hyper-condensation of centromere proximal regions could be explained through several mechanisms.

The only part of the compound chromosome that is exposed for longer to the spindle midzone is the centromere distal region. It is possible that the Ipl1 signal spreads along the chromosome arm to the centromere proximal region. A signal could for example propagate through recruitment of factors, which

promote their own recruitment. Heterochromatic regions can for example expand through recruitment of an enzyme that generates new binding sites for the enzyme complex [224].

Possibly the signal doesn't need to spread along the chromosome arm, but the compound chromosome is more sensitive to the midzone based Ipl1 signal and could condense more efficiently when exposed to Ipl1. Epigenetic marks on the chromosome could for example influence the level of Ipl1 induced condensation. The epigenetic state of the compound chromosome could for example be set in during earlier divisions.

Alternatively, condensation efficiency could be dictated by the nuclear context. On the *LC(XII:IV)cen4*Δ chromosome IV is physically linked to the *rDNA* containing chromosome XII. This means that the *TRP1-LYS4* region is now in physical proximity to *rDNA* specific protein pools. Amongst those are two proteins known to promote anaphase condensation: 1) The phosphatase Cdc14 is sequestered throughout most of the cell cycle in the *rDNA*. During anaphase, Cdc14 gets activated and released into the nucleus [155]. 2) The condensin complex accumulates in the *rDNA* in anaphase in a Cdc14 dependent manner [98, 99]. Whether anaphase hyper-condensation is specific for compound chromosomes containing chromosome XII can be tested by fusing different chromosomes.

Indeed an *rDNA*-free triple fusion chromosome did not show the same level of anaphase hyper-condensation, instead cells carrying these compound chromosomes displayed increased anaphase spindle lengths (Iris Titos and Manuel Mendoza, unpublished observations). This suggests that indeed, the *rDNA* locus affects chromosome condensation efficiency.

Despite of whether *rDNA* influences the efficiency of chromosome condensation or not, we know that adaptive anaphase condensation also takes place on *rDNA*-free chromosomes: First inactivation or mis-localization of Ipl1 causes a compaction defect of chromosome IV in anaphase. Second the correlation between spindle size and chromosome compaction can also

be observed on chromosome IV. Thus the *rDNA* may influence the efficiency, but is not required for adaptive anaphase condensation.

One of the reasons why it is difficult to understand how condensation induced at the spindle midzone can affect centromere proximal regions is our limited knowledge about how mitotic chromosomes are folded. Even though we have structural information of the nucleosome at atomic resolution [225], it has so far not been possible to extend this knowledge to segments of chromatin larger than a few nucleosomes. The reason for this is that once the limits of X-ray crystallography are reached, there is a big gap of structural information until the level of light microscopic information. Several new technologies intend to bridge this resolution gap and promise new insights into higher order chromatin structure in the coming years.

Hope lies on new microscopy techniques with resolution limits around 20nm. These should improve our knowledge about the physiological relevance of 30nm fibers and higher order folding intermediates [226]. To improve the resolution even further these techniques can be combined with electron microscopy [227].

Insight into the 3D structure of chromosomes can also be gained by using chromosome conformation capture (3C) based technologies [228]. Through a series of molecular modifications the physical distance between different fragments on a chromosome is converted into a frequency of ligation products between these fragments. These interaction data can then be used to build models of the 3D configuration of a chromosome [228, 229]. The resolution of this method is in principle limited by the size of the analyzed fragments. To start understanding the structural basis of the adaptive hyper-condensation we have started to analyze the compound chromosomes using chromosome conformation capture carbon copy (5C) (Gabriel Neurohr and Manuel Mendoza, unpublished) [230].

6. What are the consequences of chromosomal translocations on cellular fitness?

Fusion of chromosome IV and XII did not lead to any measurable defects in cell growth. We therefore assumed that cells were able to fully cope with the consequences of chromosome fusion. This assumption is however not necessarily true. As chromosomal translocations are widely observed in cancer cells, the question of whether chromosome fusions stay without any consequences or whether they are able to directly affect gene expression, chromosome stability and mutation rate is of great interest. In the following section I will point out possible consequences, weaknesses in our analysis of cellular fitness and propose experiments to overcome those.

The nucleus is compartmentalized into domains with specialized functions. Silent heterochromatic regions for example have been shown to associate with the nuclear periphery from yeast to mammals. In yeast the 32 telomeres cluster into three to eight foci of silent chromatin [231]. Changing the localization of chromatin within the nucleus can influence DNA repair efficiency [232] and transcriptional activity [233, 234] and hence influence chromatin composition, structure and stability. For the *rDNA* array it has indeed been shown that tethering to the nuclear periphery is required to suppress recombination and stabilize the number of *rDNA* repeats [207]. As mentioned before, the observed reduction in *rDNA* copy number in response to chromosome fusion may indicate that the *rDNA* array has changed its subnuclear localization to a compartment, which is less efficient in preventing recombination between repetitive regions. Increased recombiation rates can be detected by measuring marker loss within or adjacent to the *rDNA* region [207].

At the end of anaphase the two loci on the *LC(XII:IV)cen4*Δ are often found far away from the spindle pole bodies as for example in (**Fig. 14A**). This localization pattern is similar to that of the nucleolus but not to that of *TRP1-LYS4* on chromosome IV. Fusing chromosome IV to the tip of chromosome

XII thus clearly changed the localization of the *TRP1-LYS4* region within the nucleus.

Changing the nuclear compartment could affect the expression level of all genes located on a chromosome. By altering the levels of tumor suppressors and oncogenes, chromosomal translocations could thus promote tumorigenesis. Sequencing of total cellular mRNA levels could reveal changes in gene expression. Preliminary results however do not indicate a general change in expression levels of the genes located on chromosome IV or XII in LC cells when grown in glucose media in exponential phase (Francesca Di Giovanni, Leszec Pryszcz, Toni Gabaldon and Manuel Mendoza, unpublished observations). It remains to be seen whether the same holds true under different growth conditions.

As mentioned earlier we were not able to detect differences in growth rates between wild type and cells carrying compound chromosomes. In a similar study in drosophila cells, where two chromosomes were fused generating an abnormally large chromosome, the syncytial divisions failed in 3% [235]. In unicellular organisms, a complete failure in 3% of all mitosis results in an increase of doubling time of less than 5%. Such small changes in growth rate are difficult to detect by measuring growth rates. Small differences in growth rates could however be revealed more easily using competition assays.

Because it is easier to detect big differences in small numbers than small differences in big numbers, assays that directly measure the mutation rate or mitotic failure would be more sensitive too. Spindle break down for example preceded complete segregation of the compound chromosome in 1 out of 30 anaphases while this was not observed for the segregation of chromosome IV (**Fig. 20E**). This indicates that segregation of the compound chromosome is indeed error prone. Because such events happen at a low frequency, a large sample number is required to get reliable numbers. Higher sample numbers could for example be obtained by counting the percentage of dead cells in a

population using flow cytometry in combination with a vital die [236] or the mutation rate could be measured by marker loss and sectoring analysis [237].
Another reason that could have prevented us from detecting differences in viability is adaptation of the cells to the compound chromosome. It is known that yeast cells are able to adapt to alterations in the karyotype, for example an imbalance of chromosome number (aneuploidy), by accumulating suppressor mutations [238]. The strains we used for growth tests have passed through at least 50 generations since the chromosome fusion. If growth defects were only present in the first divisions after chromosome fusion they would not be detected. It would thus be informative to study cells directly after chromosome fusion either by measuring colony growth rate or by using live cell microscopy. A limiting factor to analyze cells directly after chromosome fusion has so far been the low fusion efficiency of 10^{-8} chromosome fusions per transformed cells. This efficiency could however be increased to 10^{-3} by using the Cre/loxP fusion strategy described in [239]. Using this method I was able to follow a cell under the microscope through the first division after chromosome fusion (data not shown).
Another indication that the long chromosomes can indeed impair cell fitness comes from the observation that cells with fused chromosomes fail to complete meiosis, even when the cells are homozygous for the compound chromosome (Gabriel Neurohr and Manuel Mendoza, unpublished). One possible explanation for this is that while in mitosis the increased chromosome size leads only rarely to segregation failure, this could happen more frequently in meiosis. It would therefore be interesting to see whether smaller fusion chromosomes also induce meiosis failure and where in meiosis the cells carrying long chromosomes arrest.
In general we can conclude that in order to reveal the consequences of chromosomal translocations we either have to use more sensitive assays to measure failure rates at low frequencies under standard conditions. Alternatively one can find specific conditions, like different kinds of stress or

meiosis, under which normally subtle fitness defects or advantages of cells carrying chromosome fusions become more apparent.

7. Chromosome size is plastic

To address the question whether anaphase spindle length and chromosome size are coordinated with each other we have generated a largely oversized chromosome. Cells carrying the chromosome fusion were viable and segregated their chromosomes efficiently. Cells can therefore deal with variability in the size of their chromosomes. Such plasticity may be required to cope with changes in chromosome size that are occurring naturally. One example is the spontaneous extension of repetitive regions such as the *rDNA* array or the telomeres. In budding yeast for example the number of copies of the *rDNA* gene can vary between 100 and 200 [47]. This corresponds to a 50% difference in length of the longest chromosome arm, the right arm of chromosome XII (1837kb - 2747kb).
Variations in chromosome size also occur as a result of large chromosomal rearrangements such as chromosome end to end fusions or partial translocations. Such rearrangements are often found in tumor cells [240, 241], and thus the same mechanisms that help cells to deal with naturally occurring variations in chromosome size may support the survival of tumor cells.

The number and size of eukaryotic chromosomes varies greatly between different species: Budding yeasts have 16 chromosomes (1n), which range from 250kb-2.5Mb [242] while the 23 human chromosomes (1n) are between 50Mb and 250Mb [53, 54]. This raises the question what determines the size of the chromosomes. Several processes influence the karyotype of an organism and thus contribute to genome evolution. The number of chromosomes can change as a result of chromosome fusion or fragmentation, chromosome non-disjunction in meiosis or mitosis and failure of cytokinesis. The DNA content and arrangement on chromosomes can be affected by

duplication or deletion of large segments, partial chromosome inversions, reciprocal translocations, whole chromosome fusions and also by expansion or elimination of repetitive elements. The number and size of chromosomes in a given karyotype are the result of the relative rates of these processes [243]. The efficiency of adaptive hyper-condensation we have described for the *LC(XII:IV)* compound chromosome could influence the rates for chromosome fusion, reciprocal translocations, DNA insertion, partial genome duplication and spontaneous expansion of repetitive regions, as it is a prerequisite to adapt to sudden increases in chromosome size.

Modeling of chromosome size evolution using reciprocal translocation as the only evolutionary force suggests that there is an upper and a lower limit to chromosome size [244]. Indeed limits to chromosome size have been suggested. A lower limit was proposed because very small chromosomes are segregated with a high error rate in meiosis in *A. thaliana* and the field bean *V. faba* [245, 246]. In budding yeast and vertebrate cells small linear chromosomes were shown to be unstable during mitotic divisions [247, 248]. What determines the lower limit to chromosome size is not clear, possibly short chromosomes are too small to establish sufficient cohesion between chromosome arms and are not able to correctly attach to the mitotic spindle.
Fusion of the two longest budding yeast chromosomes has not revealed an upper limit to chromosome size. Chromosome size has however also been increased experimentally in *D. melanogaster* by fusion of two homologous chromosomes. This led to an elevated frequency of lagging chromosomes in telophase and division failure in 3% of the nuclei during the syncytial stage [235], suggesting an upper limit to chromosome size. In somatic divisions of neuroblasts however no increased error rate was observed and the flies carrying the compound chromosome were viable and fertile [235]. Thus if there is an upper limit for chromosome size it is different for different cell types. Support for the idea of an upper limit to chromosome size comes from analysis of *V. faba* lines carrying different sets of chromosomal translocations.

These showed that there is a threshold in chromosome arm length, above which viability and fertility are reduced. Interestingly reduced fertility was observed at shorter chromosome arm length than impaired cell growth, suggesting that the upper limit in chromosome size are different in mitosis and meiosis [171]. This observation could be confirmed in barley [249]. In *V. faba* the limit was reached when the longest chromosome arm was increased in length by more than 30% [171]. In contrast we have shown that in budding yeast a 50% increase in length of the longest chromosome arm is tolerated without any detectable growth phenotype. Therefore in wild type budding yeast cells, the longest chromosome is still substantially smaller than a possible upper mitotic size limit. It would be interesting to further increase chromosome arm length in to determine the upper limit of chromosome size in budding yeast mitosis and meiosis.

The average chromosome size of an organism varies over 3 orders of magnitudes among eukaryotes [244]. This argues that the upper chromosome size limit is different from species to species. But what defines how big chromosomes can get? The extra long chromosome arms in *V. faba* could not be fully separated in anaphase [171]. The length of the mitotic spindle in anaphase was therefore proposed to define the upper limit of chromosome size. This can however not be the full explanation because the maximal spindle size, which is limited by cell size, is not nearly as variable as chromosome size between different eukaryotes. The *V. faba* spindle is for example only 4x longer than budding yeast spindles, while the largest *V. faba* chromosome is about 100x bigger. Another limiting factor for chromosome size therefore must be how well cells are able to axially compact their chromosomes in mitosis. We resented here direct evidence for this hypothesis as yeast cells carrying the *LC(XII:IV)* are more sensitive to loss of condensin activity. Thus the anaphase spindle length and the efficiency of chromosome condensation together determine the upper limit to chromosome size.

VI. Conclusions

1. Largely oversized chromosome arms segregate efficiently.

2. Dynamic, repetitive regions (the *rDNA* array) shorten in response to increased chromosome arm length.

3. The extra-long chromosome hyper-condenses in both, centromere proximal and centromere distal regions.

4. Anaphase specific hyper-condensation depends on spindle midzone localized Ipl1 activity and scales with the size of the spindle.

5. Ipl1 induces chromosome condensation through phosphorylation of H3S10 and possibly other targets and promotes removal of cohesin.

6. Ipl1 is important for Cdc14 re-sequestration in telophase.

VII. Future Directions

1. Chromosomal rearrangements are a hallmark of cancer cells [250]. We have developed a method that allows to investigate the effects of chromosomal translocations systematically. A thorough analysis of cellular fitness, genome expression and mutation rate could reveal highly relevant insights into the role of chromosome organization in tumorigenesis.

2. To get a better understanding the structural basis of adaptive hyper-condensation 3D models of mitotic chromosomes will be built using 5C data and modeling. This will not only allow us to compare the structure of different chromosomes, but may also allow us to build hypotheses of how mitotic chromosomes are folded.

3. To find molecular players involved in adaptive hyper-condensation, mass spectrometry on purified chromatin from H3S10 mutants should be performed. Binding patterns of identified proteins may explain how the midzone-signal propagates from the spindle midzone along the chromosome arm.

4. The increased spindle length in condensin mutants suggests a two directional signaling between spindle size and chromosome condensation. It will be important to determine how chromosomes can influence spindle size.

5. The role of Ipl1 in re-sequestering Cdc14 into the nucleolus is new and surprising. An effort should be made to understand the consequences of delayed Cdc14 re-import and how Ipl1 regulates this process.

VIII. Acknowledgements

My gratitude goes to all the people who have contributed in one way or the other to this work and have made these years so enjoyable.

Manuel, it has been a pleasure to work for and with you! Thank you for your positive and liberal way of leadership, for inspiring me and for letting me develop my own ideas. Thanks for the excellent formation in so many aspects, which includes your essential guidance for writing this thesis! Now that the end of my time in your lab is getting nearer, it starts to feel like leaving home and, although I chose it myself, I wish I had more time to stay and finish up several exciting projects.

Dear Yves, I was lucky to start my scientific career in your lab and to have your support during these years was very helpful. I have learned a lot from you and I appreciate your creativity and different way of looking at things. Thank you.

I want to thank Isabelle Vernos for her support during for my PhD and beyond and for interesting discussions in the lab meetings.

For their support as member of my Thesis Advisory Committee or PhD Defense Panel and for critically reading this PhD thesis I want to thank Jordi Torress-Rosell, Ethel Queralt Badia, Jerome Solon and Luciano Di Croce.

One important lesson that I have learned during my PhD is that science is most fun and productive when it is done together. I have profited enormously from the knowledge and work of others.

My most important collaborators were my lab mates with whom I shared my daily work, profited from their stocks, enjoyed short and long lab meetings, lunch and coffee breaks, lab retreats, endless discussions and night sessions in the lab, spontaneous mojitos and much more. Alex, Petra, Evi, Francesca, Nuno, Trini, Aina and Iris you are fantastic and I will miss you!

I especially want to thank Andreas Nägeli, Iris Titos, Dominik Theler, Basil Greber, Javier Diez and Toni Gabaldon for their collaboraion on the paper.

A thank you goes to all the members of the group of Isabelle Vernos for sharing their lab meetings with us and also to the group of Hernan Lopez Schier for sharing space, time and music of variable volume and quality. Thanks also to all the labs of the Cell and Developmental Biology Department for sharing reagents and equipment.

For helping me with tricky machines and formulas I want to thank Camilla Iannone, Ramon Tejedor, Cristina Militti, Bernhard Paetzold and Felix Campelo and the people working in the sequencing and advanced light microscopy facilities of the CRG.

So many people also outside of lab walls made this experience unforgettable and I am grateful to all of you! Sadly I cannot mention every single one, but some cannot be left out:

Ines and Jesus, I had a great time living with you guys! Being around you still feels like home and I will keep Monday nights in Gran Via 1000 and Flat-Meetings in Marroc 1 in good memory.

Joschi, Fede und Lorenzo: Die vielen Ausflüge und speziellen Momente, die wir mit euch verbringen durften werden uns für immer in Erinnerung bleiben!

Martin, danke für das Notasyl und für die Sommernächte auf der Strasse, du wirst mir fehlen!

Trini, me has enseñado hablar Español y me has vigilado muy bien! Gracias por tu apoyo en situaciones difíciles y por tu felicidad cada día. Ya sabes que eres una muy buena amiga y que te echare mucho de menos!

Liebi Mama und Papa, Gschwüsterti und Fründä i dä Schwiz. Z'wüssä dass mer immer än Ort hät wo mer chan um Rat frögä und Energie tankä isch unbezahlbar. Ihr gänd mir Sälbstvertrauä und Muet zum miini Troim verwürklichä.

Liebi Andrea, du gisch mir Stabilität und Rue und treisch än grossä Aateil a däm wo ich i mim Läbä erreichä. Ich bin dir dankbar dass du mit mir uf Barcelona cho bisch und au jetzt wider Muet zum Risiko zeigsch. Ich glaub äs hät sich glohnt und mir händ zämä vill chönä erläbä und lernä! Etwas wagen muss das Herz. Ich froi mich riisig uf oisi nächstä Etapänä i däm Abentür!

IX. Bibliography

1. Neurohr, G., Naegeli, A., Titos, I., Theler, D., Greber, B., Diez, J., Gabaldon, T., Mendoza, M., and Barral, Y. (2011). A Midzone-Based Ruler Adjusts Chromosome Compaction to Anaphase Spindle Length. In Science. p. 16.
2. Morgan, D.O. (2007). The Cell Cycle. The Cell Cycle - Principles of Control, 4-7.
3. Nurse, P., Thuriaux, P., and Nasmyth, K. (1976). Genetic control of the cell division cycle in the fission yeast Schizosaccharomyces pombe. Mol Gen Genet *146*, 167-178.
4. Hartwell, L.H., Culotti, J., and Reid, B. (1970). Genetic control of the cell-division cycle in yeast. I. Detection of mutants. In Proc Natl Acad Sci USA, Volume 66. pp. 352-359.
5. Hartwell, L.H., Mortimer, R.K., Culotti, J., and Culotti, M. (1973). Genetic Control of the Cell Division Cycle in Yeast: V. Genetic Analysis of cdc Mutants. In Genetics, Volume 74. pp. 267-286.
6. Murray, A.W., and Kirschner, M.W. (1989). Dominoes and clocks: the union of two views of the cell cycle. Science *246*, 614-621.
7. Masui, Y., and Markert, C.L. (1971). Cytoplasmic control of nuclear behavior during meiotic maturation of frog oocytes. J Exp Zool *177*, 129-145.
8. Hara, K., Tydeman, P., and Kirschner, M. (1980). A cytoplasmic clock with the same period as the division cycle in Xenopus eggs. Proc Natl Acad Sci U S A *77*, 462-466.
9. Gerhart, J., Wu, M., and Kirschner, M. (1984). Cell cycle dynamics of an M-phase-specific cytoplasmic factor in Xenopus laevis oocytes and eggs. J Cell Biol *98*, 1247-1255.
10. Morgan, D.O. (2007). The Cell-Cycle Control System. The Cell Cycle - Principles of Control, 8-9.
11. Beach, D., Durkacz, B., and Nurse, P. (1982). Functionally homologous cell cycle control genes in budding and fission yeast. Nature *300*, 706-709.
12. Lee, M.G., and Nurse, P. (1987). Complementation used to clone a human homologue of the fission yeast cell cycle control gene cdc2. Nature *327*, 31-35.
13. Dunphy, W.G., Brizuela, L., Beach, D., and Newport, J. (1988). The Xenopus cdc2 protein is a component of MPF, a cytoplasmic regulator of mitosis. Cell *54*, 423-431.
14. Alberts, B., Johnson, A., Lewis, J., Raff, M., ROberts, K., and Walter, P. (2008). The control of the cell cycle. Molecular Biology of the Cell, 1061.

15. Booher, R.N., Alfa, C.E., Hyams, J.S., and Beach, D.H. (1989). The fission yeast cdc2/cdc13/suc1 protein kinase: regulation of catalytic activity and nuclear localization. Cell *58*, 485-497.
16. Koivomagi, M., Valk, E., Venta, R., Iofik, A., Lepiku, M., Morgan, D.O., and Loog, M. (2011). Dynamics of Cdk1 substrate specificity during the cell cycle. Mol Cell *42*, 610-623.
17. Morgan, D.O. (2007). Cyclin Dependent Kinases. The Cell Cycle - Principles of Control, 30-33.
18. Morgan, D.O. (2007). Control of Cell Proliferation and Growth. The Cell Cycle - Principles of Control, 196-203.
19. Sidorova, J.M., and Breeden, L.L. (1997). Rad53-dependent phosphorylation of Swi6 and down-regulation of CLN1 and CLN2 transcription occur in response to DNA damage in Saccharomyces cerevisiae. Genes Dev *11*, 3032-3045.
20. Morgan, D.O. (2007). Control of Cdk Activity by Phosphorylation. The Cell Cycle - Principles of Control, 34-35.
21. Morgan, D.O. (2007). Effects of DAN damage on DNA Synthesis and Mitosis. The Cell Cycle - Principles of Control, 242-243.
22. Morgan, D.O. (2007). The Completion of Mitosis. The Cell Cycle - Principles of Control, 142-149.
23. Morgan, D.O. (2007). Overview: The Events of Mitosis. The Cell Cycle - Principles of Control, 88-89.
24. Goshima, G., and Yanagida, M. (2000). Establishing biorientation occurs with precocious separation of the sister kinetochores, but not the arms, in the early spindle of budding yeast. Cell *100*, 619-633.
25. Morgan, D.O. (2007). The Positioning and Timing of Cytokinesisn in Yeast. The Cell Cycle - Principles of Control, 166.
26. Morgan, D.O. (2007). Overview: The Mitotic Spindle. The Cell Cycle - Principles of Control, 112.
27. Bouck, D., Joglekar, A., and Bloom, K. (2008). Design Features of a Mitotic Spindle: Balancing Tension and Compression at a Single Microtubule Kinetochore Interface in Budding Yeast. In Genetics, Volume 42. pp. 335-359.
28. Desai, A., and Mitchison, T.J. (1997). Microtubule polymerization dynamics. Annu Rev Cell Dev Biol *13*, 83-117.
29. Sauer, G., Korner, R., Hanisch, A., Ries, A., Nigg, E.A., and Sillje, H.H. (2005). Proteome analysis of the human mitotic spindle. Mol Cell Proteomics *4*, 35-43.
30. Ruchaud, S., Carmena, M., and Earnshaw, W.C. (2007). Chromosomal passengers: conducting cell division. Nat Rev Mol Cell Biol *8*, 798-812.
31. Nakajima, Y., Tyers, R.G., Wong, C.C., Yates, J.R., 3rd, Drubin, D.G., and Barnes, G. (2009). Nbl1p: a Borealin/Dasra/CSC-1-like protein essential for Aurora/Ipl1 complex function and integrity in Saccharomyces cerevisiae. Mol Biol Cell *20*, 1772-1784.

32. Buvelot, Tatsutani, Vermaak, and Biggins (2003). The budding yeast Ipl1/Aurora protein kinase regulates mitotic spindle disassembly. In The Journal of Cell Biology, Volume 160. pp. 329-339.
33. Archambault, V., and Glover, D.M. (2009). Polo-like kinases: conservation and divergence in their functions and regulation. Nat Rev Mol Cell Biol *10*, 265-275.
34. Spellman, P.T., Sherlock, G., Zhang, M.Q., Iyer, V.R., Anders, K., Eisen, M.B., Brown, P.O., Botstein, D., and Futcher, B. (1998). Comprehensive identification of cell cycle-regulated genes of the yeast Saccharomyces cerevisiae by microarray hybridization. Mol Biol Cell *9*, 3273-3297.
35. Uchiumi, T., Longo, D.L., and Ferris, D.K. (1997). Cell cycle regulation of the human polo-like kinase (PLK) promoter. J Biol Chem *272*, 9166-9174.
36. Elia, A.E., Cantley, L.C., and Yaffe, M.B. (2003). Proteomic screen finds pSer/pThr-binding domain localizing Plk1 to mitotic substrates. Science *299*, 1228-1231.
37. Cottarel, G., Shero, J.H., Hieter, P., and Hegemann, J.H. (1989). A 125-base-pair CEN6 DNA fragment is sufficient for complete meiotic and mitotic centromere functions in Saccharomyces cerevisiae. Mol Cell Biol *9*, 3342-3349.
38. Morgan, D.O. (2007). Heterochromatin at Telomeres and Centromeres. The Cell Cycle - Principles of Control, 82-83.
39. Blackburn, E.H. (1991). Structure and function of telomeres. Nature *350*, 569-573.
40. Lowell, J.E., and Pillus, L. (1998). Telomere tales: chromatin, telomerase and telomere function in Saccharomyces cerevisiae. Cell Mol Life Sci *54*, 32-49.
41. Warner, J.R. (1999). The economics of ribosome biosynthesis in yeast. Trends Biochem Sci *24*, 437-440.
42. Kobayashi, T. (2011). Regulation of ribosomal RNA gene copy number and its role in modulating genome integrity and evolutionary adaptability in yeast. Cell Mol Life Sci *68*, 1395-1403.
43. Takeuchi, Y., Horiuchi, T., and Kobayashi, T. (2003). Transcription-dependent recombination and the role of fork collision in yeast rDNA. Genes Dev *17*, 1497-1506.
44. Warner, J.R. (1989). Synthesis of ribosomes in Saccharomyces cerevisiae. Microbiol Rev *53*, 256-271.
45. Ide, S., Miyazaki, T., Maki, H., and Kobayashi, T. (2010). Abundance of Ribosomal RNA Gene Copies Maintains Genome Integrity. In Science, Volume 327. pp. 693-696.
46. Rustchenko, E.P., Curran, T.M., and Sherman, F. (1993). Variations in the number of ribosomal DNA units in morphological mutants and normal strains of Candida albicans and in normal strains of Saccharomyces cerevisiae. J Bacteriol *175*, 7189-7199.

47. Kobayashi, T., Heck, D.J., Nomura, M., and Horiuchi, T. (1998). Expansion and contraction of ribosomal DNA repeats in Saccharomyces cerevisiae: requirement of replication fork blocking (Fob1) protein and the role of RNA polymerase I. In Genes & Development, Volume 12. pp. 3821-3830.
48. Morgan, D.O. (2007). Detection and Repair of DNA Repair. The Cell Cycle - Principles of Control, 230-231.
49. Kobayashi, T. (2006). Strategies to maintain the stability of the ribosomal RNA gene repeats--collaboration of recombination, cohesion, and condensation. Genes Genet Syst *81*, 155-161.
50. Kobayashi, T., and Ganley, A.R. (2005). Recombination regulation by transcription-induced cohesin dissociation in rDNA repeats. Science *309*, 1581-1584.
51. Lin, S.J., Kaeberlein, M., Andalis, A.A., Sturtz, L.A., Defossez, P.A., Culotta, V.C., Fink, G.R., and Guarente, L. (2002). Calorie restriction extends Saccharomyces cerevisiae lifespan by increasing respiration. Nature *418*, 344-348.
52. Kobayashi, T., Horiuchi, T., Tongaonkar, P., Vu, L., and Nomura, M. (2004). SIR2 regulates recombination between different rDNA repeats, but not recombination within individual rRNA genes in yeast. Cell *117*, 441-453.
53. Venter, J.C., Adams, M.D., Myers, E.W., Li, P.W., Mural, R.J., Sutton, G.G., Smith, H.O., Yandell, M., Evans, C.A., Holt, R.A., et al. (2001). The sequence of the human genome. Science *291*, 1304-1351.
54. Lander, E.S., Linton, L.M., Birren, B., Nusbaum, C., Zody, M.C., Baldwin, J., Devon, K., Dewar, K., Doyle, M., FitzHugh, W., et al. (2001). Initial sequencing and analysis of the human genome. Nature *409*, 860-921.
55. Watson, J.D., and Crick, F.H. (1953). Molecular structure of nucleic acids; a structure for deoxyribose nucleic acid. Nature *171*, 737-738.
56. Luger, K., Mader, A.W., Richmond, R.K., Sargent, D.F., and Richmond, T.J. (1997). Crystal structure of the nucleosome core particle at 2.8 A resolution. Nature *389*, 251-260.
57. Fussner, E., Ching, R.W., and Bazett-Jones, D.P. Living without 30nm chromatin fibers. Trends Biochem Sci *36*, 1-6.
58. Morgan, D.O. (2007). Basic Chromatin Structure. The Cell Cycle - Principles of Control, 76-77.
59. Xu, D., Bai, J., Duan, Q., Costa, M., and Dai, W. (2009). Covalent modifications of histones during mitosis and meiosis. Cell Cycle *8*, 3688-3694.
60. Johansen, K.M., and Johansen, J. (2006). Regulation of chromatin structure by histone H3S10 phosphorylation. Chromosome Res *14*, 393-404.
61. De Souza, C.P., Osmani, A.H., Wu, L.P., Spotts, J.L., and Osmani, S.A. (2000). Mitotic histone H3 phosphorylation by the NIMA kinase in Aspergillus nidulans. Cell *102*, 293-302.

62. Roig, J., Mikhailov, A., Belham, C., and Avruch, J. (2002). Nercc1, a mammalian NIMA-family kinase, binds the Ran GTPase and regulates mitotic progression. Genes Dev *16*, 1640-1658.
63. Kang, T.H., Park, D.Y., Choi, Y.H., Kim, K.J., Yoon, H.S., and Kim, K.T. (2007). Mitotic histone H3 phosphorylation by vaccinia-related kinase 1 in mammalian cells. Mol Cell Biol *27*, 8533-8546.
64. Hsu, J.Y., Sun, Z.W., Li, X., Reuben, M., Tatchell, K., Bishop, D.K., Grushcow, J.M., Brame, C.J., Caldwell, J.A., Hunt, D.F., et al. (2000). Mitotic phosphorylation of histone H3 is governed by Ipl1/aurora kinase and Glc7/PP1 phosphatase in budding yeast and nematodes. In Cell, Volume 102. pp. 279-291.
65. Giet, R., and Glover, D.M. (2001). Drosophila aurora B kinase is required for histone H3 phosphorylation and condensin recruitment during chromosome condensation and to organize the central spindle during cytokinesis. J Cell Biol *152*, 669-682.
66. Crosio, C., Fimia, G.M., Loury, R., Kimura, M., Okano, Y., Zhou, H., Sen, S., Allis, C.D., and Sassone-Corsi, P. (2002). Mitotic phosphorylation of histone H3: spatio-temporal regulation by mammalian Aurora kinases. Mol Cell Biol *22*, 874-885.
67. Gurley, L.R., D'Anna, J.A., Barham, S.S., Deaven, L.L., and Tobey, R.A. (1978). Histone phosphorylation and chromatin structure during mitosis in Chinese hamster cells. Eur J Biochem *84*, 1-15.
68. Hendzel, M.J., Wei, Y., Mancini, M.A., Van Hooser, A., Ranalli, T., Brinkley, B.R., Bazett-Jones, D.P., and Allis, C.D. (1997). Mitosis-specific phosphorylation of histone H3 initiates primarily within pericentromeric heterochromatin during G2 and spreads in an ordered fashion coincident with mitotic chromosome condensation. Chromosoma *106*, 348-360.
69. Van Hooser, A., Goodrich, D.W., Allis, C.D., Brinkley, B.R., and Mancini, M.A. (1998). Histone H3 phosphorylation is required for the initiation, but not maintenance, of mammalian chromosome condensation. J Cell Sci *111 (Pt 23)*, 3497-3506.
70. Wei, Y., Mizzen, C.A., Cook, R.G., Gorovsky, M.A., and Allis, C.D. (1998). Phosphorylation of histone H3 at serine 10 is correlated with chromosome condensation during mitosis and meiosis in Tetrahymena. Proc Natl Acad Sci U S A *95*, 7480-7484.
71. Wei, Y., Yu, L., Bowen, J., Gorovsky, M.A., and Allis, C.D. (1999). Phosphorylation of histone H3 is required for proper chromosome condensation and segregation. Cell *97*, 99-109.
72. Nowak, S.J., and Corces, V.G. (2000). Phosphorylation of histone H3 correlates with transcriptionally active loci. Genes Dev *14*, 3003-3013.
73. Finch, J.T., and Klug, A. (1976). Solenoidal model for superstructure in chromatin. Proc Natl Acad Sci U S A *73*, 1897-1901.
74. Horowitz, R.A., Agard, D.A., Sedat, J.W., and Woodcock, C.L. (1994). The three-dimensional architecture of chromatin in situ: electron

tomography reveals fibers composed of a continuously variable zig-zag nucleosomal ribbon. J Cell Biol *125*, 1-10.
75. Tremethick, D.J. (2007). Higher-order structures of chromatin: the elusive 30 nm fiber. Cell *128*, 651-654.
76. Eltsov, M., Maclellan, K.M., Maeshima, K., Frangakis, A.S., and Dubochet, J. (2008). Analysis of cryo-electron microscopy images does not support the existence of 30-nm chromatin fibers in mitotic chromosomes in situ. Proc Natl Acad Sci U S A *105*, 19732-19737.
77. Dekker, J. (2008). Mapping in vivo chromatin interactions in yeast suggests an extended chromatin fiber with regional variation in compaction. In J Biol Chem, Volume 283. pp. 34532-34540.
78. Lieberman-Aiden, E., van Berkum, N.L., Williams, L., Imakaev, M., Ragoczy, T., Telling, A., Amit, I., Lajoie, B.R., Sabo, P.J., Dorschner, M.O., et al. (2009). Comprehensive mapping of long-range interactions reveals folding principles of the human genome. In Science, Volume 326. pp. 289-293.
79. Paulson, J.R., and Laemmli, U.K. (1977). The structure of histone-depleted metaphase chromosomes. Cell *12*, 817-828.
80. Poirier, M., Eroglu, S., Chatenay, D., and Marko, J.F. (2000). Reversible and irreversible unfolding of mitotic newt chromosomes by applied force. In Mol Biol Cell, Volume 11. pp. 269-276.
81. Sun, M., Kawamura, R., and Marko, J.F. (2011). Micromechanics of human mitotic chromosomes. Phys Biol *8*, 015003.
82. Poirier, M.G., and Marko, J.F. (2002). Mitotic chromosomes are chromatin networks without a mechanically contiguous protein scaffold. Proc Natl Acad Sci U S A *99*, 15393-15397.
83. Kireeva, N., Lakonishok, M., Kireev, I., Hirano, T., and Belmont, A.S. (2004). Visualization of early chromosome condensation: a hierarchical folding, axial glue model of chromosome structure. J Cell Biol *166*, 775-785.
84. Moser, S.C., and Swedlow, J.R. (2011). How to be a mitotic chromosome. Chromosome Res *19*, 307-319.
85. Holm, C., Goto, T., Wang, J.C., and Botstein, D. (1985). DNA topoisomerase II is required at the time of mitosis in yeast. In Cell, Volume 41. pp. 553-563.
86. Uemura, T., Ohkura, H., Adachi, Y., Morino, K., Shiozaki, K., and Yanagida, M. (1987). DNA topoisomerase II is required for condensation and separation of mitotic chromosomes in S. pombe. In Cell, Volume 50. pp. 917-925.
87. Holm, C., Stearns, T., and Botstein, D. (1989). DNA topoisomerase II must act at mitosis to prevent nondisjunction and chromosome breakage. Mol Cell Biol *9*, 159-168.
88. Shamu, C.E., and Murray, A.W. (1992). Sister chromatid separation in frog egg extracts requires DNA topoisomerase II activity during anaphase. J Cell Biol *117*, 921-934.

89. Baumann, C., Korner, R., Hofmann, K., and Nigg, E.A. (2007). PICH, a centromere-associated SNF2 family ATPase, is regulated by Plk1 and required for the spindle checkpoint. Cell *128*, 101-114.
90. Hirano, T. (2006). At the heart of the chromosome: SMC proteins in action. In Nat Rev Mol Cell Biol, Volume 7. pp. 311-322.
91. Yoshimura, S.H., Hizume, K., Murakami, A., Sutani, T., Takeyasu, K., and Yanagida, M. (2002). Condensin architecture and interaction with DNA: regulatory non-SMC subunits bind to the head of SMC heterodimer. Curr Biol *12*, 508-513.
92. Nakazawa, N., Mehrotra, R., Ebe, M., and Yanagida, M. (2011). Condensin phosphorylated by the Aurora-B-like kinase Ark1 is continuously required until telophase in a mode distinct from Top2. In Journal of Cell Science. p. 13.
93. Tada, K., Susumu, H., Sakuno, T., and Watanabe, Y. (2011). Condensin association with histone H2A shapes mitotic chromosomes. In Nature. p. 9.
94. Cuylen, S., Metz, J., and Haering, C. (2011). Condensin structures chromosomal DNA through topological links. In Nat Struct Mol Biol. p. 9.
95. Ono, T., Fang, Y., Spector, D.L., and Hirano, T. (2004). Spatial and temporal regulation of Condensins I and II in mitotic chromosome assembly in human cells. Mol Biol Cell *15*, 3296-3308.
96. Gerlich, D., Hirota, T., Koch, B., Peters, J., and Ellenberg, J. (2006). Condensin I Stabilizes Chromosomes Mechanically through a Dynamic Interaction in Live Cells. In Current Biology, Volume 16. pp. 333-344.
97. D'ambrosio, C., Schmidt, C., Katou, Y., Kelly, G., Itoh, T., Shirahige, K., and Uhlmann, F. (2008). Identification of cis-acting sites for condensin loading onto budding yeast chromosomes. In Genes & Development, Volume 22. pp. 2215-2227.
98. D'Amours, D., Stegmeier, F., and Amon, A. (2004). Cdc14 and condensin control the dissolution of cohesin-independent chromosome linkages at repeated DNA. In Cell, Volume 117. pp. 455-469.
99. Wang, B.D., Yong-Gonzalez, V., and Strunnikov, A.V. (2004). Cdc14p/FEAR pathway controls segregation of nucleolus in S. cerevisiae by facilitating condensin targeting to rDNA chromatin in anaphase. In Cell Cycle, Volume 3. pp. 960-967.
100. Clemente-Blanco, A., Mayán-Santos, M., Schneider, D., Machín, F., Jarmuz, A., Tschochner, H., and Aragón, L. (2009). Cdc14 inhibits transcription by RNA polymerase I during anaphase. In Nature. p. 5.
101. Cuylen, S., and Haering, C.H. (2011). Deciphering condensin action during chromosome segregation. Trends Cell Biol *21*, 552-559.
102. Freeman, L., Aragon-Alcaide, L., and Strunnikov, A. (2000). The condensin complex governs chromosome condensation and mitotic transmission of rDNA. In The Journal of Cell Biology, Volume 149. pp. 811-824.

103. Bhat, M.A., Philp, A.V., Glover, D.M., and Bellen, H.J. (1996). Chromatid segregation at anaphase requires the barren product, a novel chromosome-associated protein that interacts with Topoisomerase II. Cell *87*, 1103-1114.
104. Hirano, T., Kobayashi, R., and Hirano, M. (1997). Condensins, chromosome condensation protein complexes containing XCAP-C, XCAP-E and a Xenopus homolog of the Drosophila Barren protein. Cell *89*, 511-521.
105. Ouspenski, II, Cabello, O.A., and Brinkley, B.R. (2000). Chromosome condensation factor Brn1p is required for chromatid separation in mitosis. Mol Biol Cell *11*, 1305-1313.
106. Strick, T.R., Kawaguchi, T., and Hirano, T. (2004). Real-time detection of single-molecule DNA compaction by condensin I. Curr Biol *14*, 874-880.
107. Kimura, K., and Hirano, T. (1997). ATP-dependent positive supercoiling of DNA by 13S condensin: a biochemical implication for chromosome condensation. Cell *90*, 625-634.
108. Poirier, M.G., and Marko, J.F. (2002). Micromechanical studies of mitotic chromosomes. J Muscle Res Cell Motil *23*, 409-431.
109. Kimura, K., Hirano, M., Kobayashi, R., and Hirano, T. (1998). Phosphorylation and activation of 13S condensin by Cdc2 in vitro. In Science, Volume 282. pp. 487-490.
110. Mora-Bermúdez, F., Gerlich, D., and Ellenberg, J. (2007). Maximal chromosome compaction occurs by axial shortening in anaphase and depends on Aurora kinase. In Nat Cell Biol, Volume 9. pp. 822-831.
111. St-Pierre, J., Douziech, M., Bazile, F., Pascariu, M., Bonneil, É., Sauvé, V., Ratsima, H., and D'amours, D. (2009). Polo Kinase Regulates Mitotic Chromosome Condensation by Hyperactivation of Condensin DNA Supercoiling Activity. In Molecular Cell, Volume 34. pp. 416-426.
112. Lavoie, B. (2004). In vivo requirements for rDNA chromosome condensation reveal two cell-cycle-regulated pathways for mitotic chromosome folding. In Genes & Development, Volume 18. pp. 76-87.
113. Lipp, J., Hirota, T., Poser, I., and Peters, J. (2007). Aurora B controls the association of condensin I but not condensin II with mitotic chromosomes. In Journal of Cell Science, Volume 120. pp. 1245-1255.
114. Hagstrom, K.A., Holmes, V.F., Cozzarelli, N.R., and Meyer, B.J. (2002). C. elegans condensin promotes mitotic chromosome architecture, centromere organization, and sister chromatid segregation during mitosis and meiosis. Genes Dev *16*, 729-742.
115. Petersen, J., and Hagan, I. (2003). S. pombe aurora kinase/survivin is required for chromosome condensation and the spindle checkpoint attachment response. In Curr Biol, Volume 13. pp. 590-597.
116. Wang, B.D., Butylin, P., and Strunnikov, A. (2006). Condensin function in mitotic nucleolar segregation is regulated by rDNA transcription. Cell Cycle *5*, 2260-2267.

117. Gruber, S., Haering, C.H., and Nasmyth, K. (2003). Chromosomal cohesin forms a ring. Cell *112*, 765-777.
118. Ivanov, D., and Nasmyth, K. (2005). A topological interaction between cohesin rings and a circular minichromosome. Cell *122*, 849-860.
119. Ciosk, R., Shirayama, M., Shevchenko, A., Tanaka, T., Toth, A., and Nasmyth, K. (2000). Cohesin's binding to chromosomes depends on a separate complex consisting of Scc2 and Scc4 proteins. Mol Cell *5*, 243-254.
120. Michaelis, C., Ciosk, R., and Nasmyth, K. (1997). Cohesins: chromosomal proteins that prevent premature separation of sister chromatids. In Cell, Volume 91. pp. 35-45.
121. Uhlmann, F., and Nasmyth, K. (1998). Cohesion between sister chromatids must be established during DNA replication. Curr Biol *8*, 1095-1101.
122. Nasmyth, K. (2011). Cohesin: a catenase with separate entry and exit gates? Nat Cell Biol *13*, 1170-1177.
123. Ben-Shahar, T.R., Heeger, S., Lehane, C., East, P., Flynn, H., Skehel, M., and Uhlmann, F. (2008). Eco1-dependent cohesin acetylation during establishment of sister chromatid cohesion. In Science, Volume 321. pp. 563-566.
124. Unal, E., Heidinger-Pauli, J.M., Kim, W., Guacci, V., Onn, I., Gygi, S.P., and Koshland, D.E. (2008). A molecular determinant for the establishment of sister chromatid cohesion. Science *321*, 566-569.
125. Gandhi, R., Gillespie, P.J., and Hirano, T. (2006). Human Wapl is a cohesin-binding protein that promotes sister-chromatid resolution in mitotic prophase. In Curr Biol, Volume 16. pp. 2406-2417.
126. Sutani, T., Kawaguchi, T., Kanno, R., Itoh, T., and Shirahige, K. (2009). Budding yeast Wpl1(Rad61)-Pds5 complex counteracts sister chromatid cohesion-establishing reaction. Curr Biol *19*, 492-497.
127. Nishiyama, T., Ladurner, R., Schmitz, J., Kreidl, E., Schleiffer, A., Bhaskara, V., Bando, M., Shirahige, K., Hyman, A.A., Mechtler, K., et al. (2010). Sororin mediates sister chromatid cohesion by antagonizing Wapl. Cell *143*, 737-749.
128. Waizenegger, I.C., Hauf, S., Meinke, A., and Peters, J.M. (2000). Two distinct pathways remove mammalian cohesin from chromosome arms in prophase and from centromeres in anaphase. In Cell, Volume 103. pp. 399-410.
129. Sumara, I., Vorlaufer, E., Stukenberg, P.T., Kelm, O., Redemann, N., Nigg, E.A., and Peters, J.M. (2002). The dissociation of cohesin from chromosomes in prophase is regulated by Polo-like kinase. Mol Cell *9*, 515-525.
130. Giménez-Abián, J.F., Sumara, I., Hirota, T., Hauf, S., Gerlich, D., de la Torre, C., Ellenberg, J., and Peters, J. (2004). Regulation of sister chromatid cohesion between chromosome arms. In Curr Biol, Volume 14. pp. 1187-1193.

131. Losada, A., Hirano, M., and Hirano, T. (2002). Cohesin release is required for sister chromatid resolution, but not for condensin-mediated compaction, at the onset of mitosis. In Genes Dev, Volume 16. pp. 3004-3016.
132. Salic, A., Waters, J.C., and Mitchison, T.J. (2004). Vertebrate shugoshin links sister centromere cohesion and kinetochore microtubule stability in mitosis. Cell *118*, 567-578.
133. Kitajima, T.S., Kawashima, S.A., and Watanabe, Y. (2004). The conserved kinetochore protein shugoshin protects centromeric cohesion during meiosis. Nature *427*, 510-517.
134. McGuinness, B.E., Hirota, T., Kudo, N.R., Peters, J.M., and Nasmyth, K. (2005). Shugoshin prevents dissociation of cohesin from centromeres during mitosis in vertebrate cells. PLoS Biol *3*, e86.
135. Uhlmann, F., Lottspeich, F., and Nasmyth, K. (1999). Sister-chromatid separation at anaphase onset is promoted by cleavage of the cohesin subunit Scc1. In Nature, Volume 400. pp. 37-42.
136. De Piccoli, G., Torres-Rosell, J., and Aragon, L. (2009). The unnamed complex: what do we know about Smc5-Smc6? Chromosome Res *17*, 251-263.
137. Torres-Rosell, J., Machin, F., Farmer, S., Jarmuz, A., Eydmann, T., Dalgaard, J.Z., and Aragon, L. (2005). SMC5 and SMC6 genes are required for the segregation of repetitive chromosome regions. Nat Cell Biol *7*, 412-419.
138. Lindroos, H.B., Strom, L., Itoh, T., Katou, Y., Shirahige, K., and Sjogren, C. (2006). Chromosomal association of the Smc5/6 complex reveals that it functions in differently regulated pathways. Mol Cell *22*, 755-767.
139. Akiyoshi, B., Sarangapani, K., Powers, A., Nelson, C., Reichow, S., Arellano-Santoyo, H., Gonen, T., Ranish, J., Asbury, C., and Biggins, S. (2010). Tension directly stabilizes reconstituted kinetochore-microtubule attachments. In Nature, Volume 468. pp. 576-579.
140. Tanaka, T.U., Rachidi, N., Janke, C., Pereira, G., Galova, M., Schiebel, E., Stark, M.J., and Nasmyth, K. (2002). Evidence that the Ipl1-Sli15 (Aurora kinase-INCENP) complex promotes chromosome bi-orientation by altering kinetochore-spindle pole connections. Cell *108*, 317-329.
141. Lampson, M.A., Renduchitala, K., Khodjakov, A., and Kapoor, T.M. (2004). Correcting improper chromosome-spindle attachments during cell division. Nat Cell Biol *6*, 232-237.
142. Rieder, C.L., Cole, R.W., Khodjakov, A., and Sluder, G. (1995). The checkpoint delaying anaphase in response to chromosome monoorientation is mediated by an inhibitory signal produced by unattached kinetochores. J Cell Biol *130*, 941-948.
143. Zachariae, W., Shin, T.H., Galova, M., Obermaier, B., and Nasmyth, K. (1996). Identification of subunits of the anaphase-promoting complex of Saccharomyces cerevisiae. Science *274*, 1201-1204.

144. Zachariae, W., Shevchenko, A., Andrews, P.D., Ciosk, R., Galova, M., Stark, M.J., Mann, M., and Nasmyth, K. (1998). Mass spectrometric analysis of the anaphase-promoting complex from yeast: identification of a subunit related to cullins. Science *279*, 1216-1219.
145. King, R.W., Peters, J.M., Tugendreich, S., Rolfe, M., Hieter, P., and Kirschner, M.W. (1995). A 20S complex containing CDC27 and CDC16 catalyzes the mitosis-specific conjugation of ubiquitin to cyclin B. Cell *81*, 279-288.
146. Sudakin, V., Ganoth, D., Dahan, A., Heller, H., Hershko, J., Luca, F.C., Ruderman, J.V., and Hershko, A. (1995). The cyclosome, a large complex containing cyclin-selective ubiquitin ligase activity, targets cyclins for destruction at the end of mitosis. Mol Biol Cell *6*, 185-197.
147. Zachariae, W., Schwab, M., Nasmyth, K., and Seufert, W. (1998). Control of cyclin ubiquitination by CDK-regulated binding of Hct1 to the anaphase promoting complex. Science *282*, 1721-1724.
148. Cohen-Fix, O., Peters, J.M., Kirschner, M.W., and Koshland, D. (1996). Anaphase initiation in Saccharomyces cerevisiae is controlled by the APC-dependent degradation of the anaphase inhibitor Pds1p. Genes Dev *10*, 3081-3093.
149. Ciosk, R., Zachariae, W., Michaelis, C., Shevchenko, A., Mann, M., and Nasmyth, K. (1998). An ESP1/PDS1 complex regulates loss of sister chromatid cohesion at the metaphase to anaphase transition in yeast. Cell *93*, 1067-1076.
150. Oliveira, R.A., Hamilton, R.S., Pauli, A., Davis, I., and Nasmyth, K. (2010). Cohesin cleavage and Cdk inhibition trigger formation of daughter nuclei. Nat Cell Biol *12*, 185-192.
151. Sullivan, Higuchi, Katis, and Uhlmann, F. (2004). Cdc14 phosphatase induces rDNA condensation and resolves cohesin-independent cohesion during budding yeast anaphase. In Cell, Volume 117. pp. 471-482.
152. Torres-Rosell, J., Machin, F., Jarmuz, A., and Aragon, L. (2004). Nucleolar segregation lags behind the rest of the genome and requires Cdc14p activation by the FEAR network. Cell Cycle *3*, 496-502.
153. Bouchoux, C., and Uhlmann, F. (2011). A quantitative model for ordered Cdk substrate dephosphorylation during mitotic exit. Cell *147*, 803-814.
154. Queralt, E., and Uhlmann, F. (2008). Cdk-counteracting phosphatases unlock mitotic exit. Curr Opin Cell Biol *20*, 661-668.
155. Stegmeier, F., Visintin, R., and Amon (2002). Separase, polo kinase, the kinetochore protein Slk19, and Spo12 function in a network that controls Cdc14 localization during early anaphase. In Cell, Volume 108. pp. 207-220.
156. Rock, J., and Amon, A. (2009). The FEAR network. In Current Biology, Volume 19. pp. R1063-R1068.
157. Mohl, D., Huddleston, M., Collingwood, T., Annan, R., and Deshaies, R. (2009). Dbf2-Mob1 drives relocalization of protein phosphatase

Cdc14 to the cytoplasm during exit from mitosis. In The Journal of Cell Biology, Volume 184. pp. 527-539.
158. Caydasi, A.K., Ibrahim, B., and Pereira, G. (2010). Monitoring spindle orientation: Spindle position checkpoint in charge. Cell Div *5*, 28.
159. Visintin, C., Tomson, B., Rahal, R., Paulson, J., Cohen, M., Taunton, J., Amon, and Visintin, R. (2008). APC/C-Cdh1-mediated degradation of the Polo kinase Cdc5 promotes the return of Cdc14 into the nucleolus. In Genes Dev, Volume 22. pp. 79-90.
160. Higuchi, T., and Uhlmann, F. (2005). Stabilization of microtubule dynamics at anaphase onset promotes chromosome segregation. Nature *433*, 171-176.
161. Pereira, G. (2003). Separase Regulates INCENP-Aurora B Anaphase Spindle Function Through Cdc14. In Science, Volume 302. pp. 2120-2124.
162. Khmelinskii, Lawrence, Roostalu, and Schiebel (2007). Cdc14-regulated midzone assembly controls anaphase B. In The Journal of Cell Biology, Volume 177. pp. 981-993.
163. Jensen, S., Segal, M., Clarke, D.J., and Reed, S.I. (2001). A novel role of the budding yeast separin Esp1 in anaphase spindle elongation: evidence that proper spindle association of Esp1 is regulated by Pds1. In The Journal of Cell Biology, Volume 152. pp. 27-40.
164. Woodbury, E.L., and Morgan, D.O. (2007). Cdk and APC activities limit the spindle-stabilizing function of Fin1 to anaphase. Nat Cell Biol *9*, 106-112.
165. Mirchenko, L., and Uhlmann, F. (2010). Sli15(INCENP) dephosphorylation prevents mitotic checkpoint reengagement due to loss of tension at anaphase onset. In Curr Biol, Volume 20. pp. 1396-1401.
166. D'Ambrosio, C., Kelly, G., Shirahige, K., and Uhlmann, F. (2008). Condensin-dependent rDNA decatenation introduces a temporal pattern to chromosome segregation. In Curr Biol, Volume 18. pp. 1084-1089.
167. Baxter, J., Sen, N., Martinez, V., De Carandini, M., Schvartzman, J., Diffley, J., and Aragon, L. (2011). Positive Supercoiling of Mitotic DNA Drives Decatenation by Topoisomerase II in Eukaryotes. In Science, Volume 331. pp. 1328-1332.
168. Renshaw, M., Ward, J., Kanemaki, M., Natsume, K., Nédélec, F., and Tanaka, T. (2010). Condensins Promote Chromosome Recoiling during Early Anaphase to Complete Sister Chromatid Separation. In Dev Cell, Volume 19. pp. 232-244.
169. Robinson, P.J., Fairall, L., Huynh, V.A., and Rhodes, D. (2006). EM measurements define the dimensions of the "30-nm" chromatin fiber: evidence for a compact, interdigitated structure. Proc Natl Acad Sci U S A *103*, 6506-6511.

170. Harrison, B., Hoang, M., and Bloom, K. (2009). Persistent mechanical linkage between sister chromatids throughout anaphase. In Chromosoma, Volume 118. pp. 633-645.
171. Schubert, I., and Oud, J.L. (1997). There is an upper limit of chromosome size for normal development of an organism. Cell *88*, 515-520.
172. Guacci, V., Hogan, E., and Koshland, D. (1994). Chromosome condensation and sister chromatid pairing in budding yeast. J Cell Biol *125*, 517-530.
173. Machin (2005). Spindle-independent condensation-mediated segregation of yeast ribosomal DNA in late anaphase. In The Journal of Cell Biology, Volume 168. pp. 209-219.
174. Hara, Y., and Kimura, A. (2009). Cell-size-dependent spindle elongation in the Caenorhabditis elegans early embryo. Curr Biol *19*, 1549-1554.
175. Wuhr, M., Chen, Y., Dumont, S., Groen, A.C., Needleman, D.J., Salic, A., and Mitchison, T.J. (2008). Evidence for an upper limit to mitotic spindle length. Curr Biol *18*, 1256-1261.
176. Vas, Andrews, Matesky, K., and Clarke (2007). In vivo analysis of chromosome condensation in Saccharomyces cerevisiae. In Mol Biol Cell, Volume 18. pp. 557-568.
177. Reed, S.I., Hadwiger, J.A., and Lorincz, A.T. (1985). Protein kinase activity associated with the product of the yeast cell division cycle gene CDC28. Proc Natl Acad Sci U S A *82*, 4055-4059.
178. Janke, C., Magiera, M., Rathfelder, N., Taxis, C., Reber, S., Maekawa, H., Moreno-Borchart, A., Doenges, G., Schwob, E., Schiebel, E., et al. (2004). A versatile toolbox for PCR-based tagging of yeast genes: new fluorescent proteins, more markers and promoter substitution cassettes. In Yeast, Volume 21. pp. 947-962.
179. Harju, S., Fedosyuk, H., and Peterson, K.R. (2004). Rapid isolation of yeast genomic DNA: Bust n' Grab. BMC Biotechnol *4*, 8.
180. Herschleb, J., Ananiev, G., and Schwartz, D.C. (2007). Pulsed-field gel electrophoresis. Nat Protoc *2*, 677-684.
181. Sikorski, R.S., and Hieter, P. (1989). A system of shuttle vectors and yeast host strains designed for efficient manipulation of DNA in Saccharomyces cerevisiae. Genetics *122*, 19-27.
182. Pop, M., Phillippy, A., Delcher, A.L., and Salzberg, S.L. (2004). Comparative genome assembly. Brief Bioinform *5*, 237-248.
183. Cherry, J.M., Ball, C., Weng, S., Juvik, G., Schmidt, R., Adler, C., Dunn, B., Dwight, S., Riles, L., Mortimer, R.K., et al. (1997). Genetic and physical maps of Saccharomyces cerevisiae. Nature *387*, 67-73.
184. Altschul, S.F., and Koonin, E.V. (1998). Iterated profile searches with PSI-BLAST--a tool for discovery in protein databases. Trends Biochem Sci *23*, 444-447.
185. Hughes, J.F., Skaletsky, H., Pyntikova, T., Graves, T.A., van Daalen, S.K., Minx, P.J., Fulton, R.S., McGrath, S.D., Locke, D.P., Friedman,

C., et al. Chimpanzee and human Y chromosomes are remarkably divergent in structure and gene content. Nature *463*, 536-539.
186. Amberg D. C., B.D.J., Strathern J. N. (2005). Methods in Yeast Genetics, (Cold Spring Harbor Laboratory Press).
187. Pfaffl, M.W. (2001). A new mathematical model for relative quantification in real-time RT-PCR. Nucleic Acids Res *29*, e45.
188. Lu, Y., and Cross, F. (2010). Periodic Cyclin-Cdk Activity Entrains an Autonomous Cdc14 Release Oscillator. In Cell, Volume 141. pp. 268-279.
189. Hill, A., and Bloom, K. (1987). Genetic manipulation of centromere function. In Mol Cell Biol, Volume 7. pp. 2397-2405.
190. Alvaro, D., Lisby, M., and Rothstein, R. (2007). Genome-wide analysis of Rad52 foci reveals diverse mechanisms impacting recombination. PLoS Genet *3*, e228.
191. Game, J.C., Birrell, G.W., Brown, J.A., Shibata, T., Baccari, C., Chu, A.M., Williamson, M.S., and Brown, J.M. (2003). Use of a genome-wide approach to identify new genes that control resistance of Saccharomyces cerevisiae to ionizing radiation. Radiat Res *160*, 14-24.
192. Hillenmeyer, M.E., Fung, E., Wildenhain, J., Pierce, S.E., Hoon, S., Lee, W., Proctor, M., St Onge, R.P., Tyers, M., Koller, D., et al. (2008). The chemical genomic portrait of yeast: uncovering a phenotype for all genes. Science *320*, 362-365.
193. Burtner, C.R., Murakami, C.J., Olsen, B., Kennedy, B.K., and Kaeberlein, M. (2011). A genomic analysis of chronological longevity factors in budding yeast. Cell Cycle *10*, 1385-1396.
194. Breslow, D.K., Cameron, D.M., Collins, S.R., Schuldiner, M., Stewart-Ornstein, J., Newman, H.W., Braun, S., Madhani, H.D., Krogan, N.J., and Weissman, J.S. (2008). A comprehensive strategy enabling high-resolution functional analysis of the yeast genome. Nat Methods *5*, 711-718.
195. Schwartz, D.C., and Cantor, C.R. (1984). Separation of yeast chromosome-sized DNAs by pulsed field gradient gel electrophoresis. Cell *37*, 67-75.
196. Shou, W., Seol, J.H., Shevchenko, A., Baskerville, C., Moazed, D., Chen, Z.W., Jang, J., Charbonneau, H., and Deshaies, R.J. (1999). Exit from mitosis is triggered by Tem1-dependent release of the protein phosphatase Cdc14 from nucleolar RENT complex. Cell *97*, 233-244.
197. Zhang, T., Nirantar, S., Lim, H.H., Sinha, I., and Surana, U. (2009). DNA damage checkpoint maintains CDH1 in an active state to inhibit anaphase progression. In Dev Cell, Volume 17. pp. 541-551.
198. Li, Z., Vizeacoumar, F.J., Bahr, S., Li, J., Warringer, J., Vizeacoumar, F.S., Min, R., Vandersluis, B., Bellay, J., Devit, M., et al. (2011). Systematic exploration of essential yeast gene function with temperature-sensitive mutants. Nat Biotechnol *29*, 361-367.

199. Bazile, F., St-Pierre, J., and D'amours, D. (2010). Three-step model for condensin activation during mitotic chromosome condensation. In cc, Volume 9. pp. 3243-3255.
200. Sullivan, M., and Uhlmann, F. (2003). A non-proteolytic function of separase links the onset of anaphase to mitotic exit. In Nat Cell Biol, Volume 5. pp. 249-254.
201. Nowak, S.J., and Corces, V.G. (2004). Phosphorylation of histone H3: a balancing act between chromosome condensation and transcriptional activation. Trends Genet *20*, 214-220.
202. Fischle, W., Tseng, B.S., Dormann, H.L., Ueberheide, B.M., Garcia, B.A., Shabanowitz, J., Hunt, D.F., Funabiki, H., and Allis, C.D. (2005). Regulation of HP1-chromatin binding by histone H3 methylation and phosphorylation. Nature *438*, 1116-1122.
203. Gillett, E.S., Espelin, C.W., and Sorger, P.K. (2004). Spindle checkpoint proteins and chromosome-microtubule attachment in budding yeast. J Cell Biol *164*, 535-546.
204. Gari, E., Volpe, T., Wang, H., Gallego, C., Futcher, B., and Aldea, M. (2001). Whi3 binds the mRNA of the G1 cyclin CLN3 to modulate cell fate in budding yeast. Genes Dev *15*, 2803-2808.
205. Kim, Y.H., Ishikawa, D., Ha, H.P., Sugiyama, M., Kaneko, Y., and Harashima, S. (2006). Chromosome XII context is important for rDNA function in yeast. In Nucleic Acids Res, Volume 34. pp. 2914-2924.
206. Duan, Z., Andronescu, M., Schutz, K., Mcilwain, S., Kim, Y., Lee, C., Shendure, J., Fields, S., Blau, C.A., and Noble, W. (2010). A three-dimensional model of the yeast genome. In Nature, Volume 465. pp. 363-367.
207. Mekhail, Seebacher, Gygi, and Moazed, D. (2008). Role for perinuclear chromosome tethering in maintenance of genome stability. In Nature, Volume 456. pp. 667-670.
208. Kobayashi, T. (2011). How does genome instability affect lifespan?: roles of rDNA and telomeres. Genes Cells *16*, 617-624.
209. Shintomi, K., and Hirano, T. (2011). The relative ratio of condensin I to II determines chromosome shapes. Genes Dev *25*, 1464-1469.
210. Kieserman, E.K., and Heald, R. (2011). Mitotic chromosome size scaling in Xenopus. Cell Cycle *10*, 3863-3870.
211. Uhlmann, F., Wernic, D., Poupart, M.A., Koonin, E.V., and Nasmyth, K. (2000). Cleavage of cohesin by the CD clan protease separin triggers anaphase in yeast. In Cell, Volume 103. pp. 375-386.
212. Goshima, G., Wollman, R., Stuurman, N., Scholey, J.M., and Vale, R.D. (2005). Length control of the metaphase spindle. Curr Biol *15*, 1979-1988.
213. Fuller, B.G., Lampson, M.A., Foley, E.A., Rosasco-Nitcher, S., Le, K.V., Tobelmann, P., Brautigan, D.L., Stukenberg, P.T., and Kapoor, T.M. (2008). Midzone activation of aurora B in anaphase produces an intracellular phosphorylation gradient. Nature *453*, 1132-1136.

214. Hayashi-Takanaka, Y., Yamagata, K., Nozaki, N., and Kimura, H. (2009). Visualizing histone modifications in living cells: spatiotemporal dynamics of H3 phosphorylation during interphase. J Cell Biol *187*, 781-790.
215. Sauve, D.M., Anderson, H.J., Ray, J.M., James, W.M., and Roberge, M. (1999). Phosphorylation-induced rearrangement of the histone H3 NH2-terminal domain during mitotic chromosome condensation. J Cell Biol *145*, 225-235.
216. Tsui, K., Durbic, T., Gebbia, M., and Nislow, C. (2012). Genomic approaches for determining nucleosome occupancy in yeast. Methods Mol Biol *833*, 389-411.
217. Duan, Q., Chen, H., Costa, M., and Dai, W. (2008). Phosphorylation of H3S10 blocks the access of H3K9 by specific antibodies and histone methyltransferase. Implication in regulating chromatin dynamics and epigenetic inheritance during mitosis. J Biol Chem *283*, 33585-33590.
218. Rea, S., Eisenhaber, F., O'Carroll, D., Strahl, B.D., Sun, Z.W., Schmid, M., Opravil, S., Mechtler, K., Ponting, C.P., Allis, C.D., et al. (2000). Regulation of chromatin structure by site-specific histone H3 methyltransferases. Nature *406*, 593-599.
219. Millar, C.B., and Grunstein, M. (2006). Genome-wide patterns of histone modifications in yeast. Nat Rev Mol Cell Biol *7*, 657-666.
220. Ohta, S., Wood, L., Bukowski-Wills, J.C., Rappsilber, J., and Earnshaw, W.C. (2011). Building mitotic chromosomes. Curr Opin Cell Biol *23*, 114-121.
221. Hauf, S., Roitinger, E., Koch, B., Dittrich, C.M., Mechtler, K., and Peters, J.M. (2005). Dissociation of cohesin from chromosome arms and loss of arm cohesion during early mitosis depends on phosphorylation of SA2. PLoS Biol *3*, e69.
222. Dai, J., Sullivan, B.A., and Higgins, J.M. (2006). Regulation of mitotic chromosome cohesion by Haspin and Aurora B. Dev Cell *11*, 741-750.
223. Indjeian, V.B., Stern, B.M., and Murray, A.W. (2005). The centromeric protein Sgo1 is required to sense lack of tension on mitotic chromosomes. Science *307*, 130-133.
224. Ottaviani, A., Gilson, E., and Magdinier, F. (2008). Telomeric position effect: from the yeast paradigm to human pathologies? Biochimie *90*, 93-107.
225. Luger, K., Rechsteiner, T.J., Flaus, A.J., Waye, M.M., and Richmond, T.J. (1997). Characterization of nucleosome core particles containing histone proteins made in bacteria. J Mol Biol *272*, 301-311.
226. Flors, C., and Earnshaw, W.C. (2011). Super-resolution fluorescence microscopy as a tool to study the nanoscale organization of chromosomes. Curr Opin Chem Biol *15*, 838-844.
227. Micheva, K.D., and Smith, S.J. (2007). Array tomography: a new tool for imaging the molecular architecture and ultrastructure of neural circuits. Neuron *55*, 25-36.

228. Dekker, J. (2002). Capturing Chromosome Conformation. In Science, Volume 295. pp. 1306-1311.
229. Umbarger, M.A., Toro, E., Wright, M.A., Porreca, G.J., Bau, D., Hong, S.H., Fero, M.J., Zhu, L.J., Marti-Renom, M.A., McAdams, H.H., et al. (2011). The three-dimensional architecture of a bacterial genome and its alteration by genetic perturbation. Mol Cell *44*, 252-264.
230. Dostie, J., Richmond, T.A., Arnaout, R.A., Selzer, R.R., Lee, W.L., Honan, T.A., Rubio, E.D., Krumm, A., Lamb, J., Nusbaum, C., et al. (2006). Chromosome Conformation Capture Carbon Copy (5C): a massively parallel solution for mapping interactions between genomic elements. Genome Res *16*, 1299-1309.
231. Taddei, A., Schober, H., and Gasser, S.M. (2010). The budding yeast nucleus. Cold Spring Harb Perspect Biol *2*, a000612.
232. Nagai, S., Dubrana, K., Tsai-Pflugfelder, M., Davidson, M.B., Roberts, T.M., Brown, G.W., Varela, E., Hediger, F., Gasser, S.M., and Krogan, N.J. (2008). Functional targeting of DNA damage to a nuclear pore-associated SUMO-dependent ubiquitin ligase. Science *322*, 597-602.
233. Andrulis, E.D., Neiman, A.M., Zappulla, D.C., and Sternglanz, R. (1998). Perinuclear localization of chromatin facilitates transcriptional silencing. Nature *394*, 592-595.
234. Taddei, A., Van Houwe, G., Hediger, F., Kalck, V., Cubizolles, F., Schober, H., and Gasser, S.M. (2006). Nuclear pore association confers optimal expression levels for an inducible yeast gene. Nature *441*, 774-778.
235. Sullivan, W., Daily, D.R., Fogarty, P., Yook, K.J., and Pimpinelli, S. (1993). Delays in anaphase initiation occur in individual nuclei of the syncytial Drosophila embryo. In Mol Biol Cell, Volume 4. pp. 885-896.
236. Aragon, A.D., Rodriguez, A.L., Meirelles, O., Roy, S., Davidson, G.S., Tapia, P.H., Allen, C., Joe, R., Benn, D., and Werner-Washburne, M. (2008). Characterization of differentiated quiescent and nonquiescent cells in yeast stationary-phase cultures. Mol Biol Cell *19*, 1271-1280.
237. Andersen, M., Nelson, Z., Hetrick, E., and Gottschling, D. (2008). A Genetic Screen for Increased Loss of Heterozygosity in Saccharomyces cerevisiae. In Genetics, Volume 179. pp. 1179-1195.
238. Torres, E., Dephoure, N., Panneerselvam, A., Tucker, C., Whittaker, C., Gygi, S., Dunham, M., and Amon, A. (2010). Identification of aneuploidy-tolerating mutations. In Cell, Volume 143. pp. 71-83.
239. Theler, D. (2007). Construction of a conditionally dicentric extraordinary long chromosome (by site specific recombination) in S. cerevisiae: Cut or No Cut? In Biology Department, Institut of Biochemistry. (ETH Zürich).
240. Dutrillaux, B., Gerbault-Seureau, M., Remvikos, Y., Zafrani, B., and Prieur, M. (1991). Breast cancer genetic evolution: I. Data from cytogenetics and DNA content. Breast Cancer Res Treat *19*, 245-255.
241. Davidson, J.M., Gorringe, K.L., Chin, S.F., Orsetti, B., Besret, C., Courtay-Cahen, C., Roberts, I., Theillet, C., Caldas, C., and Edwards,

P.A. (2000). Molecular cytogenetic analysis of breast cancer cell lines. Br J Cancer *83*, 1309-1317.

242. Goffeau, A., Barrell, B.G., Bussey, H., Davis, R.W., Dujon, B., Feldmann, H., Galibert, F., Hoheisel, J.D., Jacq, C., Johnston, M., et al. (1996). Life with 6000 genes. Science *274*, 546, 563-547.
243. Schubert, I. (2007). Chromosome evolution. Curr Opin Plant Biol *10*, 109-115.
244. Li, X., Zhu, C., Lin, Z., Wu, Y., Zhang, D., Bai, G., Song, W., Ma, J., Muehlbauer, G.J., Scanlon, M.J., et al. (2011). Chromosome size in diploid eukaryotic species centers on the average length with a conserved boundary. Mol Biol Evol *28*, 1901-1911.
245. Schubert, I. (2001). Alteration of chromosome numbers by generation of minichromosomes -- is there a lower limit of chromosome size for stable segregation? Cytogenet Cell Genet *93*, 175-181.
246. Murata, M., Shibata, F., and Yokota, E. (2006). The origin, meiotic behavior, and transmission of a novel minichromosome in Arabidopsis thaliana. Chromosoma *115*, 311-319.
247. Murray, A.W., Schultes, N.P., and Szostak, J.W. (1986). Chromosome length controls mitotic chromosome segregation in yeast. Cell *45*, 529-536.
248. Spence, J.M., Mills, W., Mann, K., Huxley, C., and Farr, C.J. (2006). Increased missegregation and chromosome loss with decreasing chromosome size in vertebrate cells. Chromosoma *115*, 60-74.
249. Hudakova, S., Kunzel, G., Endo, T.R., and Schubert, I. (2002). Barley chromosome arms longer than half of the spindle axis interfere with nuclear divisions. Cytogenet Genome Res *98*, 101-107.
250. Mitelman, F., Johansson, B., and Mertens, F. (2007). The impact of translocations and gene fusions on cancer causation. Nat Rev Cancer *7*, 233-245.

Appendix

Contains the article that resulted from the presented work:

Neurohr, G., Naegeli, A., Titos, I., Theler, D., Greber, B., Diez, J., Gabaldon, T., Mendoza, M., and Barral, Y. (2011). A Midzone-Based Ruler Adjusts Chromosome Compaction to Anaphase Spindle Length. In Science. p. 16.

Neurohr G, Naegeli A, Titos I, Theler D, Greber B, Diez J, et al. A midzone-based ruler adjusts chromosome compaction to anaphase spindle length. Science. 2011 Apr 22;332(6028):465-468.